SYNTHESIS, FABRICATION AND ANALYSIS OF BORON NITRIDE REINFORCED STEEL SURFACE COMPOSITE FOR INTERMEDIATE TO HIGH TEMPERATURE APPLICATIONS.

A Thesis

Submitted in partial fulfillment of the requirements for the award of the degree of

DOCTOR OF PHILOSOPHY

in

(MECHANICAL ENGINEERING)

By

MUKHTIAR SINGH

(41500112)

Supervised By

Dr.Ravinder Kumar

Co-Supervised by

Dr.Hitesh Vasudev

LOVELY PROFESSIONAL UNIVERSITY

PUNJAB

Declaration

I hereby declare that this thesis represents my own work which has been done after registration for the degree of PhD at Lovely Professional University, and has not been previously included in a thesis or dissertation submitted to this or any other institution for a degree, diploma or other qualifications. It is the result of my own work and includes nothing which is the outcome of work done in collaboration except as declared in the Preface and specified in the text. I further state that no substantial part of my dissertation has already been submitted, or, is being concurrently submitted for any such degree, diploma or other qualification at the Lovely Professional University or any other University of similar institution except as declared in the Preface and specified in the text. The work was done under the guidance of Dr. Ravinder Kumar Associate Professor, Lovely Professional University.

Candidate's Name: Mukhtiar Singh
Date: 30-09-2021

In my capacity as supervisor of the candidate's thesis, I certify that the above statements are true to the best of my knowledge.

Dr. Ravinder Kumar
Associate Professor
School of Mechanical Engg.
Lovely Professional University
Punjab

Dr.Hitesh Vasudev
Associate Professor
School of Mechanical Engg.
Lovely Professional University
Punjab

CERTIFICATE

I hereby certify that the work which is being presented in PhD thesis entitled "**MECHANICAL AND MICRO STRUCTURAL CHARACTERIZATION OF BN THIN FILMS DEVELOPED USING RF MAGNETRON SPUTTERING METHOD**" in partial fulfillment of the requirements for the award of the degree of **Doctor of Philosophy** is an authentic work of my own which was carried out during the period from Aug 2015 to Feb 2021 under the supervision of **Dr. Ravinder Kumar** Associate Professor, School of Mechanical Engineering, Lovely Professional University, Punjab and **Dr. Hitesh Vasudev** Associate Professor, School of Mechanical Engineering, Lovely Professional University, Punjab The matter presented in this thesis has not been submitted anywhere for the award of any degree.

Place: Phagwara
Date: 30-09-2021

Mukhtiar Singh
Reg No: 41500112

This is to certify that the above statement made by the candidate is correct to the best of my knowledge and belief.

Dr. Ravinder Kumar
Associate Professor
School of Mechanical Engg.
Lovely Professional University
Punjab

Dr.Hitesh Vasudev
Associate Professor
School of Mechanical Engg.
Lovely Professional University
Punjab

Abstract

The main property requirements expected from thin coatings are generally tribological electrical, optical, magnetic, heat resistant, corrosion-resistant, biocompatible, and decorative. The hard coatings deposited by advanced methods such as PVD and CVD etc. can meet this requirement with excellence. Although presently different kinds of thin hard coatings are routinely used in industries for better service than the uncoated samples butt still thin coating could not reach the market maturity. A significant explanation is that coatings with very good adhesion are regularly deposited, and the chances of developing a coating with poor adhesion is still present which leads to coating failure. The coating failure is not a disaster on a general component such as cutting tools. However, the failure of the coating on a critical component, may result in a catastrophic failure of the whole assembly in general machinery or an engine. Higher residual stress development in the coating and hardness gap between the coating and substrate are often addressed for poor adhesion. The development of advanced functional and intelligent protection coatings in different technological applications is currently strongly focused. Self-healing coating and smart coatings are emphasized, which incorporate much functionality to improve the protection against corrosion. Recent progress is being made by chemical engineering to incorporate functionalities focused on encompassing super hydrophobic agents, corrosion inhibitors and anti-fouling agents as well as modifications of organic and synthetic matrices. The surface coating results in the application or cultivation on the base product ground with thin layers of different materials. There is wide variation in the coating thickness ranging from less than 100 nm to few hundreds of microns.Among the various Physical Vapour Deposition techniques, sputtering is most widely employed method to prepare thin films for modern industrial applications. This process has emerged as the best choice for the thin film deposition with wide range of important coatings for modern industrial sectors. Increasing demand in the industries for high quality functional film is the main cause behind its development; examples of thin coatings are low friction coatings, corrosion resistance coatings, wear resistance coatings, decorative coatings and thin film coating with specific structural, electrical, and optical properties. In this research Boron nitride coatings were synthesised on SS316L stainless steel substrates through the radio frequency magnetron sputtering method from a target made of hexagonal boron nitride. The main objectives of the research are to improve surface, mechanical, tribological and corrosion behaviour of the coated surface.

The process of coating deposition was performed at the lab facility of Institute of Electrophysics, Yekaterinburg, Russia under the supervision of Prof. A S Kamenetskik. Cubic phase boron nitride based coatings were deposited on SS316L specimens with the help of RF magnetron sputtering technique. As a target material, a disc of h-BN (99.9% purity) measuring 80 mm in diameter and 10 mm thickness was used. for the sputtering. Prior to the deposition, plasma cleaning was performed in Ar environment at a 400 V negative bias for 10 min. The magnetron power supplied to the target plate was increased to 150 W progressively during deposition and was maintained until the deposition was completed. For varying bias voltage levels of between 100 and 200 V, the temperature ranged between 200-300^{o}C. For each experiment the coating continued to grow for 5 hours. Scanning Electron Microscopy (SEM), Fourier Transform Infrared Spectroscopy (FTIR) and X-Ray Diffraction (XRD) techniques investigated the microstructure morphology and composition of the BN films developed in three different parameter regimes. The electrochemical corrosion test and mechanical analysis was performed to study corrosion and tribological behaviour of the BN coating. This research aimed to examine the effects of changing the N_2 gas ratio on the structure and structural morphology of c-BN coatings. Using QAr / QN_2-5/2.5 gas mixing ratio an increased consistency of the microstructure and further c-BN step formation suggest a fundamental technique for producing superior quality cubic boron nitride films. Various tests investigations revealed that coating synthesised in BN-2 regime has possessed superior chemical, tribilogical and mechanical behaviour under different operating condition. From the study it has been found that in comparison to BN-1 and BN-3 more cubic phase of boron nitride found in BN-2 sample as revealed by investigation of XRD differentiation peaks. It is because of the fact that there is a bombardment of high Ar ions in sample BN-2 which results in more Ar ions residing in the BN-2 film synthesized in Ar / N_2 plasma. Because of the contamination of these Ar ions within the BN coatings, the compressive stress increases during the formation of h-BN phase on the substrate interface to promote thermodynamically cubic boron nitride nucleation and growth. The XRD investigation shows the c-BN as a major phase in the deposited coating. The results from electrochemical corrosion test confirmed that BN-2 regimes have the lowest corrosion rate due to the high c-BN contents presence

in the coating. From the study of scratch tracks it has been found that BN-2 coatings have high adhesion strength and hardness in comparison to coatings deposited in other regimes. The tribological performance test for the measurement of friction coefficient was carried out on all samples. The BN-2 regime films have excellent wear resistance as revealed by these tests. The findings of Young's modulus obtained by system of approach curves confirmed the presence of cubic phase boron nitride structure in the deposited coatings. The coatings deposited on BN-2 regime samples have possessed better adhesion than deposited on BN-1 and BN-3 regimes, as indicated by higher value of critical load. Therefore BN-2 regime is a coating with a higher adhesion strength, showing a combination of excellent durability and strength of adhesion. In porosity study due to volumetric and uniform ions bombardment associated with the sputtering technique, the porosity in the sputtered RF magnetron coating was found to be less than 0.5 per cent in all coating regimes. The dry sliding wear rate of BN-2 specimens showed the 78% minimum abrasive wear coefficient from substrate (SS-316L) material, and 50% and 40% less abrasive wear compared with BN-1 and BN-3 specimens. In terms of overall coating performance BN-2 sample has been found to be the excellent choice as it possessed superior mechanical, physical, tribological and chemical attributes.

Keywords: electrical conductivity, magnetron sputtering, surface roughness, thin film,

ACKNOWLEDGEMENTS

I would never have been able to finish my dissertation without the guidance of my faculty members, help from friends, and support from my family. I would like to express my deepest gratitude to my thesis supervisor **Dr. Ravinder Kumar** due to their excellent guidance, care, patience, and providing me an excellent atmosphere for doing research. I thank him for all the time he spent with me discussing everything about my research work to career options; his supervision has helped me during setbacks, obstacles and inspired me to give my best. I would like to express my sincere gratitude to my co-supervisor **Dr. Hitesh Vasudev**, for his valuable efforts in providing me with the advances practical knowledge of the subject matter. I would like to acknowledge the special contribution of **Prof. A S Kamenetskik**, Institute of Electrophysics, Yekaterinburg, Russia for the assistance in the coating process and providing the lab facility for the sputtering process at his institute. I would like to thank **Dr. Manpreet Singh, Dr. Chandar Prakash** and **Dr Kanishka Jha** Associate Professor, School of Mechanical Engineering, Lovely Professional University for their support and suggestions in preparing this thesis on time. At last, I am grateful to my parents and my siblings for their patience and financial support as well as for their inspiration to continue the efforts without worrying about success or failure.

Table of Contents **Page No**

CHAPTER-1

INTRODUCTION

1.1 Background

The adage quoted by the famous physicist Wolfgang Pauli, "God constructed the bulk, the surface was built by the devil," clearly demonstrates how important the characteristics of the material surface are. A basic truth that a solid surface has an external border inside a solid is explained to the diabolistic feature of surfaces. Each molecule is made up of other identical atoms or components. The properties of the surface of a solid vary considerably from those of the material in bulk. Since ancient times, people have tried to alter the surface properties of objects. In other terms, gold beating and leafing has been utilised for health, protection, and aesthetic purposes since ancient Egypt. A hatchet 900 B.C. of Brinell Hardness 444 on the edge shows it has been carburized and still used to increase surface hardness of the materials. (Pshyk *et al.*, 2017). The surface of any engineering materials has two aspects: functional and decorative. The former one has been paid the utmost importance as it meets all primary demands expected from any engineering material. Mankind has been searching for improved surfaces on various tools since antiquity. In the modem era, the traditional surface improvement process is renamed as “surface engineering” which enc compasses all of those techniques and processes utilized to induce, modify and enhance the performance (functions and /or service life) of engineering materials. Surface engineering through thin coating has become an established technique and a very diverse way to improve the performance of components. by optimizing the surface properties. Surface engineering processes tailor the surfaces of engineering materials to:

- Reduce cost.
- Wear and friction control
- Corrosion resistance improvement
- Physical properties change
- Alter dimensions
- Alter appearance,e,g color, roughness

1.2 Problems related to the thin hard coating

The main property requirements expected from thin coatings are generally tribological electrical, optical, magnetic, heat resistant, corrosion-resistant, biocompatible, and decorative. The hard coatings deposited by advanced methods such as PVD and CVD etc. can meet this requirement with excellence. Although presently different kinds of thin hard coatings are routinely used in industries for better service than the uncoated samples butt still thin coating could not reach the market maturity. A significant explanation is that coatings with very good adhesion are regularly deposited, and the possibility of depositing a coating with bad adhesion is still present which leads to coating failure. The coating failure is not a disaster on a general component such as cutting tools. However, if a coating breaks on a crucial component, it might cause the entire assembly in general machinery or an engine to fail. Higher residual stress development in the coating and hardness gap between the coating and substrate are often addressed for poor adhesion. The advanced deposition techniques require higher capital investment and some methods have poor surface coverage over complex 3D objects for practical application. The lower deposition rate compared to traditional coating deposition techniques is also another drawback. Again, many of the coatings do not have low friction value and, also do not provide the opposing surface with any protection. The coating is very hard and can cause the opposite surface to wear and abrasion quickly if the coated surface is very rough. This is an abrasive particle source if the coating is removed and acts like grits within the mechanism which can lead to the failure of the coating before the expected time. Friction can also cause higher power consumption. Liquid lubricant can solve the friction problem but it involves huge cost and threat to the environment. These performance limitations demonstrate the need for other high profile multifunctional coatings that can provide wear resistance, load-bearing and lubricating capability. The use of hard solid lubricant coating to prevent these problems in the tribological field has been proposed by a growing number of studies in the literature. These coating criteria place requirements on production equipment to provide higher performance with more stringent performance specifications. The process of deposition must therefore provide a higher rate of deposition for a wide variety of material selection while also ensuring greater uniformity of broad area thickness and lower defect level.

1.3 Coatings

In extreme environments, coatings are essential to ensure surface resilience and longevity, the design of bio-compatible devices and building systems for sustainable energy production and pollution recovery, just to name the hottest applications. Coating implies a substance added to other substances that affect the surface characteristics, such as colour, light, chemical attack, or wear resistance, without changing the bulk characteristics. Thin films are often hetero-artificial materials formed by one of many deposition methods on a substrate. The term coating often refers to paints like varnishes or enamels, but also films used in other materials such as varnishes, sealants, adhesives, inks, maskers and temporary protective coatings. Metal coatings are two facets-coated materials on metal and metals as coatings on any substrate. Coatings are adapted to protect metallic substrates from corrosion are extremely important for the long-term efficiency and reliability of the coated parts and their product value. The development of advanced functional and intelligent protection coatings in different technological applications is currently strongly focused. Self-healing coating and smart coatings are emphasized, which incorporate much functionality to improve the protection against corrosion. Recent progress is being made by chemical engineering to incorporate functionalities focused on encompassing super hydrophobic agents, corrosion inhibitors and anti-fouling agents as well as modifications of organic and synthetic matrices. The surface coating results in the application or cultivation on the base product ground with thin layers of different materials. There is wide variation in the coating thickness ranging from less than 100 nm to few hundreds of microns. The underlying process of surface coating growth is a chemical reaction with vapor or liquid on the substrate surface. The surface coating consists of thin layers of one or more materials applied or grown from the surface of the base material. There is wide variation in the coating thickness range from less than 100 nm to hundreds of microns. A surface coating is produced by a chemical reaction on the surface of the substrate with a liquid or vapor. Surface coatings provide wear, optical, corrosion, electrical, chemical, and cosmetic properties which superior to the possible surface properties of the substrate. The combination of a surface coating and base material facilitates the fabrication of components that meet the higher standard of performance, cost requirements and reliability that would not

be possible otherwise if an uncoated base material is used. The best example is the coating of zinc on carbon steel screws. The zinc protects against corrosion and the steel provides strength. Without the application of zinc coating, the steel would corrode too quickly for outdoor applications. Today, surface coatings are utilized as a part of the entire cross-area of utilizations ranging from display devices, microelectronics (Kowalik *et al.,* 2020) solar cell, tribology, wear resistance, and corrosion including cutting tool and distinctive machine parts, sunlight based cells, warm protection, high-temperature oxidation, and coatings for decoration to enhance performance and improve material's life. The first observations concerning thin films go back more than 150 years. However, during 30 years, the innovative performances in the deposition systems, plasma-based process and atomic deposition processes have progressed dramatically (Panich N *et al.,* 20016). These coatings are produced from a wide variety of materials. These are single-layer or multi-layer intermetallic compounds, metals, refractory compounds (e.g. nitrides, carbides, oxides) and alloys. The coating's thickness ranges from a few atomic layers to many atomic layers. A vital aspect of thin-film research and surface engineering is hard coatings and wear-resistant (Taube, K *et al.,* 2018).There are very much concentrated artistic thin film for modern applications particularly to electronics devices, solar cell, automobile industries, aircraft industries, wear resistance and cutting tools applications such as TiN (Ananthakumar R *et al.,* 2019), TiAlN (Zhao Y.H *et al.,*. 2019), TiC (Mateescu, A *et al.,*. 2017), SiC, TiN (Bin D *et al.,* 2020), WC (Broitman E *et al.,*. 2019), CrN and DLC (Auezhan *et al.,* 2020) as cases. A few other applications in numerous industrial sectors are used to create nano-coatings for various purposes in the form of thin films such as solar cells, display, antistatic coatings, infrared reflection, microelectronics cylinder rings in diesel engine, gas turbine rollers, shaping or forming tools and airspace components, etc. (Kelly *et al.,* 2020). But industrial requirements and expanding innovation demand thinner films with more complex properties. Sputtering technique is traditionally one of the oldest techniques of thin coating deposition and plays a prominent role among different methods of physical vapor deposition (PVD). Besides its other advantages: low temperature of deposition, fast deposition rate, improved adhesion; thin coating with controlled microstructures and properties can therefore be achieved by the sputtering, utilizing flexible controls

on deposition parameters and different possible configurations. Sir W. R. Grove, an English judge and "man of science" reported first sputtering in 1852 (Grove, W.R. 1852). He was the first one to research what was termed "sputtering," while others noted the impact during the study of glow discharge. Since the development of vacuum technology closely involves most of the physical vapor deposition, Otto van Guericke invented the first vacuum pump of a piston-type in 1640, to pump out the water from mines. However, in 1838 M. Faraday first applied the vacuum pump to form a glow discharge in a vacuum tube. Several researchers have been investigating magnetron sputtering since then and the first application of a magnetron sputter was studied in the 1960s. In 1966, Maiseel and Davidse utilized sputtering to create the dielectric film from a dielectric material. Nevertheless, due to the high costs and application of high temperatures, deposition by sputtering is not used extensively. Magnetron sputtering was then invented in the mid-1970s to sputter hard coatings on tools and became commercially available at the beginning of the 1980s. (Mattox, D.M. 2019). This technique utilizes high energy bombardment ions of a few hundred electron volts. Because of the ion bombardment to the cathode, metal atoms and secondary electrons are formed. Gas ions were accelerated in the plasma to the target material during the sputtering process. The material is removed and placed on the substrate. In various regions of today's challenging and rapid development of technology, especially in the electronic and optical industries, their one-of-a-kind physical, electrical and mechanical characteristics of thin solid films are extremely unique in comparison to the required bulk material. A thin film must meet the criteria before being considered in every possible application: high quality, a high rate of deposition, reproducibility, reasonable cost, etc. Thin films are highly dependent on deposition method, material of the substrate, deposition rate, temperature, and pressure of the background gas. One of the most complex areas in thin film innovation is the thin film deposition of visibly transparent semi-conductive and electrically conductive high-quality oxide films at high deposition rates. Numerous modern technological applications require specific properties in the fields of thin films viz. low porosity, desirable stoichiometry, adhesive, thermal resilience, etc. These characteristics are heavily dependent upon methods of deposition such as reactive evaporation, thermal oxidation, spray-pyrolysis and sputtering, etc. The latter

includes magnetron, ion beam, triode and diode sputtering (L. Hultman 2020). In the last two decades, magnetic sputtering has become increasingly popular. Essentially, this is because it enables a large scale deposition of quality films (e.g. high density, homogenous thicknesses, and stronger adhesion to the substrate) with relatively controllable substrate temperature and high rate of deposition. Traditionally, in the presence of oxygen, transparent conducting alloy oxide films have been sputtered by the magnetron technique from a single target of oxide or multi-component, using RF or DC controls. However, in comparison with DC magnetron sputtering, complexity, higher cost and lower deposition rates make RF sputtering less favourable. The main objective of research in the past decade has been to examine the mechanical properties of boron nitride thin film nano-coatings. Boron nitride has various applications in the mechanical, microelectronic and electrical industries because of its outstanding mechanical, thermal and electrical properties. Coated tools are important for industrial production in various processes of cutting and shaping. Strong coverings such as TiAlN, TiCN, TiN, or dry lubricant coatings such as MoS_2 are well known for wear reduction. The need to increase tool performance is one consequence of increasing product quality and productivity. In particular, the development of new coatings and tools is still challenging under high speed cutting, dry conditions, the machinery of lightweight materials and cutting hard material. Cubic boron nitride is very well known for being one of the hardest materials after diamonds. Due to its superior characteristics such as optical transparency, hardness and thermal conductivity, it is an excellent material for hard coating on various kinds of tools, similar to diamonds. But it has two benefits over diamond: i) There is no diffusion of boron and nitrogen atoms into ferrous; ii) c-BN is chemically inert in oxygen atmospheres and also more stable at elevated temperature against oxidation than diamonds. Thus, c-BN appears more appropriate for wearing protective coating on steel substrates. The characteristics of c-BN not only serve as a wear-protection coating on various kinds of tools but also transparent protection for various kinds of heat-dissipating or optical components coatings in laser diode and electronics technology. But process complexity and cost of c-BN are a disadvantage. The cubic form of boron nitride can be synthesized in a variety of ways, usually in large amounts at high temperatures and pressure, but in large cases, the thin films are

generally produced using CVD and PVD methods. Magnetron sputtering is a PVD method for removing material from the target act as a cathode while placing the substrate between two electrodes supported by a magnetron in a low-pressure chamber. It is often utilized at room temperature for thin film deposition. Films developed by the magnetron sputtering technique are now often far better than films developed in other PVD methods, which can act in the same manner as thicker films created by other techniques for coating the substrate. As a result, magnetron sputtering is now having an important effect in applications including corrosion-resistant coatings, hard coatings, low friction coatings, wear-resistant coatings, ornamental and special electrical or optical properties coatings (S. Eyhusen *et al*, 2020). The most widely employed magnetron sputtering methods are: i) Direct current sputtering (DC) where a DC voltage is applied across the electrode but it is only possible with targets that are conductive in nature (ii) Radio Frequency sputtering (RF) in which RF signal is applied to the electrode and it can be employed for both insulator and conductor (iii) Reactive sputtering which uses a combination of both inert gas and reactive gas during the deposition process.

1.3.1 Types of Coating Processes.

1.3.1.1 Electrolytic Plating

In the electrolytic plating process, an electric current is passed through the component dipped in a chemical solution that is conductive in nature and containing metal ions to be deposited, which act as a cathode in the electric circuit. At the surface of the component, the ions of the metal in the solution receive electrons and attach themselves to the surface. It's possible to deposit a broad range of metals with the help of the electrolytic plating process, including zinc, chromium, nickel, platinum, silver, tin, gold, lead, and copper. A variety of alloys such as bronze, brass, nickel-iron and tin-lead can be also deposited. Coatings can also be deposited onto most metals, plastics and ceramics using electrolytic plating

1.3.1.2 Conversion Coating

Conversion coatings are the types of metal coatings where a coating material that transforms the surface of the component into a decorative or protective product is subjected to an electrochemical or chemical process. In this process, components are immersed into a chemical solution and the coating is attached with or without the flow of electric current to the component. The growth of a coating layer from base material takes place due to the chemical reaction between chemical solution and base. The deposited coating becomes an integral part of the surface of the components after the process. All the mechanical interface disappears after the coating set in. Conversion coating offers many advantages like corrosion protection and enhanced surface hardness. There are the following three types of conversion coating in general (Yap et al, 2018):

- Oxide coating: This type of coating offers good adhesion and ultra-thin which is mainly used for corrosion protection of the product. In these cases, oxide treatments can be done via chemical reactions, heat, or electrochemical, the best-known example of oxide coating comprise anodizing, black oxide and chemical baths
- Phosphate coating: It is similar to coating phosphate because it is produced by chemical reactions. Manganese, zinc and iron are crystals that can build on the surface. Of these three, manganese phosphate is the best kind of cover for wear applications. It is superior for metals with low alloys, carbon steel and cast iron.
- Chromate coating: It is similar to phosphate coatings, as it is produced by chemical reactions. It includes the interaction with water solutions of chromium salts or chromium acid. This coating applies to zinc, cadmium, magnesium and aluminum. This coating generally provides excellent corrosion resistance and is widely used to protect common products such as screws, hinges and other hardware.

1.3.2 Surface Coating Processes: The use of plating and surface coatings for finishing part surfaces is common in production. These coatings are used as thin films and offer decoration, protection, and durability on part surfaces. The most popular technologies used for surface coating and plating include:

- Vapor deposition
- Chemical and electrochemical deposition
- Spraying.

1.3.2.1 Vapor Deposition

Vapor deposition refers to any method where materials are condensed into a solid material in a vapor state by condensation, chemical reaction or conversion. These techniques are employed to produce coatings to modify the electrical, mechanical optical, thermal, wear and corrosion behaviour of the substrate. These processes are also employed to produce fibre and films, free-standing bodies and to infiltrate composites into fabrics. These processes are generally carried out in the vacuum chamber (O.Tsuda *et al*, 2006). The process of vapor deposition is divided into following type.

- Physical vapor deposition.
- Chemical vapor deposition.

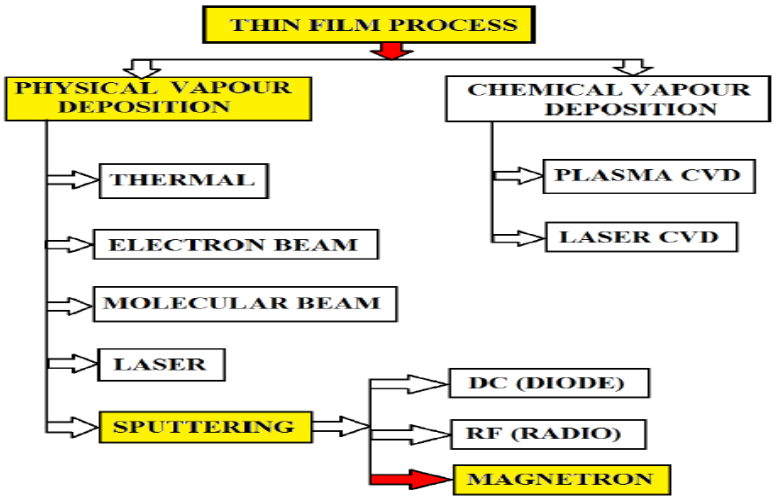

Figure.1.1. Different types of deposition methods.

In the PVD process, the material which is to be coated is evaporated first by using high energy sources (electron beam or sputtering with magnetron) and allowed this vapor to deposit on the surface of the work-piece as shown in figure 1.2. This process has been used on many metals. In the CVD process, a mixture of gases is allowed to flow overheated work-piece. Due to the chemical reaction between the gases resulting phase is deposited on the work-piece present in the chamber figure 1.3

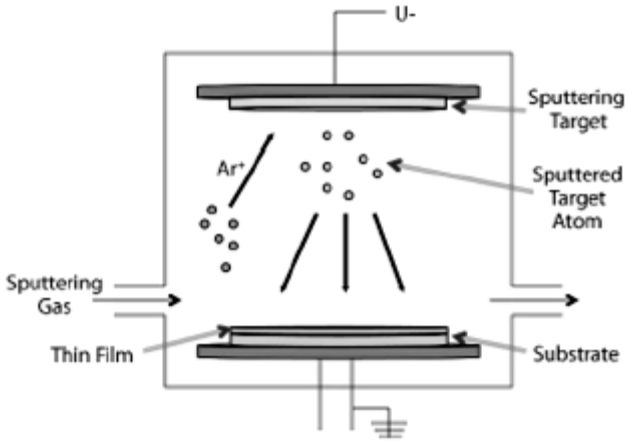

Figure.1.2. Schematic diagram of PVD

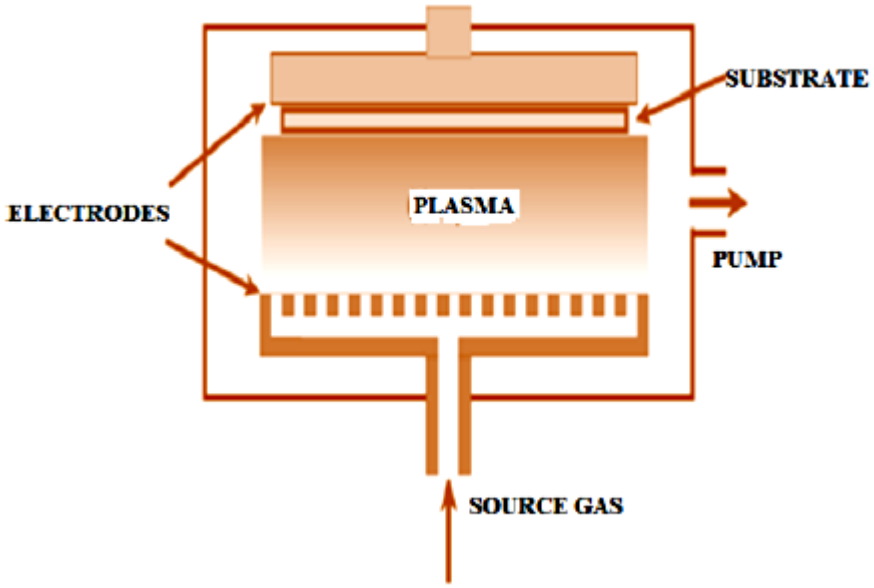

Figure 1.3 Schematic representation of CVD

PVD involves several methods of vacuum deposition to deposit thin coating on the substrate by the condensation of a vaporized phase of the coating material. The emphasis of the present work is on sputtering among PVD methods, as all the specimens examined in the research have been collected with this technique. While several variations of the technique exist, but in this present thesis work, focused on magnetron sputtering techniques. In this process, the magnets are mounted under the target material to create electrons with a closed drift path of magnetic and electric fields to increase the ionization probability. (K. Reichelt *et al.,* 1990). The below are some of the Physical Vapour Deposition techniques.

- Atomic Layer deposition
- Laser ablation
- Pulsed Laser Deposition
- Filtered arc plasma deposition
- Cathode arc plasma deposition
- Ion beam assisted sputter deposition
- High Power Impulse Magnetron Sputtering
- Electric arc plasma spraying
- Ion beam Sputtering
- Reactive magnetron sputtering

1.4 Ion Implementation

In this process, ionized particles are allowed to bombard the surface of a substrate. These particles penetrate the surface and get embedded into the subsurface of the substrate material. Physiochemical reactions occur at the subsurface regions and the properties will be changed while the bulk material retains its properties (Fei Zhou *et al.,* 2006). The process is shown in figure1.4

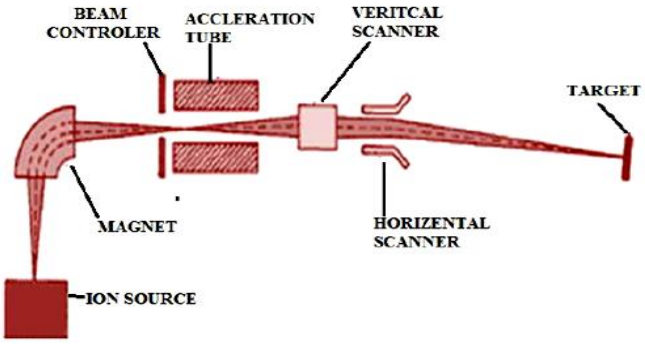

Figure 1.4 Schematic representation of Ion Implantation

1.5 Thermal Spray Coating

In this process, the coating material is feed into a gun. Then the material is heated to a molten state and forced to work-piece as molten droplets. These molten droplets get solidified as soon as they touch the substrate and get a deposit on the surface (Herman *et al.*, 1996). The process is illustrated in figure 1.5.

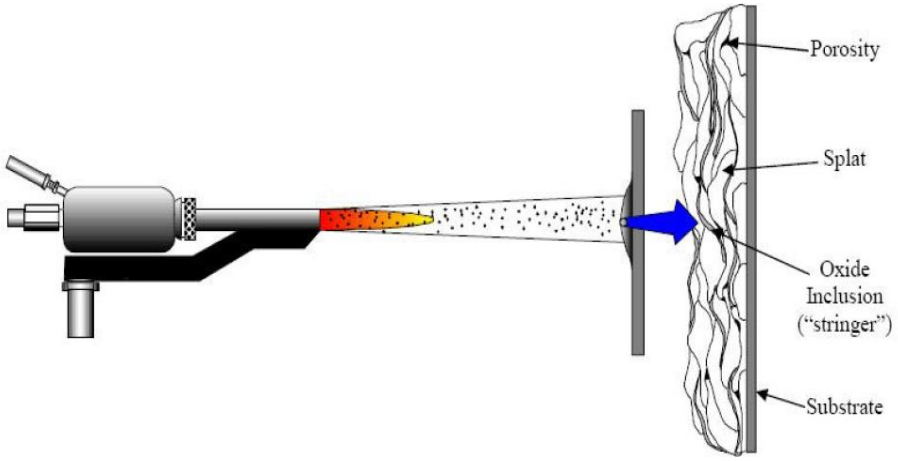

Figure 1.5 Schematic representation of Thermal Spraying.

1.6 Laser Melt Treatment

In this process, the high energy density laser beam is used to melt the surface region of the work-piece to create a metastable solid solution as shown in the figure. Coating material in the form of the particle is supplied through a nozzle by a carrier gas. After cooling, it results in the surface composite. Most of the surface modification techniques mentioned above involve liquid phase at high temperature are more susceptible to interfacial reactions and between the coating material and

substrate, and there is a probability of formation of detrimental phases. Moreover, optimization of process parameters and control is necessary to get an ideal coating surface. But, if the process takes place below the melting point temperature of the work-piece/substrate, all the aforementioned problems can be avoided (Navas *et al.*, 2006). The process of laser melt is illustrated in figure 1.6

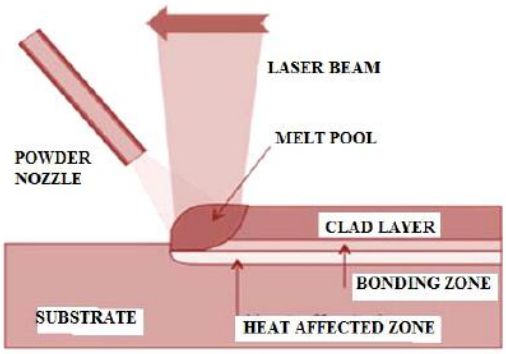

Figure 1.6 Schematic representation of Laser Melt Treatment

1.7 Sputtering

In sputtering the particles are expelled from a target due to energetic particles bombarding the target, especially gas particles. It only occurs when the kinetic energy of the incoming particles is substantially higher than that of normal thermal energies. In this process, substantial degradation of materials during sustained plasma or ion bombardment of a substance takes place which can therefore be harmful. In the simple sputtering technique, energy ions generated in the processing chamber by the glow discharge plasma are bombarded by a target plate. The ejection, or sputtering, of target atoms leads in a thin layer being formed on the substrate as a result of the bombardment as shown in figure 1.7 (Helmer *et al.*, 1996). For the sputtering gas, Argon is widely used. To form a film, the expelled atoms can be condensed at the optimal distance from the target on a substrate. Charged electrons and atoms are also released from the surface, in addition to neutral atoms. The sputtering yield'S '(number of atoms expelled per incident ion from the target surface) depends on the binding energy, composition of the target material, experimental geometry and the incident ion characteristics. It also relies on the current and voltage at which sputtering occurs.

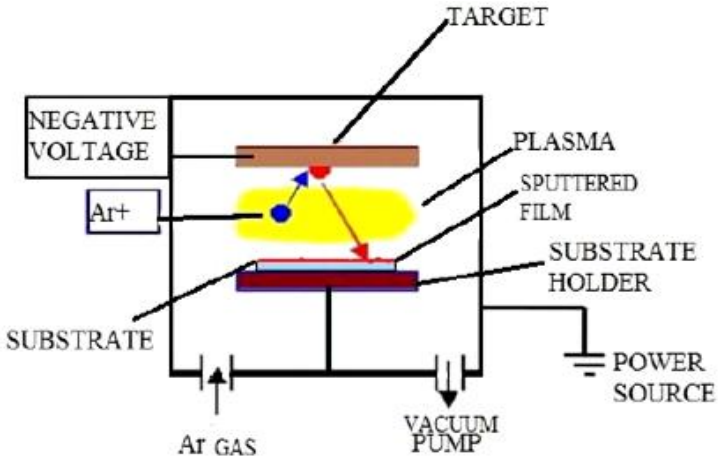

Figure 1.7 Schematic representation of Sputtering Mechanism

The illustration of the traditional process of sputtering is shown in Figure 2.2. The target material is linked to a negative supply of voltage and the substrate holder serves as the anode and faces the target during sputtering together with the chamber held at ground potential. The plasma is maintained between the substrate and the target. Because the technique works with energies in the tens of eV range, the film's adherence to the substrate is more important for sputtering.

1.7.1 Reactive Sputtering

Reactive sputtering operation is an atomistic in nature, and the majority of the atoms ejected from the cathode are emitted as atoms rather than clusters or molecules, regardless of whether it is an alloy/compound or elemental cathode. Reactive sputtering, typically combined with the inert working gas, can be described as the coating deposition of compounds on substrate surface in the presence of a reactive gas, via sputtering from targets. Chemical reactions between these atoms drifting away from the cathode towards the anode are unlikely, but it is entirely conceivable that the newly deposited atom on the surface of the film interacts chemically with the gas atoms that allow a compound film to form on the surface (P.B. Mirkarimi *et al*,2005) . A metal plate serves as the cathode in one type of reactive deposition, while an oxide or nitride of the material to be deposited serves as the cathode in the other. The most popular reactively sputtered compounds are mentioned briefly.

- Oxides (oxygen) - Ta_2O_5, Al_2O_3, SnO_2, SO_2, In_2O_3,;
- Nitrides (nitrogen, ammonia) – AlN , TiN ,TaN,Si3N4,BN;
- Carbides (propane, acetylene methane) - TiC, SiC ,WC;
- Oxynitrides and oxycarbides of Si , Ta, Al, and Ti.

It is not always clear whether to use a compound target or to sputter reactively or to sputter directly. If reactive sputtering is chosen, then simple dc diode, magnetron, or RF configurations can be used. Before making these decisions, several considerations must be taken, such as purity of the target - Highly pure metal targets are easier to develop than highly pure compound targets. The inclusion of impurities, porosity and gases is unavoidable because sintered and hot pressed powder of compound cannot be equivalent bulk densities calculated theoretically. The purity of film using elementary targets is high, especially when pure reactive gasses are commercially available.• Metal sputter rates drop drastically when compounds are formed on the targets. Due to the lower yield of sputter of the compounds relative to metals, decreases in the deposition rate well above 50% takes place. The effect depends very much upon the pressure of the reactive gas. To restore the pure metal surface and desired deposition rates, the conditioning of the target in pure Ar is needed. The sputtering reactive mode is either RF or dc magnetron when high deposition rates are required. • Stoichiometry and properties - Depending on the operating conditions, significant variance in the properties and composition is possible in films sputtered reactively.

1.7.2 Magnetron Sputtering

Initially, the word 'Magnetron' was employed to explain tubes used for radar applications to produce microwave power. This term is still employed for the same purpose, and a "magnetron" power source would be used by the owner or builder of a microwave plasma device to operate the plasma. To create an efficient sputtering cathode, the same effect of magnetron observed can be altered in these tubes in some way. These cathodes work in either DC or RF diode mode, are rarely called diodes. The current workhorse of the sputter deposition field is magnetron sputtering sources, used in the majority of all sputtering applications. In various industrial fields, especially surface processing and microelectronics, magnetrons have experienced

continuous development and are greatly used for thin coating deposition. Magnetron employs a magnetic static field positioned on the top of a cathode and the field of magnetic is positioned such that it is parallel to the surface of cathode. This magnetic field (B) constrains secondary electrons released from the cathode by the ion bombardment to travel in a perpendicular direction to both the magnetic and the electric field . It is referred to as an EB drift, and it is also fundamental to the Hall Effect. The drift results in electrons to travel away from the magnetic field parallel to the surface of cathode in a 90 degree (Deyneka *et al*, 2003). If the magnetic field is appropriately regulated, the EB drift may be managed to collapse on itself, resulting in a current loop of drifting secondary electrons. Figure 1 depicts the sputter coating method schematically. The process can operate at pressures of about 1.5 bar with high current density at a low value of voltage due to the higher efficiency of this ionization process, thereby providing high sputtering speeds. Magnetron (e.g. planar and cylindrical) sputter sources have many configurations. To develop a uniform film over wide areas, the cylindrical magnetron is a very useful tool, because in these techniques long cathodes are used. Furthermore, the hollow magnetron technique with a cylindrical form is suitable for coating complicated shapes. The cylindrical magnetron may be employed to reduce the amount of energy particles bombarding the substrate, lowering the heat generated by the substrate. As opposed to diode sputtering, dielectric films and metallic films can be deposited using planar magnetron sputtering at a high rate of deposition (Tzeng, Y., Zhu, H, 2004).

Low rate of deposition and low efficiencies of ionization in the plasma restrict the sputtering process. The magnetron sputtering development and, more recently, unbalanced magnetron sputtering has overcome these limitations. Magnetrons make use of the fact that the motion of secondary electrons in the proximity of the target can be limited by a magnetic field positioned parallel to the cathode. In this arrangement, the magnets are placed such that the central axis is fixed by a pole.

1.7.2.1 DC/RF sputtering

Based on the power supply employed, the sputtering mechanism is known as RF or DC. For depositing metals, DC sputtering is primarily used. In the case of insulators, their charge will remain localized after the ions reach the surface and a positive charge will develop on the surface of the target with time, making it harder to bombard the surface further. It can be avoided by the simultaneous bombardment of the insulator by both electrons and positive ions (Yang et al,2011). This is accomplished by applying the potential of an RF to the target surface. This RF potential gives ample energy for ionizing collisions to electron oscillating in the alternating field and retains an autonomous discharge. In comparison to the ions, the electrons have greater mobility, during the positive half cycle; more electrons can enter the insulating target surface than the negative half cycle positive ions. Therefore, the target would be negatively self-biased. The electrons are removed from the target area and a sheath is formed in front of the surface of the target enriched with positive ions. In this the target is bombarded by these ions and sputtering is accomplished. Such an ion sheath would not form at a frequency lower than 10 kHz. In the 5 to 30 MHz range, standard RF frequencies are used. However, the most common frequency employed for rf sputtering is maintained at 13.56 MHz, (Boyen *et a*l,2005) The most significant distinction between DC and RF systems is that the latter needs network matching impedance between the sputtering chamber and the power supply. The major function of this network is to enable the RF generator with optimum load matching so that adequate power can be supplied to the chamber. A schematic illustration of a typical, simple DC sputtering simple is shown in fig. 1.8. A target of the material to be deposited is situated inside a vacuum chamber where it is associated with the negative port of a DC control supply. Confronting the cathode/target is the substrate, which might be electrically floating, grounded, or biased (Reinke *et a*l,2012). An inert working gas, normally Ar, is pumped and acts as the source in which an electrical glow discharge is ignited and maintained. Forced by the field of electricity, working gas particles, Ar+, accelerate into the target material at high energy, causing target atoms to sputter upon contact with the cathode. The sputtered atoms move and condense onto the substrate through the discharge, subsequently

giving film development. At the point when the DC voltage is first connected to the electrodes, few charge bearers at first present in the working gas create a small current. Due to inelastic collisions in the gas more electron-particle sets are created, and the density of current increases. The Ar+ particles or ions target the surface of the cathode, resulting in the creation of auxiliary electrons from the surface of the cathode (and sputtering of the target atom). The secondary electrons are transported far from the target and increment the ionization of the gas using inelastic collisions. This charge multiplication causes the current to increase quickly or rapidly. At the point when the applied (connected) voltage is high to the point that the quantity of Ar+ particles created by impacts with one auxiliary electron is sufficiently high to generate another secondary electron, the discharge becomes self-maintaining and starts to glow. The light emitted from the discharge is because of the excitation of gas particles or atoms. The degrees of ionization in a typical self-sustaining DC glow discharge 10eV. The secondary electron emission coefficient, i.e. the number of optional electrons emitted at the cathode per incident ions, is around 0.1 for most metals when bombard with 100 eV Ar+ 20 (A. J. Lichtenberg &, M. A. Lieberman 1994). In this manner, to maintain the plasma the probability of collision amongst electrons and natural gas atoms must be sufficiently high. At that when the pressure of the gas is too low; the collision probability is less because of a large electron mean free path, which causes loss of electrons to the chamber wall, and the number of ionized gas molecules to be insufficient. On the other hand, at too high-pressure frequent collision prevent the electrons from getting adequate energy to ionize gas molecules or atoms, which will eventually quench the discharge. This means that at either extreme the particle or ion- generation rate is quite low and a high level of voltage is needed to maintain the plasma. An optimum pressure range, typically 14 around 1– 10 Pa, exists for a simple DC sputtering system, where a self-maintained glow discharge can be made at reasonable voltages, typically 200-1000 V (M. Ohring, 2002)]. A few features of the plasma are important in order to examine the flux of bombarding particles hitting the developing film, which is one of the key parameters in controlling and explaining the structure of the growing film. One of the plasma characteristics is because of the excess of positive Ar+ particles or ions in the space near the cathode, caused by the attraction of the particles (electrons). Any isolated surface inside the plasma charges

negatively initially because the electron flux will be higher than the Ar+ ion flux. This is a result of the dissimilarity in mass and subsequently mobility amongst electrons and ions. The surface keeps on charging negatively until the point when the electron flux equals up to the ion flux. At the point when the fluxes equal, a net positive space charge exists in closeness to the surface, and the surface will be at a potential slightly lower than the plasma. This is known as the plasma potential. In the middle of the surfaces, in the "bulk" plasma, the plasma has almost net charge zero. The abundance of positive ions adjacent to a surface is impressively expanded when an extensive external negative potential is applied, just like the case at the cathode. Solving Poisson's eqn. 1:

$$\nabla^2 V = \frac{-\rho}{\epsilon_\circ} \qquad \text{----------[1]}$$

where V is the electrical potential, $\epsilon_\circ$ is the vacuum permittivity and $-\rho$ is the charge distribution

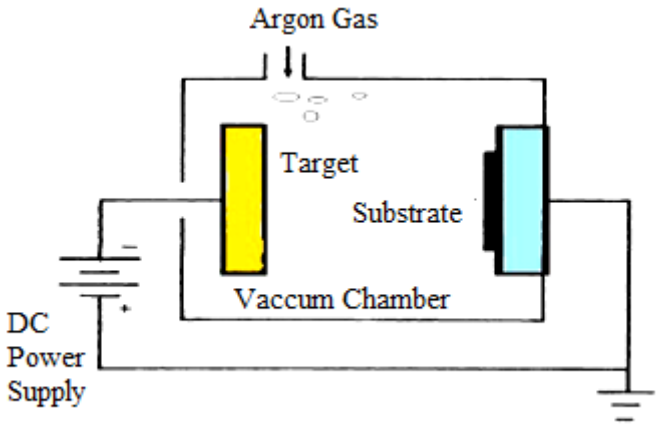

Figure 1.8 Schematic representation of Simple DC Sputtering system

1.7.2.2 DC/RF Magnetron Sputtering

In order to increase the sputter yield, sputtering sources also use magnetrons that use a strong magnetic field to restrict charged plasma particles near the target surface. On the other hand in a magnetic field, helical pathways along field lines are followed by electrons. This allows the effective path length to increase, creating further ionizing collisions close to the target surface with gaseous neutrals. The

magnetic trap has no effect on most sputtering atoms since they are neutral and hence considerably heavier. The sputtering gas is generally an inert gas such as Ar, and the Ar ions created by electron collisions speed up the deposition process. It also ensures that the plasma can be held at low-level Ar pressure. The most commonly used variant of DC sputtering is probably BMagnetron sputtering. Some of the advantages of magnetron sputtering over basic DC sputtering described so far include greater ion current (i.e. higher deposition rates) and lower operating pressure (i.e. higher deposited atom energy). (M. Ohring 2002). Permanent magnets are organized in a suitable arrangement behind the target plate during DC magnetron sputtering as shown in Fig. 1.9. The lines of the magnetic field penetrate the target and on its front surface form a closed path. The parallel component of the magnetic field with respect to the target's surface has a strength of a few hundred gauss estimated on the target's front surface. Electrons are driven slightly from the standard target initially to conduct a helical motion around the magnetic field that radiates naturally to the target area. The magnetron component also signified that electrons are obliged to drift back onto the target in a parallel region along the magnetic field (Rossnagel, 2002).

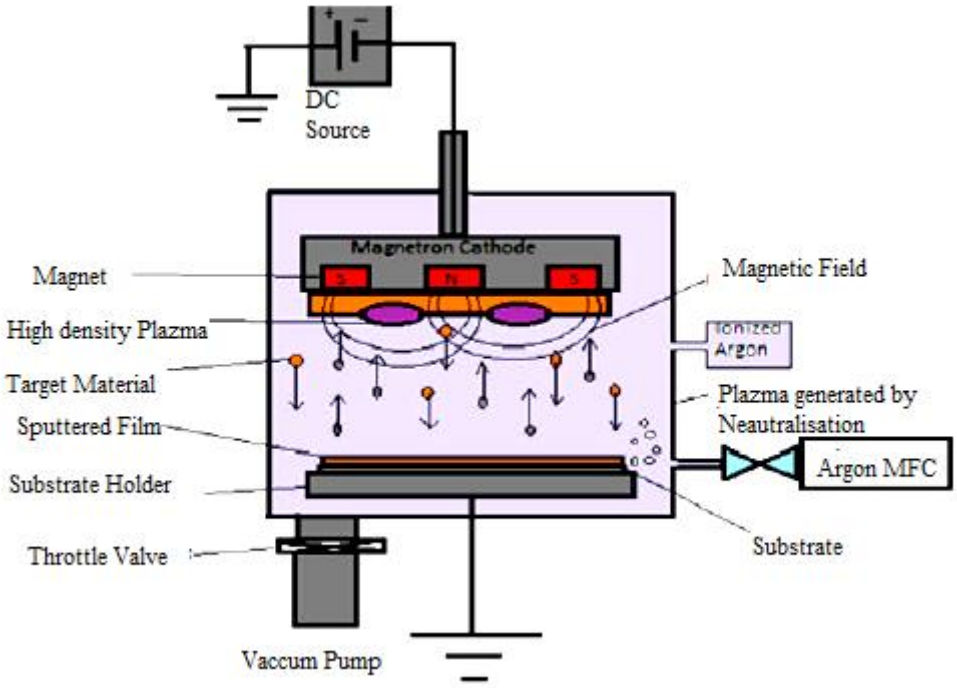

Figure 1.9 Schematic representation of DC Magnetron Configuration

When solving the movement of electrons, the electrons are following cycloid paths along the magnetic field in the direction of the target. In this way, secondary electrons make more ionising hits near the target when they are in the influence of a magnetic field and in this way increment the flux of bombarding particles or ions, resulting in a superior rate of deposition. The magnetron current-voltage characteristic is generally $I \propto V$ with n close10 (n =1 without the magnetic field). The essentially increase in ionization productivity makes it feasible to decrease the working pressure and still keep up reasonable high particles and a stable discharge and. The average pressure of magnetron-sputtering is 10-2-1 Pa, resulting in a mean free path of 1-100 cm range of sputtered molecules or atoms. Accordingly, in comparison to simple DC sputtering, the sputtered molecules' impact is lower with the atoms of gas, whereby the sputtered particles' loss of atoms in the chamber wall is brought down (i.e. increasing the deposition rate). Besides, the sputtered particles or atoms preserve a large portion of their underlying kinetic energy before targeting the substrate, which is of great significance to the final microstructure of the film. Other than the high plasma density and low working pressure, the magnetic field often prevents the substrate from being bombarded by electrons generated at the target, thereby limiting the high heat effect of the substrate. In a system of magnetron-deposition, for the most part, the deposition rate is equal to the magnetron's DC power dissipated. The substantially higher rate of deposition is achieved by magnetron sputtering is also very desirable (as opposed to simple DC sputtering). For example, because of a high flux of target atoms than for impurity atoms or particles on the substrate, the impurity level is lower in the coated samples. In addition, a high rate of deposition results in the sputtering of magnetrons desirable for modern applications in the industry. (Kelly *et al.*, 2000). In RF sputtering technique the electrons, which are present in the space between the substrate and the target (inter-electrode space), the RF field does not get enough energy to induce ionization. But if we add a field of magnetic parallel to the RF field, the electrons will be limited without being negative to the flow, thereby enhancing the efficiency of the RF discharge. For RF sputtering, a magnetic field is therefore more necessary than in DC sputtering.

1.7.3 Main features of DC Magnetron Sputtering

- Strong sputtering rate due to the confining of the plasma near the surface of the target (G. Brauer *et al.*, 2010).
- Due to the increased path length of electrons within the plasma and preventing their escape, sputtering will take place at lower gas pressure.
- When magnetic field lines are parallel to the cathode surface, a high rate of material removal from the target occurs.
- In most magnetron targets, the target consumer is 30 percent.

1.7.4 Thin Film Preparation Process

The three key phases of any thin-film deposition process are (Lee *et al.*, 2009):

- Creation of the atomic, molecular and ionic species by thermal/electrons
- Transport of these atoms to the substrate through a vacuum medium
- Via nucleation and growth processes, condensation on the substrate takes place through electrochemical/chemical reaction to form a solid deposit and thin film formation.

1.8 Sputter Deposition Process

Sputtering is described as the expulsion of atoms from a solid surface because of energetic particle bombardment. The sputtering process is a momentum exchange phenomenon, in which the momentum of the incident atom is exchanged/transfer to the target material atoms. Sputtering forms a class of physical vapor deposition and finds a significant place in thin film deposition. Sputtering depends upon different variables like the nature of the projectile, its energy, the target nature, and so forth. The incident energy of the bombarding atoms determines the nature of the particular phenomenon. Figure 1.10 demonstrates the illustration of the sputtering system in the vacuum chamber. The gas is ionized and plasma is formed at the point where a high level of voltage is supplied to a pair of electrode terminals in lower gas pressure. The particles or ions in the plasma are extremely energetic and are positively charged and drawn to the cathode, causing the expulsion known as "sputtering" of cathode material to strike. (Chopra, KL 1969). For sputtering the most regularly used gas is

Argon since it provides large particles or ions to sputtering and being an inert gas it keeps away from any chemical reaction with the target.)

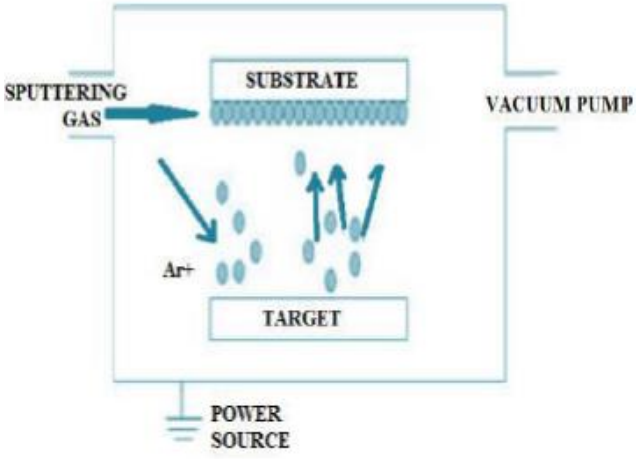

Figure 1.10 Schematic representation of Sputtering system

The following parameters influence the physical properties during magnetron sputtering of the deposited thin films and adjusting these parameters one can get a good quality of thin films.

Following are the parameters (Pelleg et al. 1991):

- Target current
- Target power
- The base pressure
- Working pressure
- Substrate temperature
- Bias voltage
- Target to substrate distance
- Deposition time etc.,

The target current specifies the deposition rate and, consequently, the time remaining for the arriving particles during either surface diffusion or agglomeration of the existing growth centres with other atoms during the production process. The goal voltage applied specifies the limit. Sputtered atomic or particle energy that can escape from the target material. The Pressure (P) in the vacuum chamber. The target to substrate distance (TSD) and pressure (P) can control the quantity of collision that happens for the atoms while in transit to the substrate. The bias voltage may be

applied to a substrate that has an effect on the substrate of accelerated electrons. Deposition time impacts the thickness of the deposited thin films. The target and substrate are parallel to each other. (Donald M Mattox, 1998), (Werner Kern & Klaus K Schuegraf , 2002).

1.8.1 Advantages

Magnetron sputtering is a deposition technique among all available PVD techniques, with carefully adjusting the energy and flow of sputtered atoms impinging and ions bombardment , the benefit of generating unique fine-grained and meta-stable structures with remarkable characteristics are obtained. Because it is easily scalable for commercial applications, magnetron sputtering is the most commonly utilized technique for industrial uses. Moreover, any material of any type can be utilized for sputtering purposes. The following are the main advantages of magnetron sputtering (G. Brauer *et al.*, 2010):

- Low plasma impedance at typical voltages about 500 V, with high discharge currents between 1 A and 100 A.
- Controlled Uniformity.
- Increased deposition rate, deposition rates vary from 1 nm/s to10 nm/s.
- Reduce wafer heating from electron bombardment.
- Lower thermal charge to a few percent coating uniformity, even for cathodes many meters long.
- Good Adhesion property.
- Well adherent, dense and easy to scale coatings.
- Evaluation has gained much attention during cost decode.
- Wide range of usable film materials (almost all compounds and metals), widely tunable film properties.
- It is easy, reliable and capable of meetings, the benefit of the technology
- The functional and economic requirements in industrial productions (M. Ohring , 2002) ; (J.Musil et al.,1999).

1.9 Sputtering Applications

In magnetron sputtering the material to be coated is bombarded with high energy ions ejected from a glow discharge. Through momentum transfer from the impinging ions to the material, atoms are being ejected or sputtered. These atoms pass through the discharge area and then deposit themselves on a substratum. In various areas of application, in notably in the fields of microeconomics and surface engineering, magnetron sputtering is actively and effectively utilised for film and coating production. (M. Ohring, 2002); (Musil *et al.*, 1999).

Following are the application areas of the thin film prepared by magnetron sputtering:

- DC Sputtering is commonly used to build microchip circuits at the molecular level in the semiconductor industry.
- It is employed for watch coatings, gold sputter jewelry and other decorative finishes, non-reflective optical and glass component coatings, as well as plastic metallic packaging.
- Physical vapor deposition (PVD) technology is used in many industrial sectors to produce thin coatings for various purposes, such as screens, solar cells, aerospace components ,antistatic coatings, microelectronics and infrared reflection, bearings in gas turbine, diesel engine parts or shaping equipment, etc. (Kelly *et al.*, 2000).
- In the manufacture of computer hard drives, one of the earliest widespread commercial applications of sputter deposition, which is still one of its most significant applications.
- In the semiconductor industry, sputtering is commonly used to develop thin films of different materials into integrated circuit manufacturing.
- Thin anti-reflection coating on the glass is often developed by sputtering for optical applications.
- Valve and valve gear coatings, connecting rods, bearings, hubs and other slipping and wearing surfaces, high corrosion resistance and strong oxidation resistance are used in automotive industry applications (M. Annunziata *et al.*, 2011).

CHAPTER 2
LITERATURE REVIEW

2.1 Boron Nitride thin films

Boron Nitride has been studied extensively in many studies due to its many superior properties such as high electrical resistivity, chemical inertness, and high thermal conductivity. In the general investigation, many parameters such as deposition rate, temperature and total flow rate have been examined to report their effects on the composition and crystalline structure of the material. In addition to the traditional CVD process studies, PECVD, LPCVD is also discussed in the literature. Due to simple parameter optimization, CVD is one of the best techniques to develop a pure form of boron nitride for the desired applications.(Aleixandre *et al*.,2000) investigated the response of ammonia gas and diborane mixtures in a hot-wall reactor on silicon substrates for chemical vapor deposition. The study was conducted with respect to the mechanism of deposition of boron nitride by CVD in a reactor at an elevated temperature and subsequently, effects of gas flow ratio and temperature (600-800^{o}C) on the formation were investigated. Reaction mechanisms have shown variation at different temperatures. At lower temperatures, an intermediate compound such as aminodiboraneis formed and at higher temperatures borazine is formed. However, the proposed mechanisms could not find kinetic data and expression rates. (Lee *et al*.,2009) developed boron nitride-based coatings from borazine by chemical vapor deposition (CVD) in a hot-wall chamber at a temperature range between 850 and 900^{o}C with a pressure of 1 kPa. As the carrier gas, N_2 was used. The layers were evenly deposited on the substrate at 900^{o}C and partly h-BN was ordered. The coatings also contained some N-H bonds at 800^{o}C. On the other hand, 900^{o}C is too high for borazine to fully decompose. As the temperature increases above 1400^{o}C, turbo-star boron nitride crystallization increases. By using the chemical vapor deposition process, (Aleixandre *et.al*. 2000) studied the effect of the rate of flow of diborane on the stability and boron nitride film's crystalline structure. The experiment performed in this analysis was at 800^{o}C and 267 Pa. Diborane (B_2H_6) and Ammonia (NH_3) that are diluted in hydrogen is the gas precursors (5 percent vol). On polished (100) silicon substrates, the film was deposited. The diborane flow rate has been concluded to influence the deposition rate. An unstable film has been found in a moist atmosphere

at low deposition. On the other hand, a more stable and uniform composition of the film was observed at a high deposition rate (high diborane flow rate).Using the CVD process, (Wang et al., 2014) examined the impact of feed speeds, temperature and pressure of ammonia gases and triethylboron on the rate of deposition and BN thin film characterization on the crystal of silicon substrate. The temperature range was 850-1100^{o}C and the ambient pressure was kept at 1 torr. As carrier gases, hydrogen and argon gases were included. The TEB partial pressure affects the deposition rate at atmospheric pressure with a power of 0.7. Owing to the rise in gas diffusivity, the deposition rate increases as the overall pressure decreases while the ammonia and TEB partial pressure remains constant. First, the rate of deposition rises to 1050^{o}C, then reduces with high temperatures. Also, XPS spectra indicated that the coating contains carbide. XRD analysis revealed that coating is turbostratic. (M. Ohring 2002) employed the DC arc jet CVD process with the gas mixture Ar-N2-BF3-H2, to deposit boron nitride coating on different substrates materials (Mo, W,Ni, Ti,Zr). The temperature of the substrates was 850-1150^{o}C in interval and pressure was kept at 50 Torr. It was found that the adhesion of BN film on W and Mo substrates was a low and pure cubic form of boron nitride film Raman peaks were observed. Due to the low W than Mo substrate reactivity, small amounts of borides were obtained on the W substratum at high temperatures. In comparison to other CVD techniques, ion bombardment produced greater stress in the coating when the production process was compared to other CVD techniques. (Ananthakumar *et al*. 2019) used the process of capacitive coupled rf discharge (CVD) to deposit BN on various materials such as Corning 7059 glass, fused silica, polished silicon crystal on both sides and silicon-coated with NiCr both on the cathode and electrode anode. Two different mixtures of gas have been used; B_2H_6 (1% v. in H2) -NH_3 and B_2H_6 (5% vol. in H_2) -N_2. As a result, the NH_3 precursor developed film on the anodic surface has very good adherence and not unscratched for B_2H_6 (1 percent v. in H_2). However, the film accumulated on the cathode surface was quickly scratched and atmospherically flaked. In addition, the cathodic film's stability is worse than that of anodic films, which is calculated by the use of optical and infrared transmission spectra. For the B_2H_6-N_2 gas precursor, the condition is the opposite. Properties and stability, therefore, rely primarily on gas mixtures and the location of the substrate (anodic or

cathodic). By producing defects, ion bombardment destroyed the film growth. (Freudenstein *et al*. 2011) researched the effects of the various mixtures of gas Ar-B2H6-N2 and Ar-B_2H_6-NH_3 on the formation of BN and aminoborane using RF as an energy source of capacitively coupled plasma. It had an RF strength of 75 W and a pressure of 0.6 torr. The coating was developed on a silicon wafer and the composition of the developed coating was calculated with the help of XPS analysis. As a consequence, the presence of ammonia in the gas mixture is observed to induce rich reactions in the gaseous phase and the formation of some amino boranes and BNs. On the other hand, there was no B-N absorption band observed in the plasma process when N_2 was present in the gas mixture. (Cheng *et al*.,2011) used LPCVD to analyze the impact of temperature and gas composition on the quantity and crystallize the degree of deposit. The kinetic deposition of the LPCVD BN output was analyzed. Gas mixtures of BCl_3-NH_3-H_2-Ar have been used as gas precursors. As a result, when NH3 is used in excess, deposition efficiency exceeds 99.8 percent. Turbostratic BN was deposited on the graphite wafer at 1000^{o}C and 1000 Pa. Turbostratic BN transforms into hexagonal BN after heat treatment above 1300^{o}C and the degree of crystallization improves. (Bello *et al*.,2015) researched h-BN film development on a plate of graphite by using a quartz cold-wall style reactor heated at reduced pressure by infrared radiation. The gas mixture of BBr3-NH_3-H_2 was used as a gas precursor, the NH_3/BBr_3 ratio remained constant at 3.0 and the pressure was estimated at 2, 4 and 8 kPa. Infrared spectroscopy and XRD determined the deposited film composition. Using SEM, surface morphology was seen. As a consequence, with increasing temperatures, the deposition rate reduces at a low rate of pressure. The increased temperature at 5 and 7 kPa induces gas-phase reactions and reactant degradation, thereby reducing the rate of deposition. Deposited films do not survive the atmosphere and become opaque after a few days. (X.W and Zhang, 2013) studied h-BN coating developed from borazine using a hot-wall reactor under atmospheric pressure on both SiBNC fiber and Si(100) wafers. Using SEM, XRD and FTIR, the characterization of the coatings was determined. It examined the effect of gas velocity, reactant concentration and temperature on the rate of deposition. As a result, at 1090^{o}C, the velocity of gas of 10.5 cm s^{-11} and 20 vol percent of concentration of ammonia was the maximum deposition intensity (plug flow assumption). Borazine

concentration has no effect on the rate of deposition in a range of 0.071 vol percent to 0.370 vol percent. Experiments with and without NH_3 have been performed. No h-BN coatings could be deposited without NH_3. In addition, SiBNC fibers have also successfully been protected.(Le *et al.*,2003) examined the pyrolytic decomposition of boron-nitride ammonia borane (H_3NBH_3). Thermal treatments (annealing) were carried out up to 1500^{o}C and H2 was the main gas product, using TPD-MSS to classify the gas composition. The film was investigated using FTIR-ATR and the result of boron nitride was analyzed using SAM, XRD, FESEM, TGA-MS, DSC in terms of composition, structure and morphology. Infrared vibrational spectra have been used to describe decomposition pathways.(Dalui R. and Pal A.R.,2008) investigated boron nitride film development on Si (100) substrate using the RF plasma CVD method at different substrate temperatures (400-600 K). As precursors, nitrogen borane-ammonia and argon gas mixtures were used. To evaluate c-BN and h-BN compositions, FTIR was used. It was observed that the composition of c-BN also enhanced by the increase in temperature. In this study, it is argued that the c-BN coating can be developed in a massive amount using inductively coupled plasma CVD although the traditional finding was that the CVD process results in less cubic BN phase in the coating.(Hirama *et al.*,2014) investigated BN coating deposition on graphite and die steel substrates with the help of RF plasma at a temperature between 550-620^{o}C. X-ray diffraction and Scanning electron microscopy were employed to characterize the composition. The coating was therefore mainly amorphous, but low quantities of h-BN were also detected. It analyzed the effects of reactor pressure and deposition time on the rate of growth. At 3 Torr, both graphite and die steel, the highest growth rate was seen. Growth rates on both die steel and graphite also increased with temperatures rising to 620^{o}C. (McKenzie *et al.*,2019) observed BN coating on quartz fibers by using dip-coating in urea and boric acid solution at 700^{o}C. To investigate the composition that showed polycrystalline h-BN properties, FTIR, XRD, HR-TEM, AND XPS spectra were used. Regulation of thickness was achieved by altering dip circles. In addition, after applying the heat process, the mechanism of the reactions was also analyzed using TGA, which measures weight changes. SEM was employed to analyze coating morphology, finding a smooth and uniform coating. During the analysis, coating thickness increased with the dipping circle and the

theoretical model of thickness was developed. (Li J and Zhang C.,2008) researched the CVD of borazine at 900-1150^{o}C on carbon fibers. The composition and structure of the BN coatings were investigated using FTIR spectroscopy, scanning electron microscopy (SEM), X-ray diffraction. The maximum rate of growth was 3.5μm/h at 1000^{o}C, according to experimental results, and the surface of the coating was loose and rough. The penetration of carbon elements was also observed from fibers to coating. It was found that control of deposition was done by the surface reaction below 1000^{o}C and the transition from mass transport control to surface reaction control was observed at 1000^{o}C in the growth mechanism. In the analysis, the crystalline rate of the coating improved with increased temperature and the presence of h-BN was observed above 1150^{o}C. Using the CVD process, (Hofsass *et al.*,2015) investigated fluffy production such as BN spheres for trimethoxyborane ($B(OMe)_3$) and ammonia catalysts support on BN sphere substrates. In this analysis, there were two phases. The action was to develop ammonia and trimethoxyborane sphere BN substrates at 1100^{o}C and then to generate sphere BN, ammonia flow was treated at 1500^{o}C. In the second level, in the presence of the same ammonia and trimethoxyborane precursors, spherical BN particles were used as substrates. In the second stage, the temperature range was 1100-1400^{o}C to produce fluffy BN-like. The TEM, X-ray diffractometer (XRD), IR spectrum and EM were used for characterization. Fluffy BN particles were developed to be used in applications supporting catalysts. In a double impinging-jet CVD reactor, (Litvinov *et al*., 2014) investigated hardness, morphology and chemical yield of β-rhombohedral boron carbide on tungsten substrates. In this research, FTIR was employed to study the chemical boron carbide yield, 13 percent of boron carbide chemical yield was observed, and with an increase in temperature, it can be increased. XRD analysis showed that without any other phase or impurities, the pure rhombohedral B4C phase can be obtained at 1300^{o}C. The highly symmetric crystalline structure of the product gives a high value of hardness of 5750 kg/mm^2.(Kim *et al*. 2013) researched boron CVD by reducing hydrogen BCl_3 in a parallel flow reactor on a hot tungsten substrate. To demonstrate the crystalline structure at varying temperatures, the impact of the substrate temperature (1100^{o}C- 1250^{o}C) on the rate of deposition of $BHCl_2$ and boron was investigated. It was found that alpha-rhombohedral boron can be obtained at

1100°C with large-sized crystals, sharp facets and β-rhombohedral boron with a small crystal of size can be developed at 1300°C. The comparison between the impinging jet reactor and the parallel flow reactor reveals that in the parallel flow method, there was a major mass transfer resistance that reduces the conversion of BCl_3 to boron.(Kiryukhantsev et al. 2010) examined the method of boron deposition in a dual impinging-jet reactor by hydrogen reduction of BCl_3. In order to obtain information on gas-phase kinetics and surface reaction kinetics, FTIR analysis was performed on the effluent gas mixture. As an intermediate product, the formation of BHCl2 was found. The experiments were performed in the 750°C-1350°C temperature range. The data collected suggested a shift in the mechanism of reaction at around 900°C. Boron formation can be noted as the decomposition of BCl_3 without the reduction of hydrogen at higher temperatures. (Kelly *et al.*,2000) researched the boron carbide formation in a dual-impinging jet reactor on tungsten substrates of BCl_3, H_2 and CH_4. The experimental data showed that during the formation of boron carbide, $BHCl_2$ and β-rhombohedral B_4C was formed as an intermediate product. The conversion of B_4C was calculated by the molar ratio of BCl_3/CH_4, and the conversion rate increased by the molar ratio. The B4C formation rate of reaction was proportional to the 1.85 concentration power of BCl_3. (Bewilogua K *et al.*, 2004) researched the ammonia-based development of boron nitride nanotubes and a powder blend of iron oxide and boron in a tubular reactor.The analysis of XRD revealed that at different temperatures and gas composition, h-BN and iron boride, iron, boron oxide and rhombohedral boron nitride were observed in the substrate. For the outlet gas chemical analysis, a mass spectrometer (MS) was used. MS findings showed that the decomposition of ammonia was the only gas-phase reaction. TEM and SEM images demonstrated the development of BNNTs in the substrate.

2.2 Parameters affecting sputtering

Various parameters that influence the process of deposition include sputtering, such as gas pressure during sputtering, base vacuum, sputter strength, the temperature of the substrate and target etc. The interplay of the above parameters results in the film microstructure or and its consistency, which accounts for surface impurity, adhesion, roughness, and film density created by the sputtering (Yamamoto K *et al.*, 2000). Such

a large number of parameters make the process complicated, but if configured correctly, it also offers a great deal of influence over the method of film growth. The geometry of the deposition, which is the relative position of the substrate and the target, also plays a significant role, apart from the above parameters, which influences the growth process of the thin film. Below are some of the significant variables that are important for sputtering.

2.2.1 Base Vacuum

The chemical purity of evaporated films varies depending on the type and the degree of impurities originally existing in or contaminated from supporting materials during a deposition in the sputtering chamber. It can also arise in the vacuum system from the residual gases present. Therefore, before thin film deposition, it is important to attain an optimum base vacuum. The sputtering device is often thoroughly baked to improve the base vacuum.

2.2.2 Target substrate geometry

A significant element affecting the overall uniformity of the film is the target-substrate geometry. It includes the orientation and the distance of the source and substrate. In sputtering, electrons are often released from the target the bombardment of ions, apart from target atoms, and these are propelled towards the substrate, where gas atoms collide with electrons. These electrons aid to preserve the plasma by the induction of ionisation, since ionised gas atoms bombard the target of secondary electrons. In case the gas pressure is too low or the distance between the cathode and the anode is too short, the secondary electrons will not suffer sufficient ionizing collisions until the surface of the substrate is struck. On the other hand, inelastic collisions slow down the generated ions when they contact a target and hence do not provide enough energy to produce enough secondary electrons when they impact a target (Deng J *et al*., 2000) Therefore, for better deposition, the substrate and target space has to be optimized. Since sputtering is a line of sight deposition, it can also result in a uniform deposition over a region of substrate rotation.

2.2.3 Sputtering gas pressure

The deposition on the substrate of the target atoms depends on its surface binding energy (Ye J. *et al.*, 2009). The rate of deposition of the film also relies on the pressure and strength of sputtering. The mean-free electron between collisions is high at low pressures. Ionization efficiencies are therefore low, and it is not possible to maintain self-sustained discharges below a certain pressure range (~10-4 mbar). The electron medium-free path decreases, the ions are produced and the current stream increases with the pressure at a fixed voltage. If the pressures are too high then the sputtered atoms are subjected to the increased collision, so they are dispersed to the substratum and are not deposited efficiently (Jiang L *et al*, 2012). An acceptable pressure should therefore be placed on the maximum deposition rate attainable. A standard deposition rate/speed efficiency compared to the residual gas pressure is shown in Fig.2.1. With magnetic sputtering the number of Ar ions can be increased with no additional number of Ar neutrals so that 15 to 10^{-3} mbar can be operated.

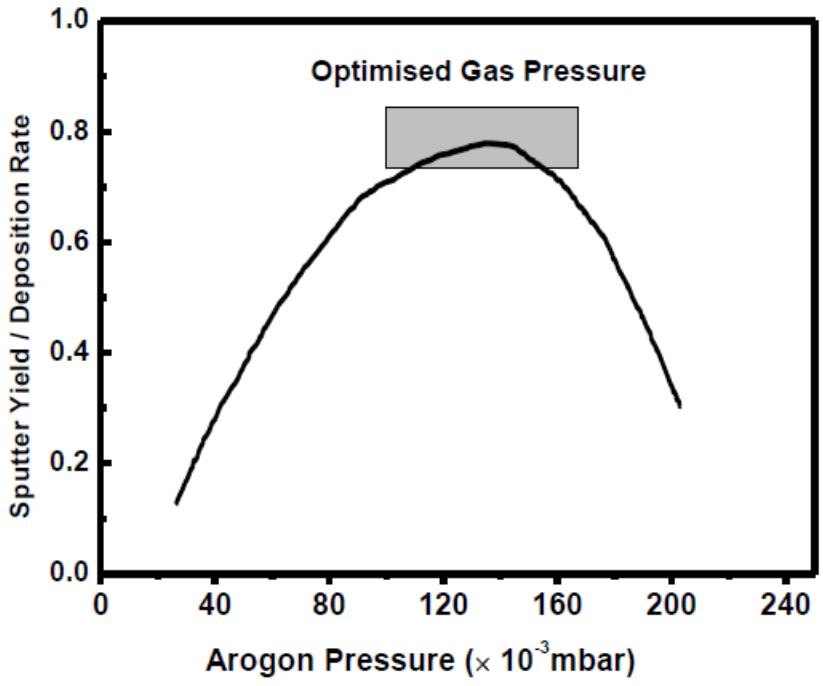

Figure 2.1: Sputter Yield/ Deposition rate as a function of sputter gas pressure (Ar Target/Substrate Temperature) (Jian *et al*,2012)

Sputtering is a low-temperature operation, and the sputtered particles and secondary electrons are expelled in a small fraction (~1 percent) of the total energy applied. The ions that hit the cathode dissipate a considerable amount of energy and warm up the cathode. Temperature increase depends on the conditions of sputtering. Although the yield of sputters increases with temperature, it should not exceed a tolerable threshold that can cause gas problems. The temperature of the substratum also influences the characteristics of thin films, such as adhesion, surface rugging uniformity, etc. The temperature of substrates is thus also an important parameter for the deposition of thin coatings, which may differ for individual films.

2.3 Boron nitride synthesis techniques

To date, the synthesis method of high temperature –high pressure (HPHT) is the only way to grow a single crystal c-BN. The cubic form of boron nitride in a high-pressure cell is normally made of h-BN powder as the starting material that comes into contact with a fluxing precursor (Keunecke M *et al.,* 2016). Many researchers, including alkaline metals, alkaline earth metals and other metal alloys, as well as oxides, nitrides and fluorides, have been using many types of Catalysts content. The obtained crystals typically are small in size and are usually amber to yellow since the precursor material contains them (submicron of approx.1 mm diameter). Recently, Taniguchi and colleagues have been able to synthesize c-BN crystals with a thickness between 1 mm and 3 mm, transparent and colorful (H.Oechsner,2006). In addition, they achieve high optical transmission and a low impurity by the use of a particular Ba-BN solvent method. (Wiemann E *et al*.,2016).The fact of the stable modification to BN under standard conditions, has led to a search for a way of c-BN rising directly from the vapor phase in a low pressure, near the balancing process. Until now, attempts have remained unsuccessful to form c-BN through the use of "classical" chemical vapors (CVD). In c-BN synthesis studies, either phase characteristics have been carried out by inadequate numbers of additional methods or data from the characterization contain anomalies or inconsistencies. In addition, none of the submitted experiments could be replicated. Consequently, there is no low pressure process allowing c-BN film to form pure and well crystallized with CVD methods. This is, however, very easily manufactured in different substrates using pure polycrystalline, adhesive

diamond coating and thick free-standing layers. (Setsuhara Y *et al.*,2019) This seems surprising, considering that diamonds are the normal metastable carbon change, and graphite is stable. In the boron case. Nitride is a stable cubic phase and metastable h-BN. However, the metastable h-BN forms are still metastable in normal and low pressure experiments. Bohr and colleagues gave a qualitative reason for this conduct (Boh *et al.*,2005) By referring to the two scientific principles that are general thumb rules for the kinetic behavior of chemical reactions, Ostwald and Ostwald-Volmer. The Ostwald rule notes that withdrawing energy from a system with many states of energy does not directly bring about the stable ground, but instead passes through all intermediate metastable states gradually. The rule of Ostwald-Volmer noted that the least dense stage first comes into being. If the law between Ostwald and Volmer contradicts one another, it takes precedence over the rule of Ostwald. The diamond/graphite system has succeeded in implementing both laws. The graphite process is typically produced during a daily CVD in a gas atmosphere that carries a carbon precursor such as carbon dioxide or methane. Although the rule of Ostwald predicts the development of the metastable diamond phase and this behavior coincides with the stronger rule of Ostwald-Volmer that says the less dense phase, that is the graphite, is first nucleated. So the Ostwald-Volmer rule must be removed in order to grow diamond films. This is normally achieved with the help of atomic hydrogen addition to the gas phase, which stabilizes the diamond surface growth areas permanently and thus prevents the growth of graphite by preventing the formation of sp^2 bonds. (I. Konyashin *et al*., 2009). The rule of Ostwald then becomes prominent and the diamond nucleates to metastable, which can develop into pure crystals of diamond. The development of h-BN in the CVD technique is a function of both rules for the boron nitride system. The Ostwald rules predict the production of h-BN and the less dense h-BN phase is first nucleated according to the Ostwald-Volmer law. Both laws must therefore be circumvented to generate c-BN in the gas phase directly. Seeding c-BN is one way that h-favored BN's nucleation can be solved and c-BN development begins. Also, the continued growth of the stable c-BN phase requires a high movement of atoms N and B sufficient atomic fixation kinetics to produce pure and large crystals of c-BN (A. Bartl *et al*.,2006). Higher temperatures could be used as a mobility means, but the temperature always needs to be within the thermodynamics.

Atmospheric pressure c-BN stability regime. In the CVD-synthesis of c-BN, more complications are anticipated since BN is a binary compound. Care should be taken to preserve the stoichiometry of BN during a deposition in order to prevent a relative loss of solid nitrogen.Strong deposition of chemical vapor. The work of Matsumoto and Zhang has recently made considerable progress in the production of c-BN thin films. Using an Ar-N2-BF3-H2 blend plasma jet and biased substratums.Microwave CVD plasma and DC plasma jet process can produce up to 20 μm thick c-BN films at 0.3μ m/min.(figure 2.2) (S. Matsumoto and W. Zhang, 2000). The thin films were deposited with a high purity of process, c-BN.

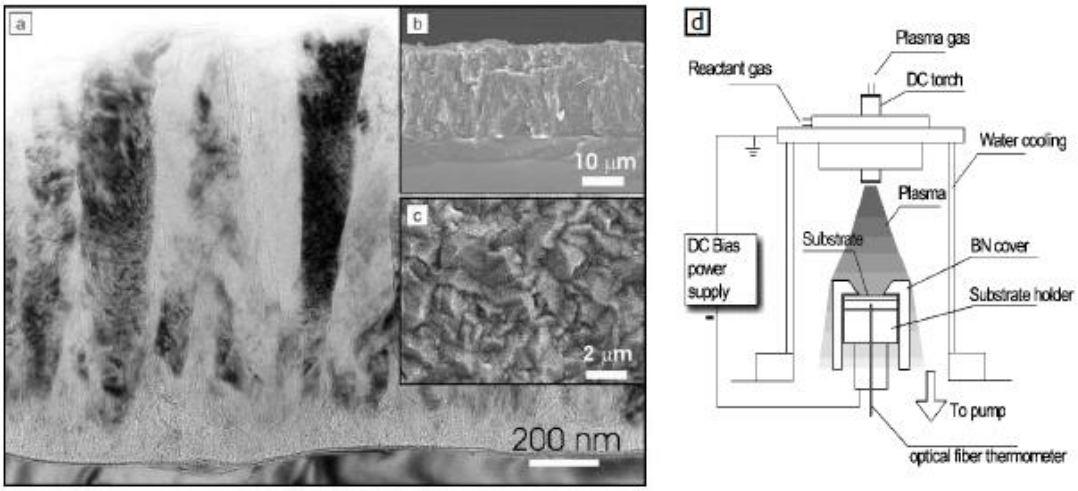

Fig.2.2 SEM cross-sectional (a,b) and plan-view (c) images of c-BN thin films deposited with DC plasma-jet CVD process. (d) DC jet plasma chemical vapor deposition reactor.

It was observed that the columns grew and each column was almost a single crystal with a side up to 0.54 μm in size and a film thickness of length. However, a lot of defects were found within the crystals, including stacking failures and twins. The films, however, displayed a strong substrate adhesion due to very little stress values of approximately 1 to 2 GPa and these values are substantially less than the 4-20 GPa values usually seen in c-BN films (P.B. Mirkarimi *et al.*,1997) Although Matsumoto's and Zhang's depositional conditions are similar to diamond CVD's, the differences to a "classical" CVD method continue to be striking. Three factors have been identified as crucial for c-BN deposition: I fluorine gas use, (ii) negative bias in substrates and

(iii) high plasma density (S. Matsumoto and W.J. Zhang, 2001). Fluorine usage was considered crucial for c-BN growth and no cubic phase formation was achieved by substituting BF_3 with B_2H_6 and BCl_3. Also, no c BN deposition occurred with fluorine, but the substratum was an etched little bit when no bias voltage was applied. That implies that the formation of the sp^3 ties, a similar feature to that of PVD methods, should involve ion bombardment caused by substrate bias. Since Fluorine effectively etches BN is well known from several studies (W. Kalss *et al.,* 2008) Zhang and Matsumoto proposed the predominant position of fluorine in c-BN formation by etching h-BN preferentially (N. Deyneka *et a*l.,2003) In addition, not only the amount of fluorine in the gas phase but also the hydrogen/fluorine ratio was found essential for c-BN development. The following reaction is preferred when hydrogen is added to the reactant gas (W.J. Zhang *et a*l.,2004).

$$2BF_3+N_2+3H_2\rightarrow 2BN+6HF$$

With the rise of H_2, the sum of BN is calculated to increase. Furthermore, HF output decreases fluorine etching of the BN due to HF stability (H. Feldermann,2002) Therefore, hydrogen flow rates regulate solid BN formation during the gas stage, and the hydrogen/fluorine ratio maintains the balance between formation and grafting. It is therefore concluded. The bisection of the sustratum will then be required to balance fluorine with hydrogen, leading to etching, and growth of c-BN and h-BN phases (H. Feldermann,2002). The experiments carried out by (N. Deyneka *et al.*,2003) further support this assumption (W.J. Zhang et al.,2004), who deposited c-BN thin films with plasma-enhanced chemical vapor deposition on the diamond substrate (PECVD). Also bias voltages as small as -20V (unlike -40V necessary for c-BN silicones to develop in the same way), was able to produce good quality c-BN thin films, and indicated that ion bombardment is needed to break down B-F bonding to allow for more B-N bonding. In brief, c-BN growth has not already been achieved in the thermal CVD phase. Although a process that Matsumoto and Zhang introduced is capable of rendering c-BN film near-stress, dense and adhesive, it does have some problems such as the need for extremely high deposition temperatures (T 1100^oC). Boron nitride thin films are available with different synthesis techniques of PVD (physical vapor deposition). The substrate should be heated during the deposition process (usually to some 100^oC) to form a cubic phase, while the rising film should be irradiated

simultaneously with high energy particles. The synthesis methods, therefore, vary mainly from N and B sources and how energetic particle bombardment is carried out. The film is normally irradiated by high energy ions, but c-BN film growth has been shown that energetic neutrals are often used instead of ions (Ming Lu *et al.*,2014). The simplistic pattern representation of the two fundamental processes typical for c-BN thin-film development is shown in Figure 2.3: plasma-assisted and ion-assisted deposition.

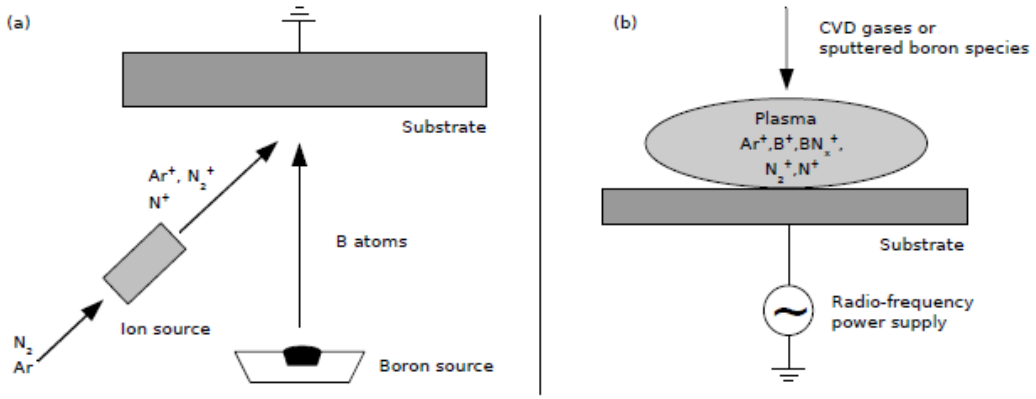

Fig.2.3 Schematic diagram of (a) an ion-assisted deposition process, (b) Plasma-assisted process.(Mir 2005)

Plasma-assisted processes use an extremely densely vacuum plasma source and a low gas processing pressure..In this process plasma can be formed with several sources, e.g. PACVD, gaseous boron-containing processes, such as borazine or diborane, as a plasma source, plasma can be generated. The material is also sputtered in PVD-like processes, boron-containing targets such as BN , B_4C , $AlMgB_{14}$, FeB, TiB_2, CrB_2 , as well as various types of hexaborides such as YB_6,LaB6, SmB_6, CeB_6 either by employing direct current (d.c.) or radiofrequency (r.f.) magnetron sputtering. In DC sputtering only targets like B_4C can be implemented, but typically with a higher growth rate as opposed to RF sputtering. However, the latter operates with pure B or h-BN targets. This method has in the past been generalized and updated to boost the start of c-BN nucleation, e.g. by adding negative bias stress in a sample in some cases (S. Matsumoto and W.J. Zhang,2001). In addition, using magnetic fields will increase ion flux, which means that the repository rate is greater, and the plasma has been extended by both uneven magnetron sputter and traditional magnetron sources along with external coils or magnets. In ion-assisted processes, either electron beam

evaporation (IBAD), laser ablation (PLD), or the sputtering of a beam by a solid h-BN or B target are given by the boron-containing species. (figure1.5a). Then, thermal energy is put onto the substratum with boron atoms and/or BN molecules. At the same time, various noble gases such as nitrogen ions with typical energies of some 100 eV are bombarding this growing film. Thus, the resulting process is very intricate and various effects, such as thermal desorption and condensation, ion implantation, surface deposit recoiling and sputtering, must be taken into account. Moreover, it is difficult to interpret the data obtained in the current c-BN growth templates because the substratum is irradiated not only by ions (with specified energy) but also by the molecules, neutral atoms and clusters. Such are the problems for a particular type of PVD process, namely the deposition of mass-separated ion beams. Unlike other PVD techniques, thin films are only prepared under ultra-high vacuum (UHV) conditions by deposition of alternative energetic N+ and B+ ions cycles. (H. Hofs¨ass *et al*.,2015) The parameters of the deposition, in this case, are clearly defined and independently controllable, including ion energy, the temperature of the substrate and ion stream ratio of different ion species. In comparison to the IBAD, nitrogen and boron are either stored as neutral atoms or molecules with no individual charged energy ions and no noble gas or any other ion. Figure 2.4 Schematic representation of the MSIBD process.

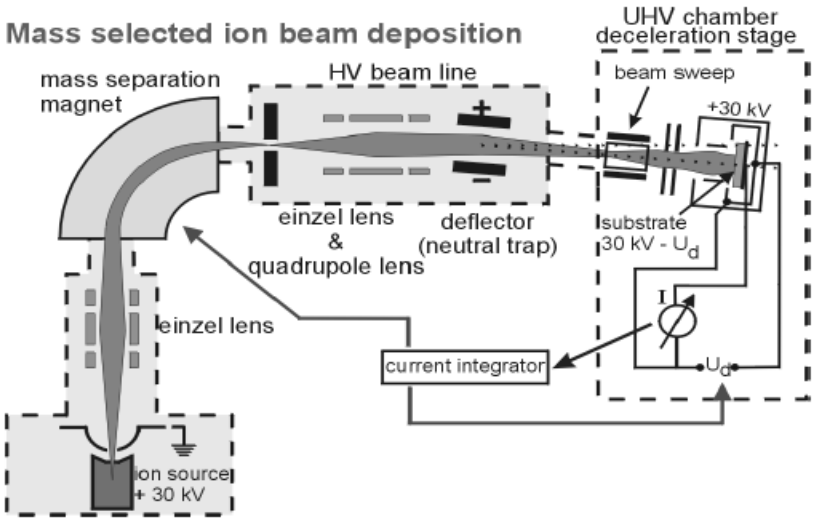

Figure 2.4: Schematic diagram of the mass separated ion beam deposition technique (Hofsass *et al*,1994)

The ions are produced from a source of ion of the Sidenius kind, accelerated to a magnet mass of 30 KeV. The isotopically pure ion beam then led to the chamber where deposition takes place and it reduces the energies of the ions from 10 eV to 50 keV. The quantity of the ions deposited is precisely measured in a suitable ion source and accelerated to high energy for the formation of a strong radius of magnetic mass. It is then directed to the chamber of deposition where the ions are slowed to energy between 10 eV and various keV which affect the heatable substratum. By calculating ion load, the volume of stored ions can be precisely calculated. MSIBD is the perfect method for studying the effect of deposition parameters on c-BN growth through this relatively simple deposition technique. Its deposition rate is however only about 10 nm/h, making it almost impossible for industrial applications.

2.4 Boron Nitride Film

In thin film applications and ion implantation, boron is commonly used. Boron ions, for instance, are used to dop semiconductors ion-bonding, surface alteration by ion implantation, films containing boron and boron nitride coatings are synthesized and particle detectors are trench-filled. Coatings based on boron can considerably enhance the surface characteristics of substrate for a broad range of applications, provided that

they are highly hard, tough, resistant to corrosion and resistant to wear. The use of h-BN as a protective coating, gating insulators, in metal- insulating semi-conductive field transistor, as a streaming source and as a film voltage /varistor is important in electronics. Boron-nitride films have big application potential in the electronics industries. Even transparent materials for X-ray lithography protective coverings and masks may also be used as cubic boron nitride film (Jiang L. *et al.*,2012). Moreover, for many industries of metalworking, the production of c-BN coating is of great relevance for instruments, combining the benefits of cutting material and c-BN coating particularly when the diamond reactivity renders this unsuitable. Thin films that form a group of composite materials are increasingly used in machine optics, electronics and manufacturing industries. The main tasks of coatings are to improve the mechanical properties like hardness, elastic module, corrosion resistance and, above all, reduce wear and friction . Boron nitride is one of the most promising materials for this purpose that best fits all the above criteria. Industrial needs such as component lifespan extension, energy savings, cost reduction, and performance enhancement are driving the development of new and unique protective coatings with high hardness, high wear resistance, and extra functionalities. Many materials have been utilised as protective coatings in many sectors, including diamond, transition metal nitrides and carbides, and DLC, but there are still many issues to be resolved. Because of its higher temperature stability, stronger oxidation resistance, and lower reactivity with iron, c-BN outperforms diamond in high temperature wear applications. Because a protective layer of B_2O_3 is generated by interaction with the oxygen in the air, c-BN has a significantly better resistance to oxidation in air up to 1200 °C than diamond. This layer protects c-BN from further oxidation. As a result, c-BN is mostly utilised for steel processing, whereas diamond is favoured for stone, ceramics, and Al-alloys processing (Vel L, Demazeau *et al.*,1991). Boron nitride is a chemical inorganic compound consisting of the same number of boron and nitrogen atoms and isostructural and carbon isoelectronic. BN forms strong, diamond-like, sp3-bound phases, graphite-like, carbon-like, bonding sp^2 phases. The most stable phases and common phases are hard cubic boron nitride (c-BN) and soft hexagonal boron nitride (h-BN) phases (Audronis M *et al.*,2015). All phases of boron nitride compounds have several common properties such as a high level of chemical and thermal stability, high

resistance to corrosion, low solubility in most common acids and water. In contrast to diamonds, there is no reaction between BN phases and ferrous metals below 1500^{o}C. Also, there are stark differences between sp^2 and sp^3 hybridization phases. Sp^2 phases, like rBN, hBN, are very soft and have graphite-like lubrication capabilities (Neo K.-S *et al*.,2013). The hexagonal phase of boron nitride has possessed superior lubrication properties at both low and high temperatures (in the presence of oxidizing atmosphere up to 900^{o}C). Because of its structural arrangements (weak between layers and strong bonds within the layers), hBN has anisotropic characteristics, such as thermal expansion and conductivity. On the other hand, the Cubic Boron Nitride has possessed a covalence- ionic structure that results in an extremely hard phase (second only to diamonds). It has high wear resistance and a low friction coefficient. Furthermore, the layered nanocomposites consisting of soft hBN and hard cBN phases with good lubrication properties are most suitable for covering bearing surfaces. The Wurtzitic boron nitride phase with c-BN like hardness has lower thermodynamic stability but it also possessed a tendency to become a stable h-BN phase.Boron Nitride coatings are deposited on silicone substrates most frequently due to the highest content of the c-BN phase has been observed on covalent and hard substrates such as sintered carbides, diamond, SiC, Si. Cubic boron nitride study (c-BN) over the last 10 years has made considerable progress. Today, the high temperature and pressure (HPHT) and many PVD techniques can be used to synthesize both the c-BN single crystals and thin filters, respectively (X. Yang *et al.*,2009). The films deposited typically have a reasonably high level of defect density, like cereal limits, dislodges, pillage defects, and impurities. In addition, cubic boron nitride-based thin films are also affected by high pressure, leading to the disintegration of the film and the delaminating of the substratum at thicknesses over 100 nanometers. The problem of reducing pressure and developing adequate low-pressure synthesis methods that can create films that are enough dense, attaching, and stress-free has been put to a great deal of effort. Many techniques for deposition have been used in the production of c-BN films. It is shown that ion bombardment for the cubic phase is absolutely important. Every attempt to directly expand cubic boron nitride from the gas stage has so far failed. Therefore, the growth of c-BN is not thermodynamically balanced and the effect of the bombardment is the subject of active study. Nevertheless, the basic

mechanisms involved are still not adequately described. Thin BN coating on relatively softer metals such as Ag and Al results in substantially less cubic phase content than those on hard metal substrates (Ni,Nb, Ta,) . In many publications, the authors point out that it is difficult to obtain hard coatings with good adhesion if deposited directly on steel. The possibility of soft, hard or stable phases of boron nitride on stainless, high - speed, bearing steels with very good tribological properties is described in a few papers .(Sokolowski *et al.*2016) recorded first of all the development of thin c-BN films with low temperature and pressure in 1979. There have been great efforts to produce c-BN thin films using the gaseous phase. In the early 90s, low-pressure and temperature deposition methods for c-BN film preparation were developed by various laboratories. C-BN prepared by physical vapor deposition and chemical vapor deposition were the processes adopted by these researchers. The most popular methods of CVD are plasma-based chemical vapor deposition, CVD plasma coupling induction coupling (ICP), CVD assisted plasma cyclotron ECR, and CVD enhanced plasma microwave (E. Weißmantel *et al*.,2002) For deposition in C-BN films, c-BN films are used with PVD techniques such as ion-assistant evaporation e-beam (K. Teii *et al*.,2015) pulsed laser ion deposition, RF and DC magnetron sputtering. The c-BN jet of plasma output CVD and plasma microwave CVD with Ar-N_2-BF_3-H_2 gas were reported to Matsumoto and Zhang. In comparison to other PVD-like CVD-assisted plasma procedures, fluorine ions and a high gas pressure of approximately 6.67, 10-2 mBB are the obvious characteristic benefits of the plasma jet. Owing to the dispersion mechanism in the gas phase, the energy of ions entering the foil surface must be greatly decreased. Low-processing gas pressure, high plasma density and higher vacuum conditions are used for processes like CVD plasma-assisted (A. Werbowy *et al*.,2000). The substratum is normally twisted to remove ions from plasma several hundred eV. Plasma may be made from a variety of source materials, e.g. the use of GB-containing methods such as borazine or diborane as plasma sources, through plasma-assisted chemical vapor deposition (PACVD). The content is also generated by the sputtering of a B, BN, or B_4C target by the use of either RF or direct current in PVD-like processes. Direct current sputtering is only feasible with targets such as B_4C, but typically comes with a higher rate of growth than RF sputtering. However, the latter deals with isolated objectives such as h-BN or pure B. This procedure has in

the past been expanded and revised to boost the onset of the c-BN nuclide, e.g. when a negatively biased voltage is used for the sample (I. Bello *et al.*,2005). The application of magnetic fields also allows for increased deposition by increasing the flux of ions. The rate has been used to expand plasma both unbalanced magnetron sputter sources and traditional magnetron sources in conjunction with external magnets or spools. Boron-containing species, in ion-assisted processes, are produced by electrons, laser ablation and ion beam sputtering (IBS) of a solid B or h-BN targets. Then, thermal energy is put onto the substratum with boron atoms and/or BN molecules. At the same time, the increasing film is being bombarded with standard energies of several hundred eV, with nitrogen and noble gas ions. Therefore, the growth process is very complex and various effects must be taken into accounts, such as thermal desorption, condensation and ion implantation, recoil implantation of the atoms inserted on the surface and reconstitution. Furthermore, it is difficult to interpret the data obtained within the c-BN growth model since the substratum is irradiated not only with ions but also with clusters, molecules and neutral atoms. These are issues for a particular type of PVD process, namely the deposition of mass-separated ion beams (MSIBD). Thin film is prepared only in ultra-high vacuum (UHV) conditions (B. Wang *et al.*, 2014) in comparison with all other PVD techniques by the deposition of alternating energy cycles N+ and B+ ions. The ion energy, ion flow rate of various ion and substrate temperature parameters are, in this situation, well described and independently controllable deposition parameters. In contrast to IBAD, both boron and nitrogen deposited into a suitable ion source are separately loaded energy ions and no noble gas, molecules or neutral atoms. The ions are accelerated to a high energy level, producing a powerful beam and magnetically separating mass. By calculating the ion charge, the number of deposited ions can be measured accurately (F. Xu *et al.*,2014). MSIBD is the perfect method to investigate the effect of deposition parameters on c-the growth of BN through this relatively simple phase of deposition. Their deposition rate only amounts to some ten times nm/h, rendering industrial use almost impossible. A successful deposition is presented in cubic nitride films synthesized through the sputtering of RF magnetrons. To detail the process of growth of such a highly stable material, several models were proposed to explain. (Reinke *et al*. 2014) proposed a model that is based on the assumption that

c-BN sputter yields were observed to be less than h-BN and also c-BN deposition occurs immediately in a sputtering zone. However, the h-BN growth at high ion present densities recorded by several researchers cannot be explicated in this model. (Bewilogua *et al*.2016) and (Yoshida, 2006) have also attempted RF bias sputtering, by adding a bias to the substrate to maximize the bombardment of ions. There is interference dephasing in RF bias sputtering method between the substrate electrodes and RF power sources. This may cause the energy distribution of charged particles to be distracted and can moderate film deposition supported by electrons or ions. Although the ion-assisted methods have performed well for the above-mentioned groups, some researchers report a non-cubic phase of BN adjacent to the substratum and c-BN (H. Yang *et al*.,2011) deposition. Therefore, to boost the c-BN growth a better observation of the process of deposition is required. Particularly for c-BN films deposited by different techniques, there remain significant difficulties in intricate stress and adhesion to the substrate. For the fruitful exploitation of this technically imported ant stuff, the most advantageous technology route has yet to emerge. One common feature of all methods of PVD for the development of c-BN thin-film is the need for ion bombardment at a low-energy level during the growth of the film, leading to the view that the formation of the cubic nitride phase involves direct or indirect ion-sound interaction. This is expressed in various supplantation-based growth models (H.S. Kim *et al*.,2011), c-BN phase formation induced by stress and c-BN growth induced by thermal spike. Based on a comprehensive collection of experimental data compiled, for example, by (Mirkarimi et al.2004) and recently by (Kulisch *et al*. 2009), it has been possible to develop a window of experimental parameters for c-BN film development. Certain parameters were found to be critical for the developed phase during PVD of thin boron nitride : ion energy - linked to the applied energy; ion mass - connected to the gas mixture and pressure of the gas during deposition, which is capable of regulating the stoichiometry of films sprayed from a target; Substrate biasing – R.F or DC added to or sustaining on the substratum in a substratum that has the impact of the electrons or ions being accelerated; deposition pressure, substrate distance, target, number of collisions takes place from the target to the substrate path. The temperature of the substrate can have a major effect on the growth behaving of the crystalline or sample density. However, these criteria are not

separate. This parameter can be used to estimate the important parameters of deposition to determine c-BN growth for various techniques of growth. The dynamic transfer criterion might not, however, be true for low ion energy.

2.5 Cubic boron nitride: properties and applications

In 1957 the physical chemist Robert H. Wentorf of General Electric Company first developed cubic boron nitride (c-BN) just after two years of the synthesis of artificial diamonds first time (Bun et al.,1955). Cubic boron nitride was made from h-BN under the conditions of high temperature and high pressure (HTHP), analogous to the manufacture of diamond crystals. For c-BN and diamond, the process of synthesis is not only similar: c-BN is sometimes referred to as "the better diamond," mainly because both materials share such extreme characteristics. Although in some instances c-BN outclass the diamond. It is the second hardest material after diamond with Vickers hardness of approximately 50-70 GPa. However, the chemical inertness and thermal stability of c-BN are much higher. Diamond readily reacts at temperatures above 1000 C with iron, cobalt and nickel or is subject to oxidation at T > 800 C, resulting in the diamond surface being disintegrated into gaseous CO_2. By comparison, c-BN, for temperatures of up to 1800^oC, is chemically inert from iron group metals, and its high stability against oxidation is the product of liquid or solid B2O3 forming, which protects the surface against further oxidation (A. Bartl *et al.*,1996). C-BN is therefore a promising material for machinery and cutting devices with a wearing resistance to corrosion, particularly in cases in which the diamond reactivity does not make this necessary. In light of electronic applications, the cubic form of boron nitride also superior to diamonds. The thermal conduciveness of the second-highest at room temperature after diamond (2-13W/cm/K) is not only strong in band-gap (Eg = 6.4eV), yet it can also easily be doped for p-type- and n-type conductivities (O. Mishima *et al.*,1990), contrary to diamond. By using this property, Nishima and co-workers created a high-temperature p-n joint diode and an ultraviolet p-n joint based on c-BN HPHT content. The majority of industrial applications, however, are not feasible, primarily because there are a very high impurity concentration and defect density of the c-BN crystals. From the late 1980s, interest in c-BN has increased tremendously, primarily due to the reason that c-BN films can be synthesized on a routine basis by employing ion beam assisted methods of deposition.

c-BN films were thoroughly deposited with a wide range of physical and chemical deposition techniques, and ion bombardment was found to be necessary to develop the cubic phase. Various attempts at c-BN growth have failed so far only through chemical processes. Thus, ion bombing plays a major role in the development of cubic BN is widely agreed upon. Designs were developed to investigate the impact of the beam of ions on c-BN growth but the mechanisms leading to the production of c-BN remain unclear. The fact that the structure of the film consists of a standard laying of a sequence of cubic and hexagonal stages (A. Lousa *et al*., 2000) is very complex is that cubic BN does not typically ever have a direct link with the substrates, but is followed by Sp^2 thin layer -linked BN. Recently, the heteroepitaxial c-BN growth in some substrates was not possible (W.J. Zhang *et al*., 2004). The synthesis of highly crystalline phase-pure c-BN films was not completed until now, because epitaxial growth has proven very difficult. The optical and electronic characteristics of c-BN thin films, therefore, have not been well studied. The developed c-BN thin films typically are nanocrystalline in shape and display a great compressive ion-bombardment strain equivalent to 25 GPa (D.R. McKenzie *et al*.,2013)), causing the film to be damaged by delamination over a few hundredths of a nanometer in thickness. The intrinsic stress has suffered greatly because, in view of tribological applications, the film's thickness limit is a serious issue. Nevertheless, c-BN films have been successfully used in micro-electronics and x-ray lithographic masks as passivation, isolating and low-dielectric-constant layers/coats (D.R. Cote *et al*.,2005). In addition, cutting tools and abrasive components were developed using c-BN, particularly for low carbon ferrous metals. The instruments are similar to diamond tools in this application but can be applied without a chance of reaction on low carbon alloys or iron. Cubic boron nitride is also used in installations where a high level of thermal conductivity provides for the effective dissipation of heat of high power and density electronic components. While enormous improvement has been observed in recent years, it is still important to have a better knowledge of the basic mechanisms resulting in the creation of c-BN film. To develop suitable procedures for deposition at low-pressure that are capable of preparing sufficiently dense, stress-free and adherent films. The category of superhard diamond-like materials is also known as cubic boron nitrideSuperhard means materials whose hardness exceeds 40 GPa by

definition (S. Veprek and J. Vac 1999). When characterizing hard materials, the Vickers method is used very often; in general, the indentation left by a diamond stylus is determined and then the hardness is indicated by the ratio of load applied to the indenter impression. It is possible to distinguish superhard materials into intrinsic and extrinsic (such as diamond or c-BN) materials (materials based on nanocomposite or superlattices). Its hardness is derived solely from its atomic scale features, while extrinsically hard materials reduce plastic deformation by avoiding the leading mechanisms. Dislocations and micro-crack growth movement and multiplication. Moreover, quite recently (Solozhenko *et al* 2016) reported that their Vickers 76 GPa ,cubic BC_2N was synthesized, which was even bigger than that of c-BN. The definition shows already: all super-hard materials consist of either nitrogen, boron or carbon (see figure 1.1). Because of their validity or oxidation, only certain elements may form a three-dimensional arrangement of directional links, and they are mostly covalent links and show high bond energy due to the high electron density between the atoms. This comment has resulted in a semi empirical formula for the B [GPA] bulk Module of strictly covalent and partly covalent/ionic compounds consisting of elements close to the center of a periodical table. In 1985, Cohen and Liu theorized that an especially strong and short bond in a highly stable gill in a ratio of 1:1,3 could be formed from carbon and nitrogen atoms in this principle and Cohen's form (C_3N_4). For the first time in 1989 (A.Y. Liu and M.L. Cohen,1989), this material was proposed to be harder than diamonds. But the reproducible synthesis of one-crystalline -C3N4 was not achieved despite a considerable worldwide effort (C. Ronning *et al*.,1998). This is possible because it's planning. It has proved extremely challenging, particularly the synthesis of stoichiometric films. Energy ion bombardment is seen as important for promoting carbon into metastable 4 times coordination (sp^3 hybrid) during the development, but in several previous experiments (S. Veprek, and J. Vac,1999) it has also resulted in the nitrogen loss from the films. In addition to the technological challenges in producing high quality C_3N_4 films, Vickers' hardness recorded only reached about 30 GPa, far less than that of diamonds or other super hard films, for amorphous stoichiometric films. Furthermore, the C_3N_4 shear module is just 60% of the diamond. In investigation C_3N_4 has proven to be a stronger atomical indicator of hardness for various types of materials than the bulk modulus (D.M. Teter

and MRS Bull,1998), the strength of diamonds, or c-BN is possibly not even reached by the C_3N_4. The B-C-N framework provides a wide range of hard materials, but most of these are highly stable under environmental conditions only. Moreover, they can only be synthesized under HPHT conditions, i.e. by ion bombs, and in a limited window with process parameters except for diamond.

2.6 Research Gaps

Traditional thermo chemical treatments on stainless steel are associated with a loss of corrosion resistance as Nitrogen, Boron and Carbon react with Chromium to form Nitrides/ Borides/Carbides, thus removing chromium from the solid solution. C-BN can be synthesised on various metals such as aluminium, gold or silver as well as compound semiconductors such as silicon carbide or titanium nitride. Despite the fact that films with a high c-BN content (i.e. > 85 percent) had been synthesised in certain circumstances, heteroepitaxial development had not been achieved. The c-BN content of the films reduced as the metal substrate hardness decreased [Mir95], a phenomenon that was explained using stress-induced c-BN production models. More ductile metals are intended to absorb the stresses created in the developing film better, delaying or even inhibiting c-BN nucleation. The films produced with pure Ar ion bombardment have low peak frequencies. The fact that the high cubic content BN films created by Ar as a reactive gas frequently delaminated in air has been reported. In the cubic boron nitride thin films development; so far there have been numerous significant concerns. The delamination of c-BN films from the substratum is among the most important challenges. C-BN films have been shown to have high-pressure between 1 and 25 GPa. Surface oxidation due to humidity after air exposure is responsible for the delamination of non-stoichiometric c-BN films.

2.7 OBJECTIVES OF THE RESEARCH WORK

The objectives of the present research work are listed below:-

- To develop BN based coating on SS316L steel substrates using Radio Frequency Magnetron Sputtering Technique.
- To examine the developed BN thin films for comparison in terms of mechanical and micro-structural characteristics.
- To characterize the wear and corrosion performance of BN thin films

CHAPTER 3

EXPERIMENTAL DETAILS

In this chapter, the deposition method of the RF sputtering has been reported along with the process parameters of the equipment used for depositing thin films. The various tools used for the characterization of the substrate, thin-film specimens at various stages of the research work have been described. The procedures of the corrosion test at room temperature and wear (abrasive) test have also been mentioned. The various characterization techniques used to evaluate the performance of the coating for the analysis of wear and corrosion products formed during various tests have also been explained in this chapter.

3.1 SELECTION OF SUBSTRATE MATERIAL

Stainless steel (SS-316L) was selected as a substrate material for the current research study. The Stainless steel (SS-316L) substrate material has been selected due to its extensive use in high temperatures like furnace parts, exhaust manifolds, Heat exchanger, jet engine parts, marine environment and; which requires high-temperature corrosion resistance and mechanical strength. The substrate material was procured from Allied Engineering Industries Pvt. Ltd, Limited, Ludhiana, India. This industry manufactures automotive parts of the engine like turbocharger housings and supplies to reputed automobile industries in India. The chemical composition of the (SS316L) substrate was checked using an optical spectrometer (Make: Metal Vision, Model: 1008i).

3.1.1 CHARACTERIZATION OF MATERIALS

The characterization of substrates stainless steel (SS-316L) was performed to determine its microstructure, grain size and element composition. Figure 3.1 (a) shows typical austenitic microstructures of the SS-316L observed through FE-SEM. The elemental composition of (SS-316L) was checked by an optical spectrometer (Make: Metal Vision, Model: 1008i). The composition of SS-316L is given in Table 3.1.

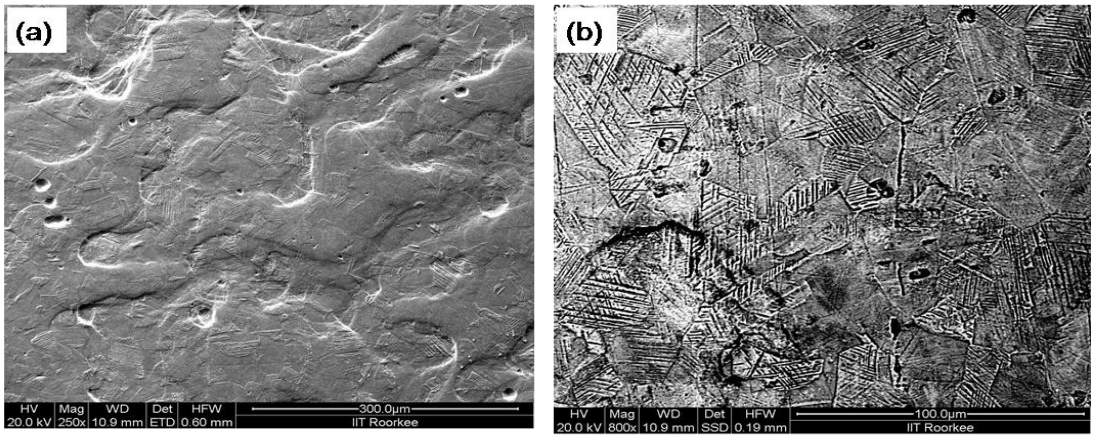

Fig. 3.1 Microstructures of bulk stainless steel: (a) SEM micrograph and (b) BSE image.

Composition	Cr	Mo	Fe	Si	C	Mn	Ni
Stainless Steel (SS316L)	17.3	2.66	Bal	0.73	0.022	1.77	13

Table 3.1: Chemical composition of the SS-316L substrate

3.2 BN target details and RF magnetron sputtering

The process of coating deposition was performed at the lab facility of Institute of Electrophysics, Yekaterinburg, Russia under the supervision of Prof. A S Kamenetskik. Cubic-BN films were deposited on SS316L substrates using the RF magnetron sputtering method. All substrate underwent ultrasonic pre-treatment in a petroleum ether solution for 3 min then were washed by deionized (DI) H_2O. Figure 3.2 shows the diagram of the experimental setup. The plasma system consisted of a flat balanced magnetron *(1)* and a large (50 cm^2) electron beam source *(2)*, positioned at a diameter of 3300 mm in the vacuum chamber *(3)*. The sputtering targets were an 80 mm diameter disc and a 10 mm thickness made of hexagonal boron nitride (99.9% purity). The main reason for the selection of h-BN target is the lowest amount of intrinsic stresses required for c-BN formation (A S Kamenetskikh *et al* 2017) .According to the static stresses model (McKenzie D R *et al.* 1996) , is 4 GPa. Thus, the amount of inherent stress in coatings formed by RF sputtering of h-BN target is 2.5 times lower than in coatings deposited by sputtering of B target at equivalent Ar/N ratios. This increases coating adhesion and enables for thicker coatings. The BN target

was mounted on a water-cooled magnetron gun, which was coupled on an RF (13.56 MHz) generator via a matching network. In RF mode (13.56 MHz), h-BN target with 150 W discharge power was sputtered. Discharge was employed in the electron source using a self-heated hollow cathode of titanium nitride. In the 2–20 A range, discharge power was adjusted and the voltage was changed from 300 V to 25 V. Coatings were deposited on the polished surfaces of SS316L samples measuring 15mm x 10mm. Samples were cleaned with trichloroethylene (TCE), acetone, methanol, and deionized water to remove any foreign substances, and then they were ultrasonically cleaned for 10 min. The working chamber was pumped off till 10^{-5} torr by the turbo-molecular pump. Samples were also cleaned by ion etching in Ar plasma generated by the electron beam. The pulse bias of samples during ion etching was 500 V (50 kHz, 12.5 μs) and ion current density was 2mA/cm^2. The bias voltage during coatings deposition was 200 V. Gas mixtures Ar/N_2 was feed through an electron source. Four deposition parameters such as gas mixture ratio, pressure, temperature and plasma energy were varied during the coating process in the three different regimes. The coating was deposited using three distinct coating regimes, BN-1, BN-2, and BN-3, with gss flow rates of QAr/QN_2 -5/1, QAr/QN_2 -5/2.5, and QAr/QN_2 -5/5 s.c.c.m, total gas pressures of 0.5^{-5} torr, 0.6^{-5} torr, and 0.7^{-5} torr, plazma energy of I00ev,120eV and 130eV respectively.

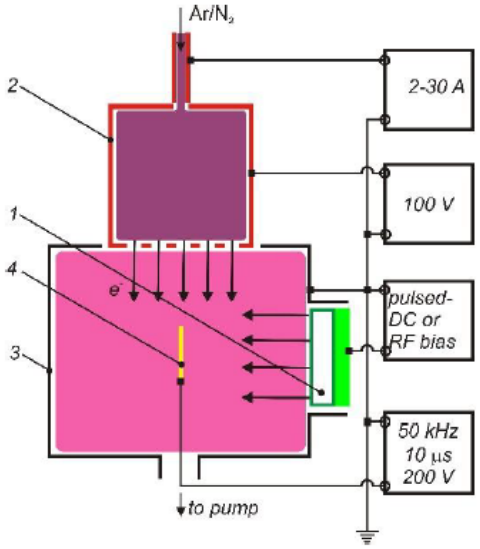

Figure.3.2 The diagram of the experimental setup: 1- magnetron, 2- electron source. 3- Working chamber, 4- samples.

Following sputtering parameters were varied for three different deposition regimes.

Table 3.2. Sputtering parameters used for different coating regimes

RF Sputtering Parameters	
Deposition parameter	RF Magnetron Sputtering
RF Frequency	13.56 MHz.
Target Material	h-BN(99% purity),80mm dia.
Ar flow rate	5 sccm.
N_2 flow rate for BN-1	1 sccm.
N_2 flow rate for BN-2	2.5 sccm.
N_2 flow rate for BN-3	5 sccm.
Magnetron discharge power	150 W in all regimes
Plazma energy for BN-1	100eV.
Plazma energy for BN-2	120eV
Plazma energy for BN-3	130eV.
Substrate temp. for BN-1	$220^{O}C$
Substrate temp. for BN-2	$275^{O}C$
Substrate temp. for BN-3	$300^{O}C$
Base pressure	10^{-5} Torr
Work pressure for BN-1	0.5^{-5} Torr
Work pressure for BN-2	0.6^{-5} Torr
Work pressure for BN-3	0.7^{-5} Torr
Deposition process time	5 Hr.
Coating Thickness	500 nm

The deposition of the coating is performed under different sputtering parameters in order to identify the best parameters to obtain maximum cubic boron nitride contents with minimum compressive stress in the coating.

3.3 DEPOSITION OF thin films

3.3.1 Preparation of Substrate Material

Substrate material (SS316L) was machined to get the required size for the purpose of its characterization and destructive testing. The material was cut on Wire-cut Electro Discharge Machine (WEDM) (ELECTRONICA HITECH Pvt Ltd. ,Model : Ultracut F2, year of Manufacturing:2010) in sizes of ($600\times400\times300mm^3$). A typical optical macrograph of the cut specimens is shown in Fig 3.3(a). After cutting the samples on the WEDM, the specimens were polished down to 1200 emery paper grade followed

by mirror finish using alumina powder particle on the polishing machine. Typical optical macrographs of the polished specimens are shown in Fig. 3.3(b). The WEDM used for the cutting of the sample is presented in Fig 3.4

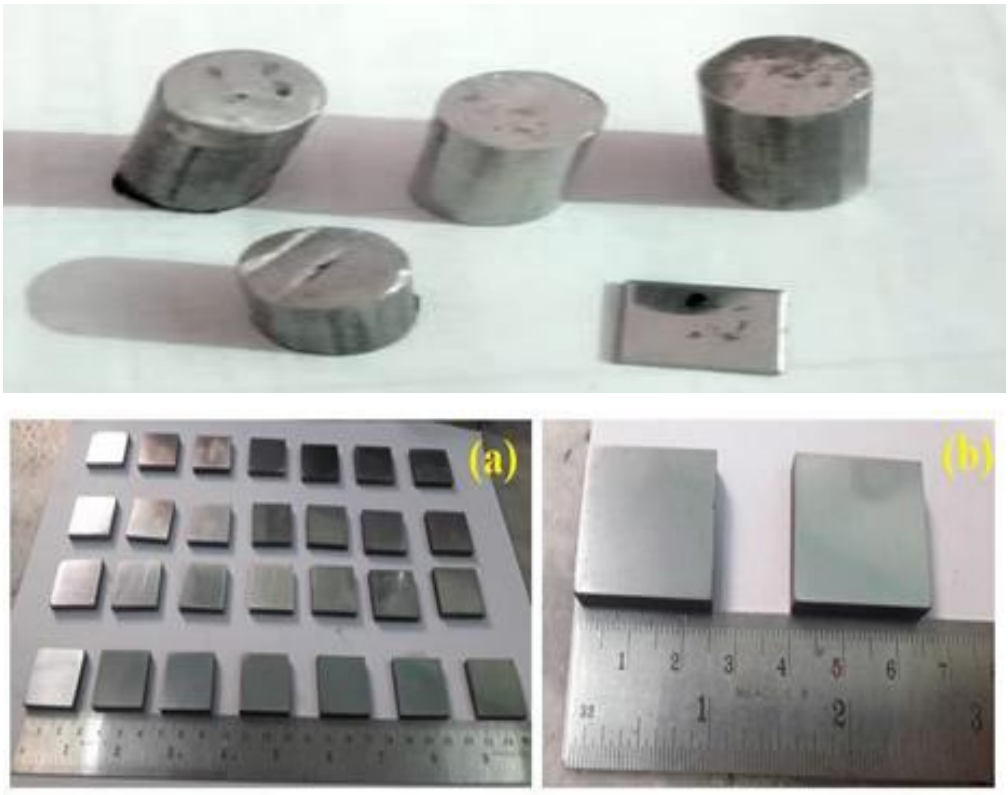

Fig. 3.3 Optical micrograph of the prepared samples before deposition of the coating (a) unpolished specimens, (b) polished specimens.

Fig. 3.4: Photograph of the wire-cut Electric discharge machine (WEDM**)**

3.4 **Metallurgical Characterizations of the RF sputtered coated specimens at various regimes:**

RF sputtering coated specimens at various sputtering regimes were mounted across the thickness using a low-speed diamond saw and were cold mounted in epoxy. The cold mounted specimens were ground and polished with different grade of emery papers. The metallurgical characterization of the coated specimens was carried out by using X-ray Diffraction (XRD), Field Emission-Scanning Electron Microscopy (FE-SEM), and optical microscope. The following section briefly explains the procedures and equipment used in the metallurgical characterization of RF sputtering coated specimens.

3.4.1 X-ray Diffraction (XRD) Analysis

The detection of various phases present in the coating at various sputtering parameter conditions was revealed by utilizing an XRD machine. The XRD patterns obtained through XRD machine were used to analyze the phases formed on the surface of the thin film and the feedstock powder X-ray diffraction (XRD) was done with a scanning rate of 1°/min and a step range (2-θ range) of 10°-100° on Bruker AXS diffractometer. The XRD was carried out with a Cu-Kα radiation source produced at 40 mA and 40 kV. The detail of the XRD facility used in the present study is presented in Appendix A (Fig. A-1).

3.4.2 Microstructural characterizations of the RF sputtered coating at various regimes using Field Emission-Scanning Electron Microscopy (FE-SEM) and Energy Dispersive Spectroscopy (EDS) Analysis.

A field emission scanning electron microscope (FE-SEM) acceleration with a voltage of 15kV (Make: JEOL, Japan; Model: JSM-6610LV) and equipped with an energy dispersive spectroscopy (EDS) attachment was used for the study of the morphology of the as-deposited and the heat-treated specimens. All specimens were initially silver pasted between the samples and stub for having conductivity, thereafter, gold-coated for obtaining elemental-maps for the analysis of different elements present on the surface and across the cross-section of the coating. The energy dispersive spectroscopy (EDS) analysis provides the elemental compositions (weight %) at the selected region in the form of point and line analysis were taken at

any region of the as-deposited coated specimens. Samples were prepared as per the procedure given in section 3.3.1 for the cross-section analysis of the samples before and after the testing. The SEM micrographs at different magnifications were taken along with the point and line scans. EDS analysis was performed for the elemental composition at different regions of the coated surface. SEM/EDS analysis of the substrate, as coated has been reported in Chapter 4 of the current research work-study.

3.4.3 Porosity and surface roughness measurement of the coating

The coated samples were polished before the measurement of porosity. Both samples were polished down to emery papers of 1200 grit size for porosity measurement. This involved the measurement of porosity on the Dewinter inverted optical microscope (Model: LT-2B, Make: Chennai metco Pvt. Ltd, Chennai, India) using image analyzer software (Dewinter Material Plus, Version 4.3) as per STM B276 standard. The detail of the Dewinter inverted optical microscope is presented in Appendix A (Fig. A-2). Ten values of porosity were taken and their averages have been reported. The surface roughness of deposited coatings has been reported during the Surface roughness tester (Model: SJ 201; Make: Mitutoyo, Japan). The porosity values and surface roughness of the deposited coatings are the average of the ten measurements and are given in Chapter 4 of the current research study.

3.5 Mechanical characterizations of the RF sputtered coating at various sputtering regimes:

The evaluation of mechanical properties was carried out in terms of microhardness. Details are explained in the following subsections.

3.5.1 Measurement of Micro-hardness

The micro-hardness of the coatings was obtained by utilizing a Vickers's micro-hardness tester (Model: Econom et VH1 MD, Make: Chennai metco Pvt Ltd, Chennai, India) at 50 g load with a dwell period of 10 s. The detail of Vickers's micro-hardness tester used in the present investigation is presented in Appendix A (Fig. A-4). The micro-hardness of the coating along the layer thickness was determined. A total number of ten indents were taken over the cross-section of the coating at two different locations and out of these five indents were taken along the layer thickness at each location. Finally, their average values are reported and the distribution of micro-

hardness values for coated specimens at various conditions is presented in chapter 4 of the current study.

3.6 Tribological Characterizations of the coated specimens:

The tribological characterization determines the functional performance of the microwave coating. Accordingly, aspects of the thin film were evaluated using dry sliding wear. The procedure and details of tribological characterizations of the specimens are explained in the following sections.

3.6.1 Dry sliding wear study (Pin on disc)

Tribological tests were carried out using a high-temperature pin-on-disc tribometer in unidirectional dry sliding conditions. High-temperature pin–on disc tribometer used for testing coated specimens at various conditions as shown in Fig.3.5. Before conducting wear and friction tests, specimens were polished using various grit sandpapers, and Ra values were decreased to less than 1 m for each specimen. The tests were carried out in accordance with ASTM G99–04 guidelines. As a result, an induction heater was utilised to warm the disc in order to achieve the necessary test temperature in this experiment. A pyrometer was used to determine the temperature of the disc. The test parameters for the wear and friction were selected based on features of typical hot forming processes. The experiments were conducted using the parameters listed in Table 3.2:

3.2:The details of the various process parameters used for performing the pin on disc test for the RF Sputtered coatings at various conditions:

Parameters	Units	Values
Sliding distance	M	5000
Speed	M s−1	1
Load	N	10
Track diameter of the disc	mm	80
Temperature	°C	800

Friction was measured using a strain gauge force transducer. The tribometer is equipped with a computerised data acquisition and control system to manage and observe many elements. A schematic diagram of the pin-on-disc facility was used for performing testing on coated specimens at all conditions as shown in Fig.3.6. The surface morphology of all samples at different magnifications after performing the tribological testing (High temperature solid air-jet erosion test, & Dry sliding wear) were analyzed by field emission scanning electron microscope (FE-SEM) (Make: JEOL, Japan; Model: JSM-6610LV) equipped with an energy dispersive spectroscopy (EDS).

Fig. 3.5 High-temperature pin–on disc tribometer used for testing coated specimens at various conditions.

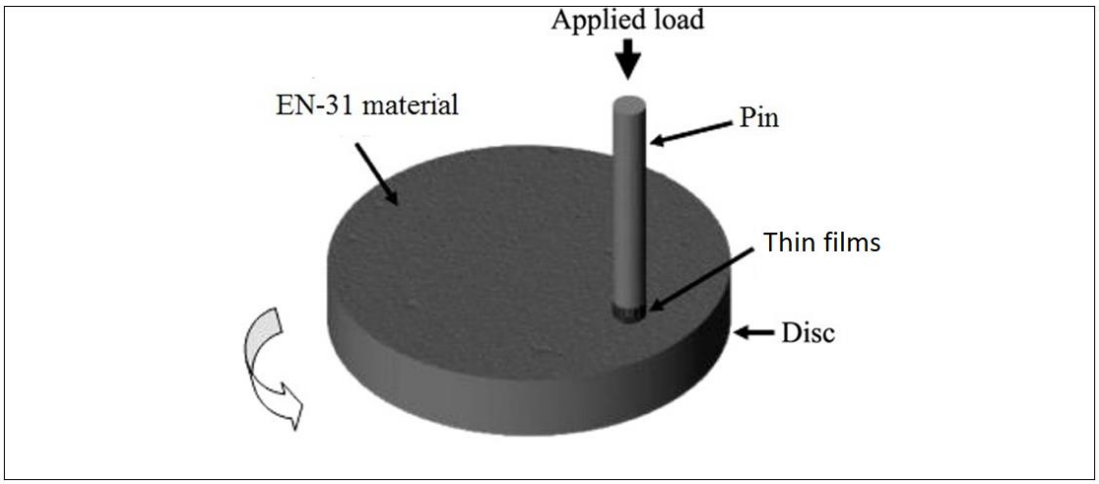

Fig. 3.6 A schematic diagram of the pin-on-disc facility used for performing testing on coated specimens at all conditions.

3.7 Corrosion behavior of the coated specimens:

Corrosion is generally initiated from the surface of the material by the interaction of the environment at the surface. The electrochemical reactions act as a catalyst for corrosion to occur on the surface/ sub-surface of the material. Thus, electrochemical testing is best for the investigation of the corrosion mechanism. For performing the electrochemical study, the main requirement of the tested sample is that it must be electrical conductors and further size of the sample is small enough (few square centimeters) to be properly fitted in the Gamry instrument used for investigating the corrosion behavior of the metal in a corrosive environment. There is a three-electrode configuration used in the Gamry instrument for performing the corrosion testing. All electrodes used for studying the corrosion behavior are immersed into the solution, and they are joined to an appliance called potentiostat. The electrolytic solution used in the study has closely resembled the actual application environment of the specimen being tested. Further, with the help of potentiostat, the potential of the metal sample can be changed at the desired level and to evaluate the current flows as a function of potential. This configuration helps in finding the corrosion current density (I_{corr}) at the corrosion potential (E_{corr}). Using electrochemistry techniques, a range of corrosion phenomena can be evaluated. In the present study, the electrochemical corrosion test was performed on both (base metal and as-deposited coated specimens. Already

defined it nomenclature Figure 3.7 illustrates the schematic construction utilized for performing the electrochemical test for investigating the corrosion behavior of the coated specimens. All potentials were calculated in relation to the standard calomel electrode (SCE), which was used as a reference electrode.. The counter electrode was made of a pure graphite rod. The coated specimens at different heat treated conditions having a corrosive area of 1.5836 cm^2 were employed in the present study and it served as a working electrode. During the electrochemical study, only the active part of the coated specimen was subjected to a corrosive environment, while the remaining part of the sample was properly insulated with epoxy. Before carrying out the electrochemical tests, the active part of the coated specimen was polished with different grades of emery papers of size varying from 200 to 1000 grit size, followed by cleaning using an ultrasonic cleaner and finally hot drying with air. The potentiodynamic polarization curve was plotted for investigating the electrochemical behavior of coated specimens at all conditions and the tests were performed in a 3.5 wt % NaCl solution at room temperature. The Potentiostat/ Galvanostat (Series G-750; Gamry Instruments, War-Minster, PA) equipment coupled with a computer with DC105 Gamry electrochemical software is utilized for performing the potentiodynamic polarization test. . During the electrochemical testing, the potential was swept from -500 mV to 1500 mV against Ecorr. A potentiostat with a scan rate of 1 mV/sec was utilised to keep the electrode potential within 1 mV of a predetermined value across a wide range of applied current. The tests were conducted using a fresh solution for each experiment and testing was carried out at ambient temperature. The procedure for performing experiments using Gamry Instrument is as follows:

a) Green–Blue: Working and Working Sense, connected. A black cable was attached to the connection point, referred to from here on as Black. This is the conventional "positive" electrode. The black cable was connected to the counter electrode (i.e. the "anode" in the electrochemical test set up).

b) Red–White: Counter and reference electrodes were also connected together. A red cable was attached to the connection point, referred to from here on as Red. This is the conventional “counter” or “negative” electrode.

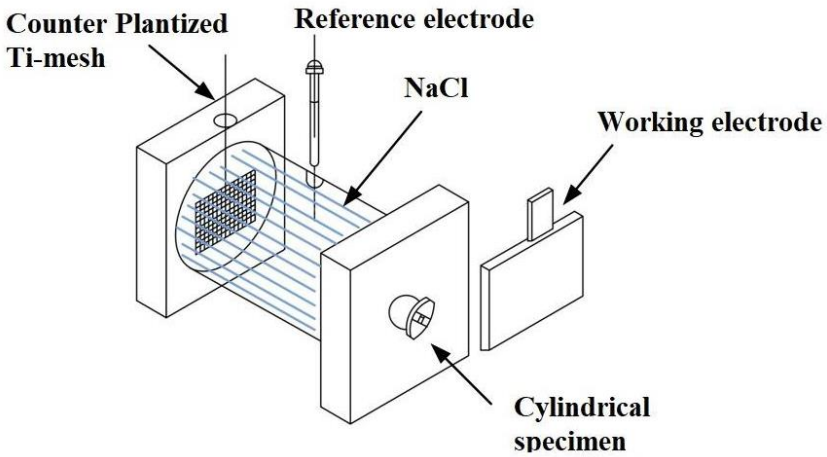

Fig 3.7. The schematic diagram indicates the setup used for performing the corrosion behavior of the coated specimen**.**

The electrochemical equivalent weight ($E_{quivalent))}$ and density (ρ_{BN})) for the BN was calculated.

The $E_{quivalent}$ of BN is as follows:

$$E_{equivalent} = 24.80 \text{ gm/mol}$$

The equivalent density (ρ_{alloy}) of BN is as follows:

$$= 3.45 \text{ gm/cm}^{3.}$$

3.7.1 Tafel Plot Experiment

The electrochemical study of the coated samples at all conditions was performed by utilizing a Tafel extrapolation method. To ensure the repeatability of the test results, the electrochemical corrosion study was done on three coated samples for each heat-treated condition. The Tafel extrapolation method is based on mixed-potential theory for determining the corrosion rate of samples. The data captured from anodic or cathodic polarization measurements were used in a mixed-potential theory. Further, during the electrochemical study, the cathodic polarization data are generally taken because these data are easier to assess using an experimental method. Schematic construction for performing a cathodic polarization measurement is shown in Fig.3.8. The sample, whose corrosion rate is to be measured served as a working electrode (W.E.), and the cathodic current was provided to it using an auxiliary electrode which

is generally made from an inert material such as platinum or graphite. The current in the experimental process was measured using an ammeter *A*, and the potential of the coated specimens was measured with respect to a reference electrode by a potentiometer-electrometer circuit. The results were obtained during the cathodic polarization of coated specimens in an air-free 3.5 wt% NaCl solution. Before the application of the cathodic current, the voltmeter indicates the corrosion potential of the tested coated specimen with respect to the standard reference calomel electrode. A graph of E vs logi is generated by plotting the electrode potential against the logarithm of the applied current. The tangents were then created on the graphical plot of logi vs E, which crossed at a point when extrapolated to the corrosion potential (Ecorr). The corrosion current (Icorr) value is represented by this point on the X-axis. The log axis is selected because of the broad range of current values to show during a corrosion test. Because of the phenomenon of passivity, it is not uncommon for the current to alter by six orders of magnitude during a corrosion experiment. After completion of the electrochemical study, the scanning electron microscopy associated with an energy dispersive spectroscopy was utilized to examine the surface characteristics of the corroded specimens to understand the corrosion mechanism and to investigate the microstructure/ composition analysis of the corroded surfaces of the coated specimens.

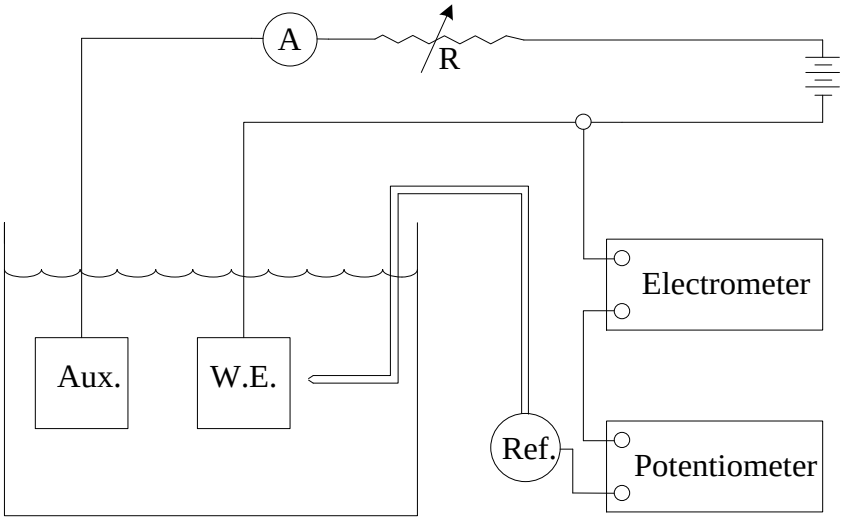

Fig. 3.8 Schematic illustration of the electric circuit for cathodic polarization measurement.

3.8 SUMMARY

The austenitic stainless steel (SS-316L) substrate material and BN thin films were used for the present study. The BN thin films were successfully developed on SS-316L substrates using the RF magnetron sputtering technique. A detailed description of the various steps in the RF magnetron sputtering technique has been described. A detailed description of different characterization techniques/tools (metallurgical, mechanical) used for finding the characteristics of developed BN thin film specimens has been presented in this chapter. A detailed description of methods/conditions used for assessing the Corrosion and tribological characteristics of BN thin films has been discussed.

CHAPTER 4

CHARACTERIZATION OF RF MAGNETRON SPUTTERED THIN FILMS

In the present work, the RF magnetron sputtering technique was employed as a method for synthesizing boron nitride coating on the SS-316L substrate surfaces. The inherent attributes of the RF magnetron sputtering technique are uniform coating resulted in the reduced thermal gradient, and less residual stresses in the deposited coating compared to the other thermal processes. Three different coating regimes in terms of varying Ar and N_2 ratios were employed. The chapter deals with characterization (metallurgical and mechanical aspects) of the as-deposited coated specimens by utilizing the various characterization techniques. The SEM/EDS analysis from the cross-section of the as-deposited coated specimens is reported. The micro-hardness of all the specimens at all conditions was evaluated along the cross-sectional direction and porosity along the cross-sectional direction is reported in the present chapter. The presented results are discussed with regard to the available literature.

4.1 SEM/EDS AND XRD ANALYSIS OF THIN FILMS SPECIMENS

The metallurgical aspects of thin film specimens at different coating regimes were characterized by examining X-ray diffraction, microstructural features and measurement of porosity. The characterizations results are explained with appropriate illustrations in the following sections:

4.1.1 Microstructural study of thin films specimen and elemental analysis:

The SEM and EDS study of the BN thin coatings at three different regimes are represented in Fig.4.1-4.3. The quantity of nitrogen and boron in the regime BN1 decreases in accordance with Fig.4.1 (b) of the EDS, due to low bombardment of the nitrogen atoms on the substrate surface during the BN1 regime. At low temperature and low plasma energy less number of nitrogen atoms bombard the substrate surface.As per the rectangle shown in Fig.4.1 (b).The EDS spectrum of the thin film synthesized on BN1 confirms the elements present in the coatings as per Fig. 4.1(b). The thin BN coatings at regime BN2 show the substantial amount of nitrogen and

boron on the BN thin film surface as illustrated by Fig.4.2.(b). Figure 4.2(a) and 4.2,b) displays the SEM and EDS of BN coatings synthesized in Regime BN2 respectively

.

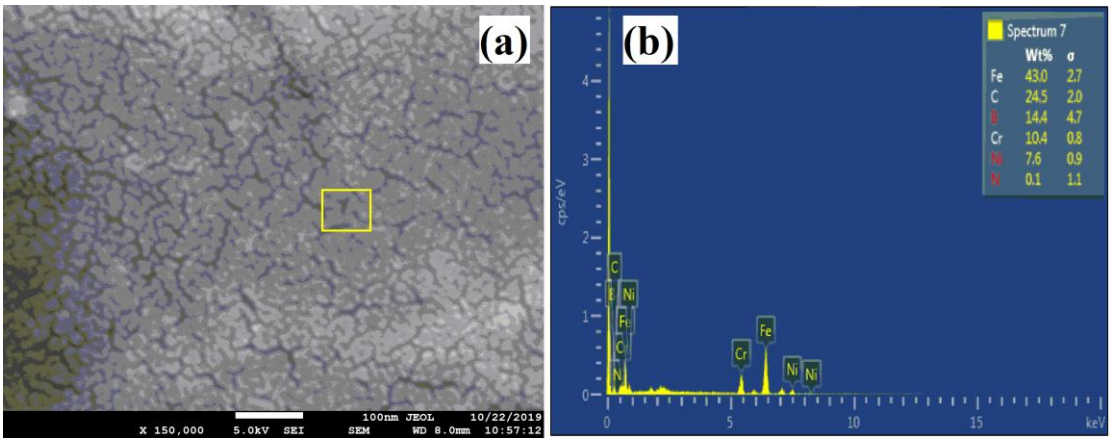

Fig.4.1. (a) SEM images of BN1 film regime, and (b) EDS micrograph of BN1 film

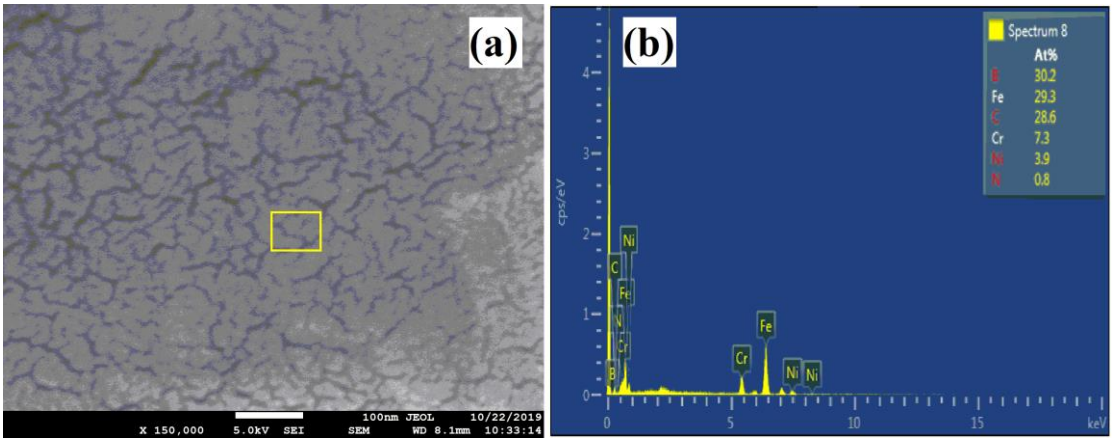

Fig.4.2. (a) SEM images of BN2 regime and (b) EDS micrograph of BN film

Figure 4.3 shows the SEM and EDS of BN thin coatings deposited on the BN3 substrate. The contents of boron and nitrogen increase (B-31.80 wt%, C-39.80 wt%) as shown in the EDS in Fig.4.3(b) of the rectangle in fig.4.3(a).

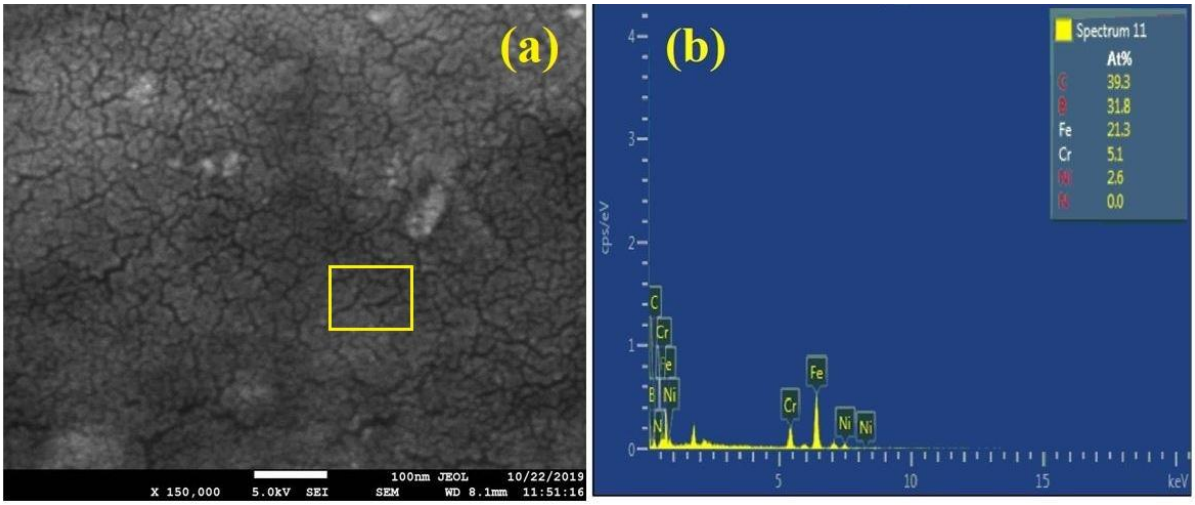

Fig.4.3. (a) SEM of BN3 film regime, and (b) EDS micrograph of BN film

Image 4.4(a) and 4(b) exhibits the cross-sectional view of the coating on the BN1 samples. The coating morphology consists of irregular shapes with the dendritic type structure. In the image 4(c) and 4(d) relatively smoother coating morphology was found on the samples BN-2. In the image 4(e) and 4(f) the grain size of the coating on the BN-3 sample is larger as compared to other regimes. The bombardment ions energy is dissipated into phonons in what has been termed a thermal spike. The BN transforms from hexagonal phase to cubic phase at the action of thermal spike which results in very high temperature and pressure locally in a very brief period of time. At the low plasma energy and temperature, the bombardment ion energy is not high enough to make the hexagonal phase transform to cubic phase as shown in BN1 regime. Similarly in BN3 regime the high plasma energy and temperature high ion energy makes deposited atoms resputter from the substrate, which is not favorable to the cBN formation and lead to the decrease of cBN content and poor surface morphology. At moderate plasma energy and temperature there is sufficient bombardment ion energy and surface morphology is relatively smoother in BN2 regimes

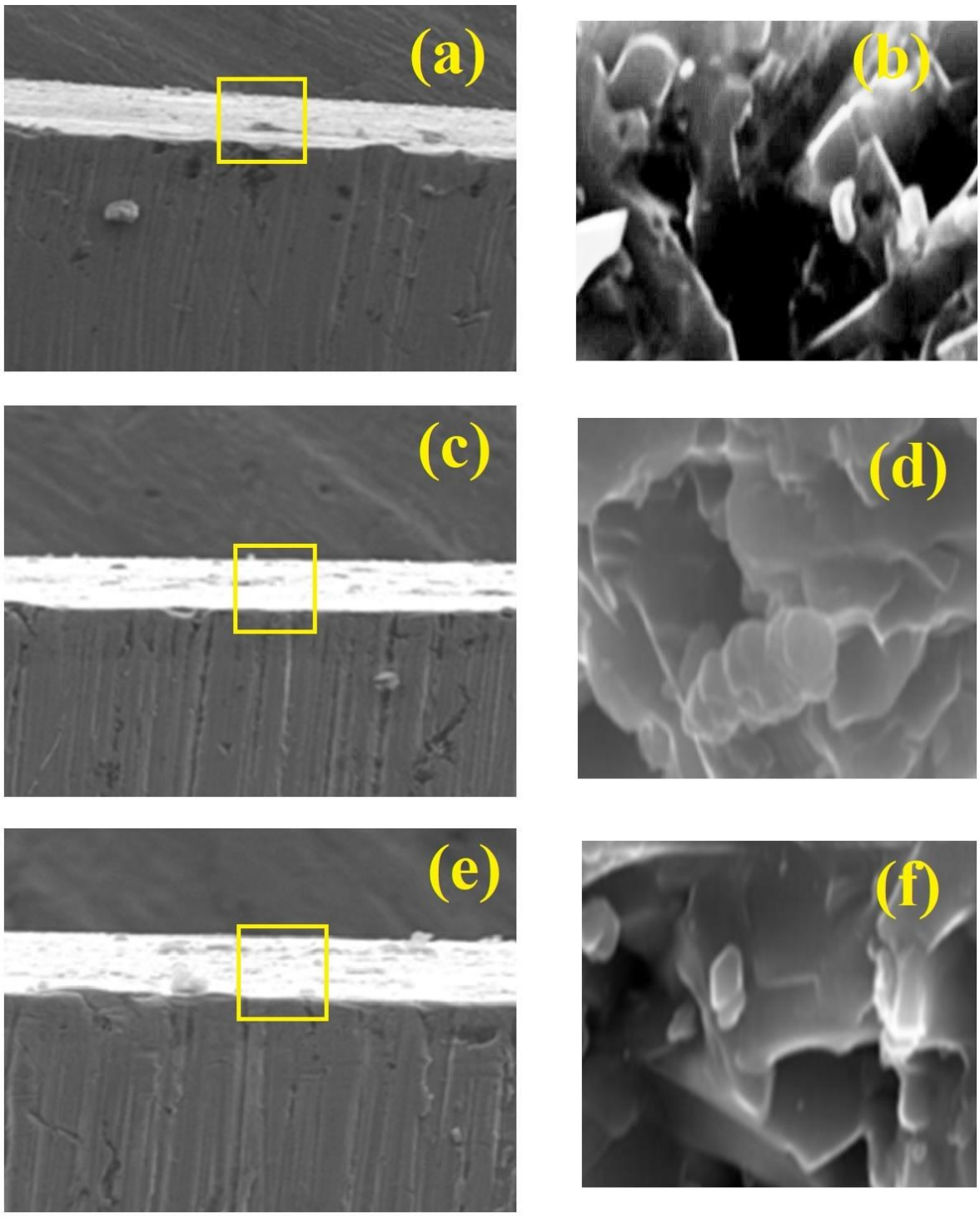

Fig.4.4 SEM micrographs of cross-section at different magnifications of (a-b) BN-1, (c-d) BN-2 and, (e-f) BN-3 thin films

4.2 XRD analysis

Fig.4.5 displays the XRD spectrum of the thin BN films. The XRD shows the c-BN in the deposited coating as a major phase. However, soft phase h-BN is also found in the surface along with presences of phases such as amorphous-BN and t-BN phases. In contrast to the BN-1 and BN-3 samples, more peaks of c-BN have been identified in BN-2. Diffraction peaks of 43.254° and 50.306° in sample BN-2 correspond to that of the cubic phase of boron nitride while BN-1 coatings consisted of softer boron nitride phases such as orthorhombic-BN, h-BN and rhombohedral-Boron Nitride with a small amount of c-BN phase. In BN-3 regimes mostly orthorhombic-BN and h-BN phases were found and various phases are present in Table 4.1.

Regime	Theta-2θ	Phase
Regime 1	20.45	Orthorhombic-BN
	25.436	Orthorhombic-BN
	27.343	Orthorhombic-BN
	26.76	h-BN
	43.163	c-BN
	59.718	Rhombohedral-BN
Regime 2	26.627	h-BN
	29.578	orthorhombic-BN
	43.193	c-BN
	50.395	c-BN
Regime 3	29.56	orthorhombic-BN
	32.436	orthorhombic-BN
	36.343	orthorhombic-BN
	48.75	h-BN
	50.355	c-BN
	62.162	Rhombohedral-BN

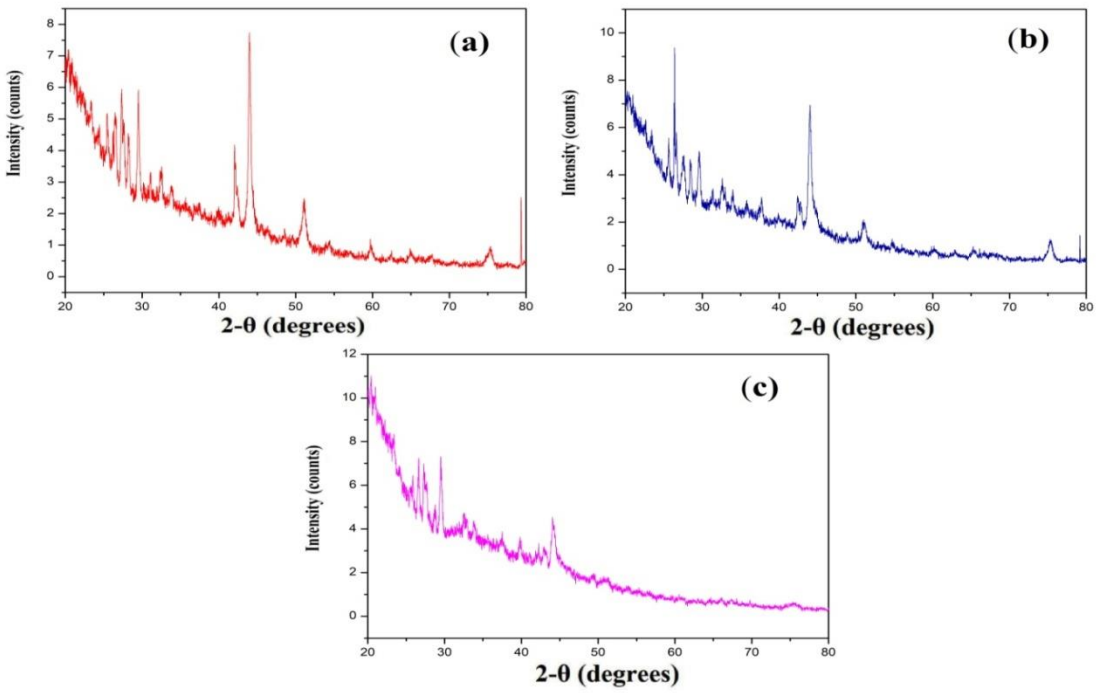

Fig 4.5. XRD pattern of (a) BN1, (b)BN2, and (c)BN3.

In comparison to BN-1 and BN-3, more cubic phase of boron nitride found in the BN-2 sample as revealed by the investigation of XRD differentiation peaks. It is because of the fact that there is a bombardment of high Ar ions in sample BN-2 which results in more Ar ions residing in the BN-2 film synthesized in Ar / N_2 plasma. Because of the contamination of these Ar ions within the BN coatings, the compressive stress increases during the formation of the h-BN phase on the substratum interface to promote thermodynamically c-BN nucleation and growth. From the study of scratch tracks, it has been found that BN-2 coatings have high adhesion strength and hardness in comparison to coatings deposited in other regimes. The higher substrate temperature enhanced the adsorption state and surface diffusion length of the hBN atoms clusters sputtered from the hBN target. According to thermal spike model, higher substrate temperature will be beneficial to the condition of cBN formation. At a lower substrate temperature, a higher substrate bias voltage will be applied to obtain more cBN content, which probable will cause high stress in the film.The cBN content increases to 50% when N_2 gets to 2.5 %. But cBN content decreases to 20% with the N_2 ratio changes from 25% to 50%. The balance of nitride and boron atoms in the film is an important factor for cubic phase BN deposition. The cBN cannot be

obtained at the mismatch of nitride and boron atoms in the film. At the bombardment of argon ions, the nitride and boron atoms will sputter from the deposited film at the different yields. The nitride atom sputtering yield is higher than that of boron atom from our previous molecular dynamics simulation. The nitride gas is added to make up the loss of nitride atoms in order to keep up with the balance of nitride and boron atoms in the film. From the experimental investigation, 25% N_2 in the gas composition is more suitable for cBN preparation.

4.3 FTIR Test

Fourier transform infrared spectroscopy (FTIR) was used to determine whether the phase was hexagonal or cubic in deposited boron nitride films. Figure 4.6 (a,b,c) shows the IR spectra of BN films on SS316l substrates deposited at a different ratio of Ar and N_2 mixture in transmission mode with a resolution of 4 cm^{-1}. Uncoated SS316l samples were used for the background spectra. There is only hexagonal BN absorption at 1350 cm^{-1} and few cubic BN absorption at 1050~1100cm^{-1} at the QAr / QN_2-5/1 sccm flow rate observed. The c-BN content increases to 50% at QAr / QN_2-5/2.5 sccm flow rate. But c-BN content decreases to 20% at QAr / QN_2–5/5 sccm flow rate. For cubic phase BN deposition, the balance of nitride and boron atoms in the film is critical. The mismatch of nitride and boron atoms in the film prevents the formation of c-BN. The nitride and boron atoms sputter from the deposited layer at different rates when bombarded with argon ions. Because the sputtering yield of nitride atoms is larger than that of boron atoms, the addition of optimal nitrogen gas compensates for the loss of nitride atoms in order to maintain the nitride and boron atom balance in the film. From the experimental investigation, QAr / QN_2-5/2.5 sccm flow rate gas composition is more suitable for c-BN preparation. In BN-2 samples, an absorbance peak for the cubic phase was seen at around 1060 cm^{-1}, whereas two absorbance peaks for the hexagonal phases were observed at around 780 and 1380

cm^{-1}.

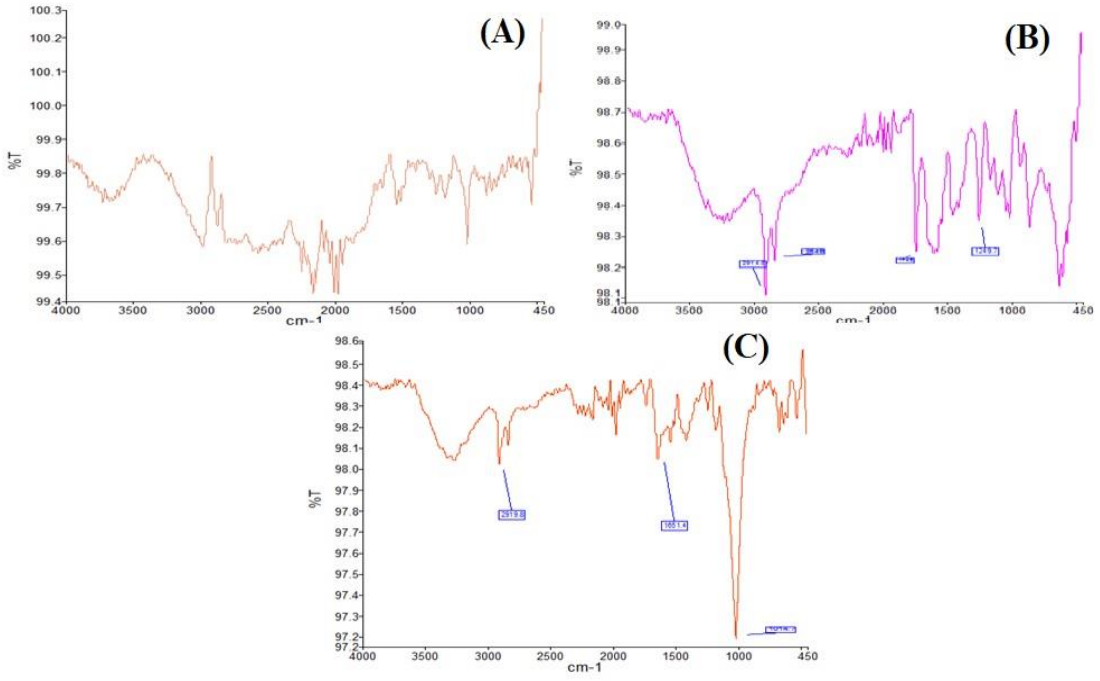

Fig.4.6. (a) FTIR pattern of BN thin film of Regime 1, (b) FTIR pattern of BN thin film of Regime 2 and (b) FTIR pattern of BN thin film of Regime 3.

4.4 Porosity measurement of the coating

The existence of porosity tends to reduce the deposited coating's mechanical and tribological performance in applications involving abrasion, surface fatigue, and so on. As a result, the porosity of magnetron sputtered coatings was assessed using an image analysis software tool (Dewinter material plus, version 4.3) in accordance with ASTM B276 utilising five regions. The porosity of deposited coating samples was observed less than 2%. The observed porosity of RF sputtered coating is found to be lower than other surface modification methods. The low value of porosity is attributed to a low thermal gradient setup in RF sputtering process, which consequently results in the low solidification rate.

4.5 Mechanical and microstructural characterization of the deposited coating

For microstructural analysis, a diamond cutter at slow speed was used to cut the coated samples along the transverse covering direction. The cut specimens were assembled on epoxy and prepared in accordance with the standardized procedure of metallographic. The polished samples were ultrasonicated in alcohol during microstructural analysis. The micro-indentation technique was employed in the direction of the coated samples to determine the hardness value towards the depth. The test was carried out for 10 s at a standard load of 50 g with Vickers indenter which is a function of the distance from the top surface to the depth of the coating. The investigation of porosity was carried out with the assistance of an image analysis technique *(Dewinter Material Plus)* on the obtained optical images of the coatings. The magnification was selected in such a way that the coated microstructure image covers the screen and allows the resolution of the void which contributes significantly to the percentage of the porosity area in total. The pore area in the viewed field was calculated by transforming the area of the pore into a background color, while the remaining microstructure is in its first colour. In this investigation, a total of 10 readings were taken at different points in the cross-section of the BN coating for the measurement of porosity. The porosity of the sputtered coating in the RF magnetron was determined as explained in the procedure above. Due to volumetric and uniform ions bombardment associated with the sputtering technique, the porosity in the sputtered RF magnetron coating was found to be less than 0.5 percent. The porosity observed is normally very small compared to other commonly performed surface processes. The low porosity value in the BN coating is due to the low solidification rate and reduced thermal gradient of the process.

4.6 Summary:

The SEM/EDS analysis from the cross-section of the as-deposited coated specimens is reported. The micro-hardness of all the specimens at all conditions was evaluated along the cross-sectional direction and porosity along the cross-sectional direction is reported. The thin BN coatings at regime BN2 show the substantial amount of nitrogen and boron on the BN thin film surface in comparison to other regimes. In

comparison to BN-1 and BN-3, more cubic phase of boron nitride found in the BN-2 sample as revealed by the investigation of XRD differentiation peaks. It is because of the fact that there is a bombardment of high Ar ions in sample BN-2 which results in more Ar ions residing in the BN-2 film synthesized in Ar / N_2 plasma. Because of the contamination of these Ar ions within the BN coatings, the compressive stress increases during the formation of the h-BN phase on the substratum interface to promote thermodynamically c-BN nucleation and growth. From the study of scratch tracks, it has been found that BN-2 coatings have high adhesion strength and hardness in comparison to coatings deposited in other regimes. Fourier transform infrared spectroscopy (FTIR) was used to determine whether the phase was hexagonal or cubic in deposited boron nitride films. It is found from the study that BN2 coating regimes possessed relatively more cubic phase of boron nitride in comparison to other regimes. The porosity of magnetron sputtered coatings was assessed using an image analysis software tool (Dewinter material plus, version 4.3) in accordance with ASTM B276 utilising five regions. The porosity of deposited coating samples was observed less than 2%. The observed porosity of RF sputtered coating is found to be lower than other surface modification methods. The low value of porosity is attributed to a low thermal gradient setup in RF sputtering process, which consequently results in the low solidification rate

CHAPTER 5

CORROSION BEHAVIOUR OF THE BASE METAL (SS-316L) AND THIN FILMS AT DIFFERENT REGIMES

Corrosion is an avoidable phenomenon in many industrial applications such as nuclear reactors etc. Therefore, high corrosion resistance is desirable in the materials used in such applications. Austenite stainless steel (SS-316L) is a widely used engineering material attributed to its moderate corrosion resistance and low cost. However, the moderate corrosion resistance limits its use in potential corrosion applications. Boron nitride-based coating is one of the most commonly used materials having an excellent combination of mechanical properties and corrosion resistance. Further, the characterization of the coated specimens was performed in terms of their corrosion behavior using various characterization techniques. The detailed results after performing characterizations are explained in this chapter.

5.1 CORROSION RATE OF THE BASE METAL & THIN FILMS

Corrosion is a damaging and unexpected metal assault and usually begins on metal surfaces. The electrochemical reactions on metal surfaces are exceptionally caused by corrosion. Electrochemical tests are therefore perfect for corrosion investigation. The term open-circuit potential (OCP), frequently called corrosion potential [Ecorr], is defined as the difference of potential between the reference electrode and the working electrode in an electrolyte (3.5wt% NaCl) and there is no associated current or potential connection to the cell. When the electrolyte attains its stable state, the OCP is estimated and there is no current flow between the anode and cathode. At this point the reduction half and oxidation half-rate reaction is equal. In this way, the calculation of the potential of open-circuit is the accompanying step for evaluating a material's corrosion vulnerability or the protective characteristics of a coating. The specimen of the coated substrate with a surface area of a few square cm was used in electrochemical investigations to examine the corrosion incidence of the metal in a corrosion test device. In the system under experimentation, the coating samples are submerged in the solution of a metal. There are also two other electrodes immersed in

the solution. All the electrodes are connected to a potentiostat. Using the potentiostat, allows specimens to change their potential in a controlled manner and to determine the flow of current as of the potential function. It offers Icorr prompt assurance at Ecorr. The electrochemical tests on the base substrate were performed in the present analysis. The inputs in the polarization tests are the density of material equivalent, and alloy weights are given in Table 5.1. Whereas the termination connections with electrodes used for gamry potentiostat are illustrated in Table 8. All potentials are measured against the regular calomel electrode (SCE), which acted as a reference electrode, and a counter electrode was used as a pure graphite rod. In this analysis, base metals and coatings were used for the corrosive area of 0.38 cm2 which acted as the working electrode. The samples were coated with insulating material so that only the active component with a surface area of 0.38 cm^2 was exposed to the samples for corrosion analysis. Before performing electrochemical tests, emery paper ranging from 100 to 8000 grit was utilized for mechanical cleaning of exposed areas, followed by acetone cleaning and hot air drying. The potentiodynamic polarization curve was designed to investigate the electrochemical response of the coatings and base metal, performed at room temperature in 3.5wt% percent NaCl solution. The Potentiostat/Galvanostat (G-1000 series; War-minster, Gamry Instruments, PA) was employed to conduct a potentiodynamic polarization check, interfaced with a system and assisted by DC105 software. The potential was varied within the -1 V to +1V range versus Ecorr during the electrochemical testing. The electrode potential was held at 1 mV as a predetermined value using a potentiostat over a broad range of applied current and a scanning rate of 1 mV/sec was used. For every experiment, the fresh solution was used at room temperature

Table: 5.1 Density and equivalent weight and of the coating material.

	Equivalent weight(Ew)(g/mol)	Density (g/cm^3)
SS-316	27.56	7.99
BN	24.82	3.45

5.2 The method for using Gamry Instrument to perform experiments

Potentiostat/ Galvanostat *(Series G-1000; Gamry Instruments, War-minster, PA)* is connected to the electrochemical cell. The test, Tafel, or polarization is selected and the input data is given to the computer screen for setup and to wait for 1800 s before launching an experiment to balance out the potential of the open circuit. The test was run and took for Tafel run 1800 s and for polarization run 5-10 min. The screen showed output results (I_{corr}, E_{corr} and corrosion rate) and output curve. For each coating state, the Tafel test was performed only once to obtain Tafel constants

5.2.1 Potentiodynamic Polarization test

In this research, BN coating formed by the RF magnetron sputtering technique coatings and base metal were studied at normal temperature in 3.5wt percent of the NaCl electrolyte solution using the polarization curve shown in figure 5.1. The test of electrochemical corrosion was performed on the surface area of 0.38. The samples were immersed in the electrolyte for the the1800s before through corrosion analysis so that the value of OCP was reached in a steady state. The BN coating corrosion rate was calculated as 0.0402 mili inch per year by Tafel extrapolation. The parameters of corrosion kinetic: corrosion rate (CR), corrosion current (I_{corr}), and corrosion potential (E_{corr}) are presented in Table 5.2.

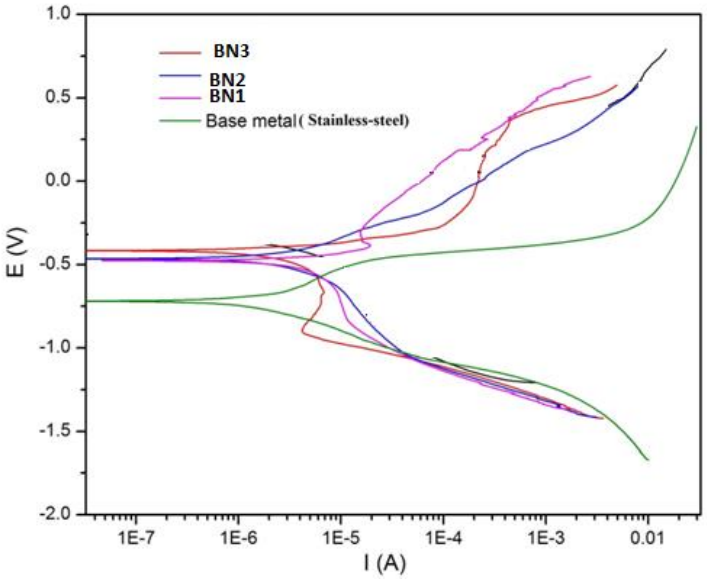

Fig.5.1. Tafel plot of different thin BN coatings

Table 5.2. Parameters of corrosion kinetic: corrosion rate (CR), corrosion current (Icorr), and corrosion potential (Ecorr)

Specimens	E_{corr}(mV)	I_{corr}(μA)	*CR* (mpy)
Base metal (Stainless steel)	-718	2.307	2.249
BN-1	-405	1.599	1.402
BN-2	-308	1.399	1.114
BN-3	-564	4.858	4.625

From the above table, it has been found that the BN3 corrosion rate is the highest (CR (mpy)= 4.625) as compared to BN-1 and BN-2 samples. For BN-2 corrosion rate is the lowest (CR (mpy)= 1.114)

5.3 MICROSTRUCTURAL STUDY OF THE CORRODED SURFACES

The micro structural features of the corroded surfaces of the base metal and coated specimens at different coating regimes were determined by employing SEM, the secondary electron images of the base metal and corroded surfaces of the coated specimens at various conditions are shown in Fig. 5.2 & Fig. 5.3 respectively. From Fig. 5.2, it is clear that the base metal was preferentially attacked during the corrosion testing, and the severe pits of size ranges 0.5 to 1 μm were observed in the microstructure of the corroded base metal surfaces.

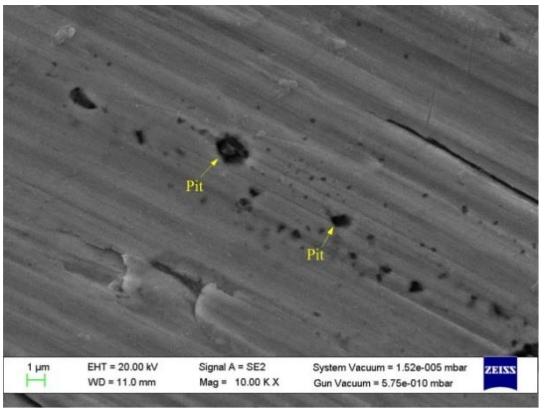

Fig. 5.2 The SEM micrographs of base metal after corrosion testing in 3.5wt% NaCl solution.

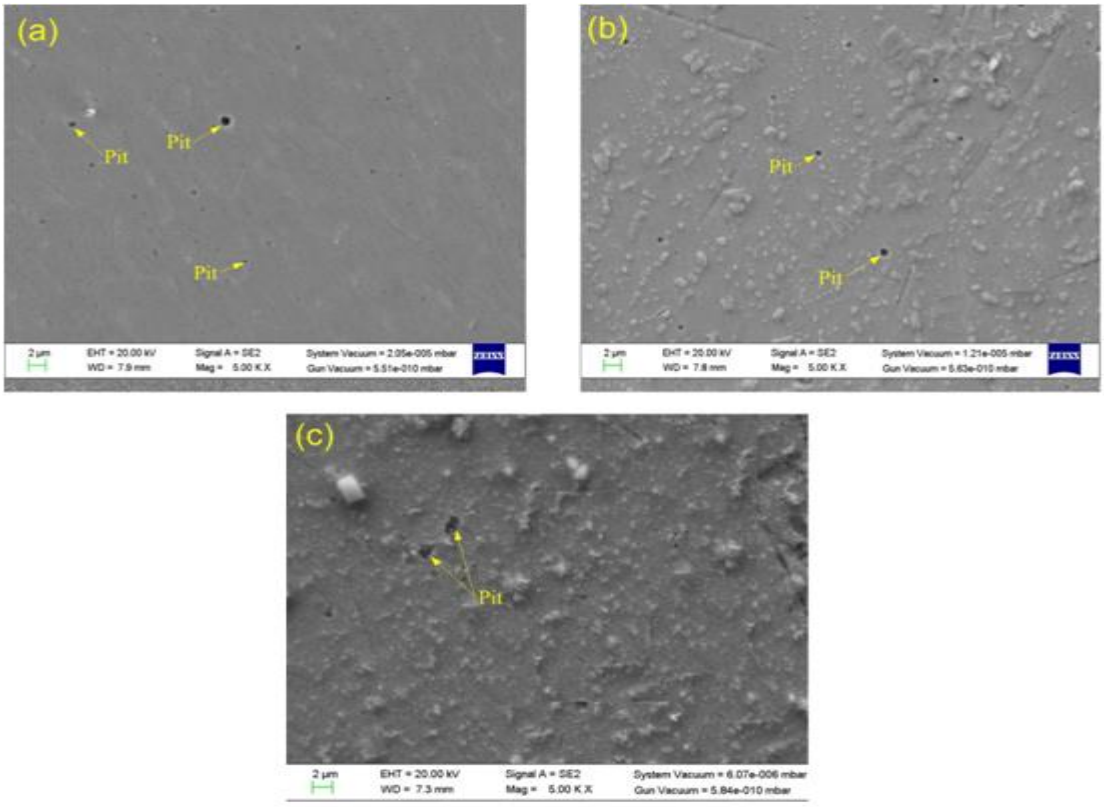

Fig. 5.3 The SEM SEM micrographs of (a) BN2, (b) BN1, (c) BN3 specimens after subjected to 3.5 wt % NaCl solution at room temperature.

From the above images it is observed that BN2 regime coating has less corrosion effect in comparison to other regimes dute to the presence of more cubic boron nitride in the coating.

5.4 Summary: The test of electrochemical corrosion was performed on the surface area of 0.38. The samples were immersed in the electrolyte for the the1800s before through corrosion analysis so that the value of OCP was reached in a steady state. The BN coating corrosion rate was calculated as 0.0402 mili inch per year by Tafel extrapolation. It has been found that the BN3 corrosion rate is the highest (CR (mpy)= 4.625) as compared to BN-1 and BN-2 samples. For BN-2 corrosion rate is the lowest (CR (mpy)= 1.114). The micro structural features of the tested base metal coated specimens and at different coating, conditions were determined by employing SEM. It is found that the base metal was preferentially attacked during the corrosion testing, and the severe pits of size ranges 0.5 to 1 μm were observed in the microstructure of the corroded base metal surfaces

CHAPTER 6

WEAR CHARACTERISTICS OF SUBSTATE AND BN THIN FILMS

6.1 SCRATCH TEST:

Figure.6.1. shows the SEM images of scratch tracks for the different coatings investigated in this paper. Scratch test was performed out on adhesive measurements of thin films of boron nitride to steel substrates. Rockwell indenter with a radius of 200 mm was used to scratch the coatings surface up to 1.5 mm distance at 3 mm / min constant speed with increased vertically load applied to the indenter during the tests. The various values of load for three thin films are shown in Table 6.1. Scratches were generated with the recording of acoustic emissions and friction force simultaneously. Based on microscopic observations, acoustic emission and friction force, the critical load for the BN films was calculated. From these results, it is possible to see only a slight delamination present on the scratch track (Figure 8b), showing that the substrate has a high adhesion resistance of the BN-2 coating. This can be attributed to the behavior of elastic recovery that occurs next to the indenter path, triggered by the compressive stresses produced by the indenter and the failure of the coating to plastically deform. This mode of failure was observed among the three coating systems in L2 for BN-2 with the highest load (126 N), indicating thus the highest adhesive strength. Delamination for BN-1 and BN-3 coatings is also created in the scratch line. The load measured in L was 102 N and 96 N respectively for these coatings, which confirms that the coatings have lower adhesion strength. Therefore BN2 is a coating with a higher adhesion strength, showing a combination of excellent durability and strength of adhesion.

Table 6.1. The various values of load for three thin films.

BN1		BN2		BN3
Load (N)	Critical Load	Load (N)	Critical Load	Load (N)
82±2	L1	96±2	L1	110±2
102±2	L2	126±2	L2	132±2
120±2	L3	146±2	L3	172±2

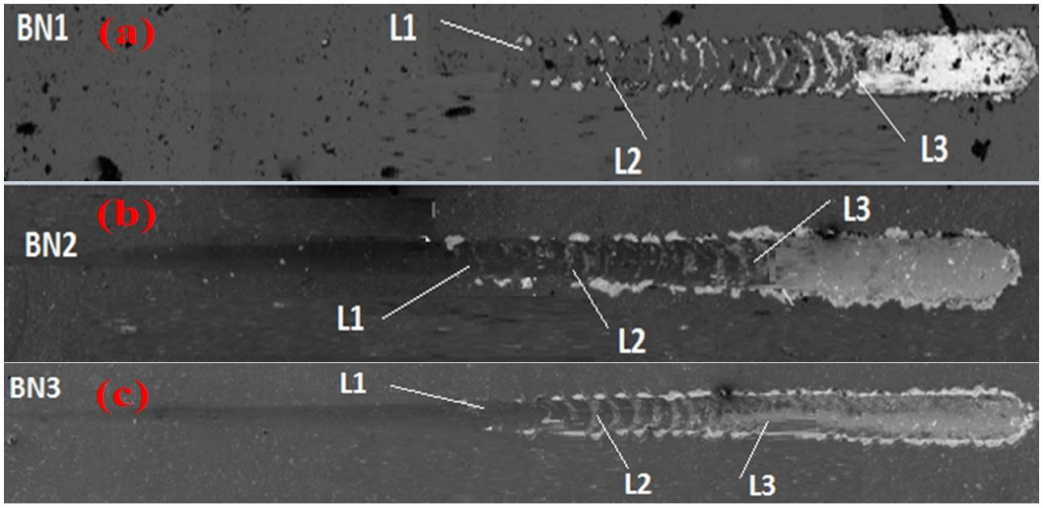

Fig.6.1. SEM micrographs of worn-out (a) BN-1, (b) BN-2 and, (c) BN-3 thin films

6.2 Elastic modulus and nano hardness

The elastic modulus and nano hardness of the coatings were examined using NanoAnalyzer- the microscope for scanning force (SFM) working in a rigid contact regime between the tested surface and the cantilever with high bending rigidity. Nano hardness of the coatings was done by the sclerometric method. In this method, scratch is produced with a constant load, and the average scratch width is then measured. Based on the calibration curve created for the material of known nano hardness (width of scratch versus load), the Hardness is calculated for tested material. Scratches with loads from 700 to 3600 N were produced for the coatings under study. The average depth of scratches did not exceed 150 nm (about 20 percent of the thickness of the coating) to remove or greatly minimize the effect of the properties of the substrate on the results obtained. Unlike nano hardness, the elastic module (Young's modulus) was tested pointwise in several dozen points using the so-called approach curves. The oscillating probe is moved down into the surface of the sample. When the tip interacts with the surface, because of the forces of elastic repulsion the resonant frequency of the oscillation changes. For each probe position, frequency change is recorded which forms the approach curve. The approach curves have different slopes for different materials. The curve slope is equal to the magnitude of the contact area for the elastic

modulus. The process mentioned allows the practical calculation of the elastic modulus of coatings with a thickness of 1 nm. The magnitude of nanohardness and Young's modulus of BN thin films are shown in Fig.6.2.

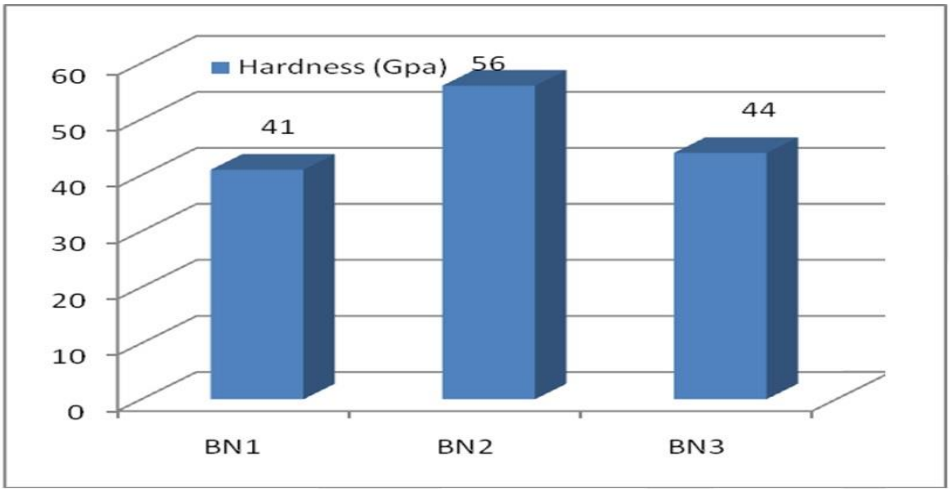

Fig. 6.2. Nano hardness values of BN thin films.

Due to high compressive stress build up during the coating deposition in regime BN2, more cubic boron nitride contents are found in the coating, which results in more coating hardness.The findings of Young's modulus obtained by the system of approach curves confirmed cubic phase boron nitride structure deposited on BN films. The critical loads for BN film thins are shown in Fig.6.3.

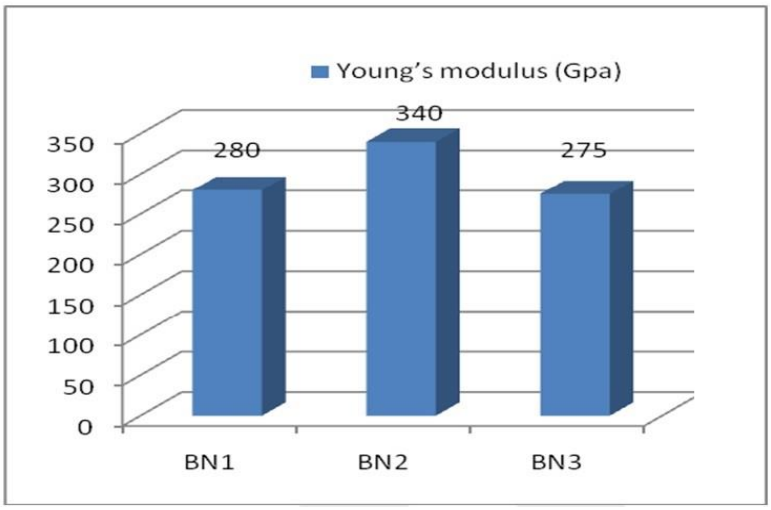

Fig.6.3. Young's modulus of BN coatings.

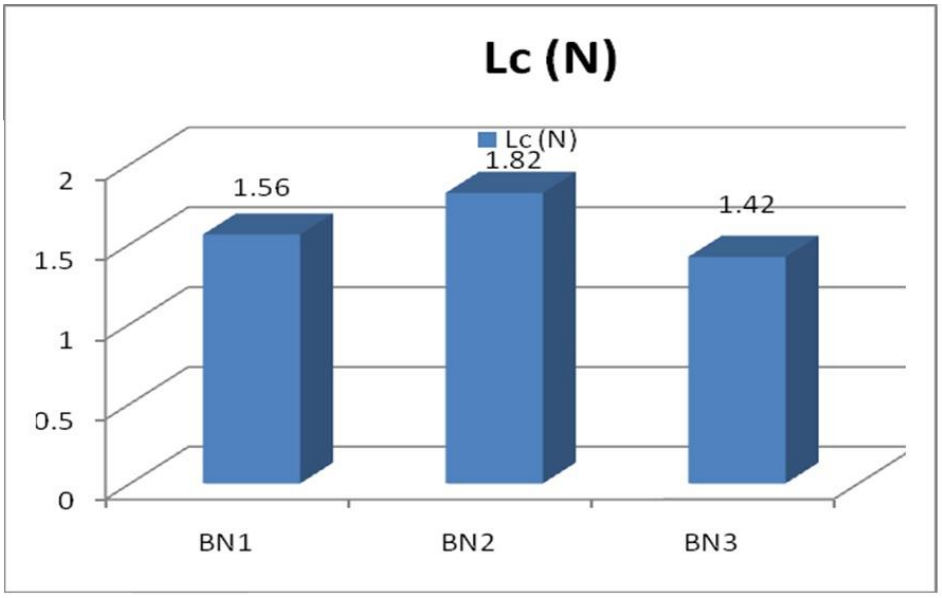

Fig. 6.4. Critical loads for BN film thins.

The coatings deposited on BN2 samples have possessed better adhesion than deposited on BN1 and BN3, as indicated by the higher value of the critical load. The 52100 Steel ball on cBN film with 80g loads at 1.64 cm/s in a tribological test is shown in Fig.6.4 and Fig.6.5, respectively.

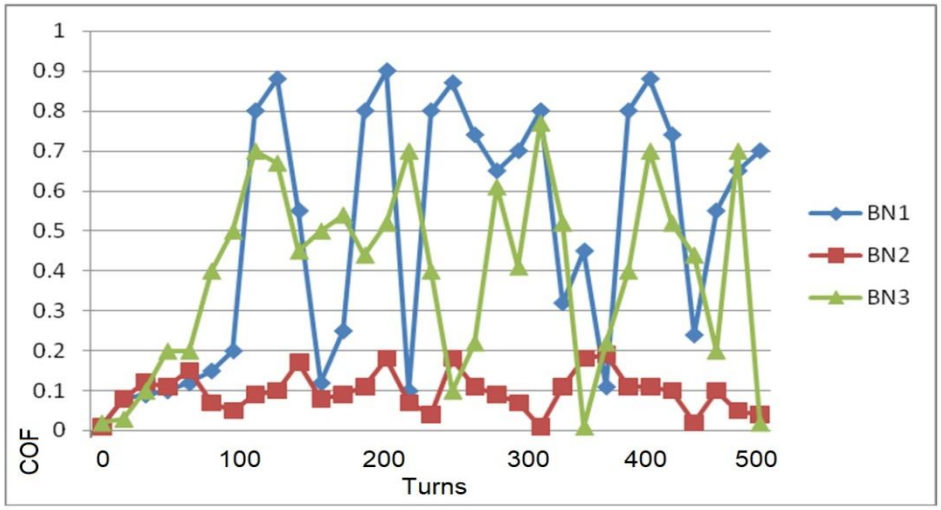

Figure 6.5.: 52100 Steel ball on cBN film with 80g loads at 1.64 cm/s in a tribological test.

All samples were subjected to a tribological performance test to determine the friction coefficient. These experiments were carried out using an 80-gram weight and a 1.64-centimeter-per-second velocity. For 100 turns, the friction coefficient of BN-2 samples is 0.052-0.148, whereas BN-1 and BN-3 samples have friction coefficients of 0.074-0.103 and.091-0.125, respectively. Within 30 cycles, the coefficient of friction for c-BN was 0.158-0.20, and certain sections of the film were eliminated, according to the literature review (S. Miyake et al., 1992).For these experiments, the friction coefficient effects are constant and identical within a hundred cycles, during which the coefficients of friction increased. The BN-2 films has excellent wear resistance as reported from these tests.

6.3 DRY SLIDING WEAR

Sliding is characterized by relative motion between two smooth solid surfaces in contact under load. High local pressure between the contacting asperities results in the plastic deformation of contacting asperities, adhesion, and consequently the formation of junctions locally. Repetitive sliding between the contacting surfaces cause rupture of these junctions and frequently transfer of material from one surface to the other. Material loss occurs in the form of small particles which are usually transferred to the other surface or get dislodged from the candidate surface. Sliding is one of the most prevalent forms of tribo-contact that functional surfaces such as machine tool slides, gears and cutting tools, etc. experience. During sliding contact, adhesion, abrasion, tribochemical reaction, and surface fatigue may occur. Adhesion causes a welded junction to develop with the counter surface, whereas abrasion causes material to be removed from the counter surface due to the presence of hard particles. Tribochemical reactions result in the formation of loose wear particles on surfaces, which function as abrasives. Sliding wear applications of engineering components have led to significant research in this field (Deuis and Kailas, 2009). In the present study, dry sliding wear performances of the substrate material (SS-316L), as-deposited coatings in different regimes were investigated by utilizing a pin-on-disc tribometer as per ASTM G-99 standards as explained in chapter 3. Further, the wear results were correlated with the SEM micrographs of the worn surfaces.

6.3.1 Wear rate and Cumulative weight Loss Characteristics

The abrasive wear (Pin on disc) performance of the coated specimens was determined as per the procedure explained in chapter 3. The cumulative loss of weight characteristics and abrasive wear coefficient of all the coated specimens and the substrate SS-316l are presented in figure 6.6. The cumulative weight loss data showed the significant weight loss of substrate (SS-316l) followed by BN1, followed by BN3, and then followed by BN2 as shown in figure 10(a). It is observed that the BN2 coated sample was exhibited minimum weight loss among all the tested specimens. This was attributed to the significant increase in the hardness and strength of the coatings. It is clear from Fig. 6.7 that during the initial run-in-wear period, all the samples such as substrate SS-316l, and coated specimens show a sudden increase in weight loss. For the calculation of the coefficient of wear rate for all the tested specimens (substrate, and coated samples), Archard's wear relation (Equation 6.1) was used.

$$Q = \frac{KW}{H} \text{ ----------(Eq-6.1)}$$

Where,

Q = Wear rate in g/m,

H = Hardness of the material

W= Load in N.

K = Dimensionless constant known as abrasive wear coefficient

The wear rate of the substrate (SS-316l) was high during the initial stage of contact with the disc and gradually reduces afterward. The wear in the substrate (SS-316l) was mainly due to plastic deformation due to the surface and sub-surface deformation, formation of debris, material transfer and reaction due to the environment. It is observed that the wear rate of the coated specimens was reduced significantly beyond 2000 m and steady wear can be seen in **Fig 6.6** The calculated

value of the abrasive wear coefficient of all the tested specimens (substrate, and coated samples) are shown in **figure 6.7.**

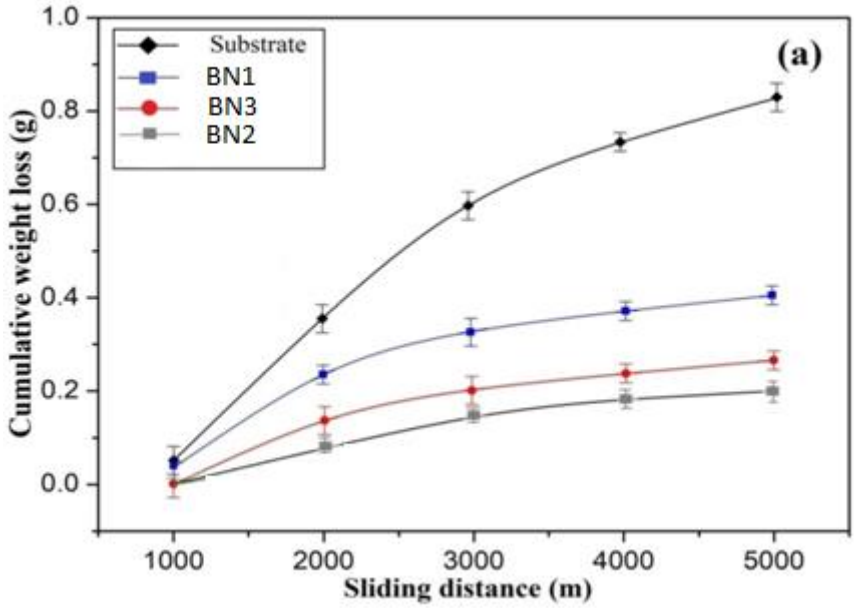

Fig. 6.6. Cumulative weight loss versus sliding distance for substrate, BN1, BN3 and BN3 specimen.

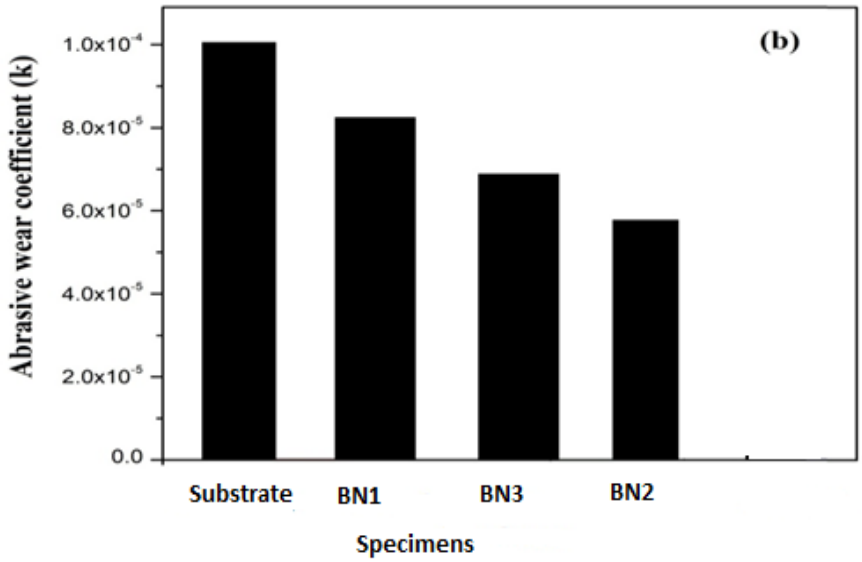

Fig.6.7. Dry sliding wear co-efficient for substrate, BN1, BN3 and BN2 specimens.

The BN2 specimens showed the 78% minimum abrasive wear coefficient from the substrate (SS-316L), 60% minimum abrasive wear coefficient compared with as-

deposited BN1, and 50% and 40% less abrasive wear from the BN3 and BN2 specimens.

6.3.2 SEM Analysis of the Worn Surfaces

After the wear testing, all specimens (substrate SS-316L, and coated specimens) were analyzed by using SEM/EDS for examined the wear mechanism of all the specimens. The surface material of the substrate was plastically deformed and abraded in a dominant way. The adhesion, abrasion and plastic deformation were responsible for the wear of substrate material (SS-316l). The material detached from the substrate (SS-316l) was occurred due to the adhesion between counter disc and substrate; this resulted in material transfer and generation of the crater in the worn surface. The deep marks formed on the surface depict the pull-out of the material. As shown in figures 6.8 the significant abrasion was also seen as a wear mechanism on the worn-out substrate (SS-316l) surfaces in the form of ploughing marks, deep grooves, craters, and scratching. The worn-out surfaces of the BN3 specimen showed some deep grooves, craters and material deboned take places, abrasion marks on the surface with formation of pits as shown in SEM/EDS Fig.6.12. The scratches formed at some locations during the sliding. Furthermore, the ploughing can be seen on the surface and micro-cutting action takes place. The worn-out surface of the BN2 specimen showed the abrasion and depressing impression of the counter surface which shows enhanced wear resistance of the BN2 specimen shown in fig.6.11. It is observed that BN1 treated samples suffered a severe material loss due to ploughing and pitting. Due to ploughing some scratches are shown in SEM/EDS image as shown in Fig.6.9. On the other hand, there is no material pull-out or deep grooves were shown in BN2 treated specimens.

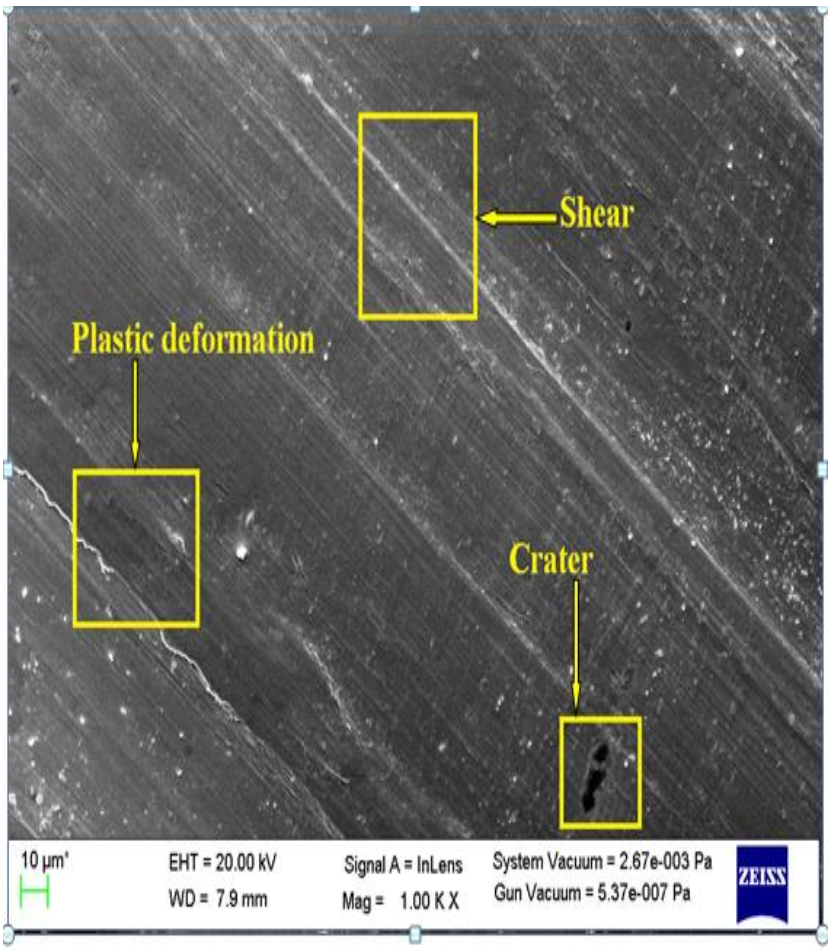

Fig. 6.8 Typical SEM micrograph of the worn surface of substrate (SS-316L).

The material detached from the substrate (SS-316L) due to adhesion between the counter disc and substrate due to this more material transfer and generation of wear debris. The deep marks formed on the surface depict the pull-out of the material. As shown in figures 6.1, the significant abrasion was also seen as a wear mechanism on the worn-out substrate (SS-316L) surfaces in the form of ploughing marks, deep grooves, and scratching

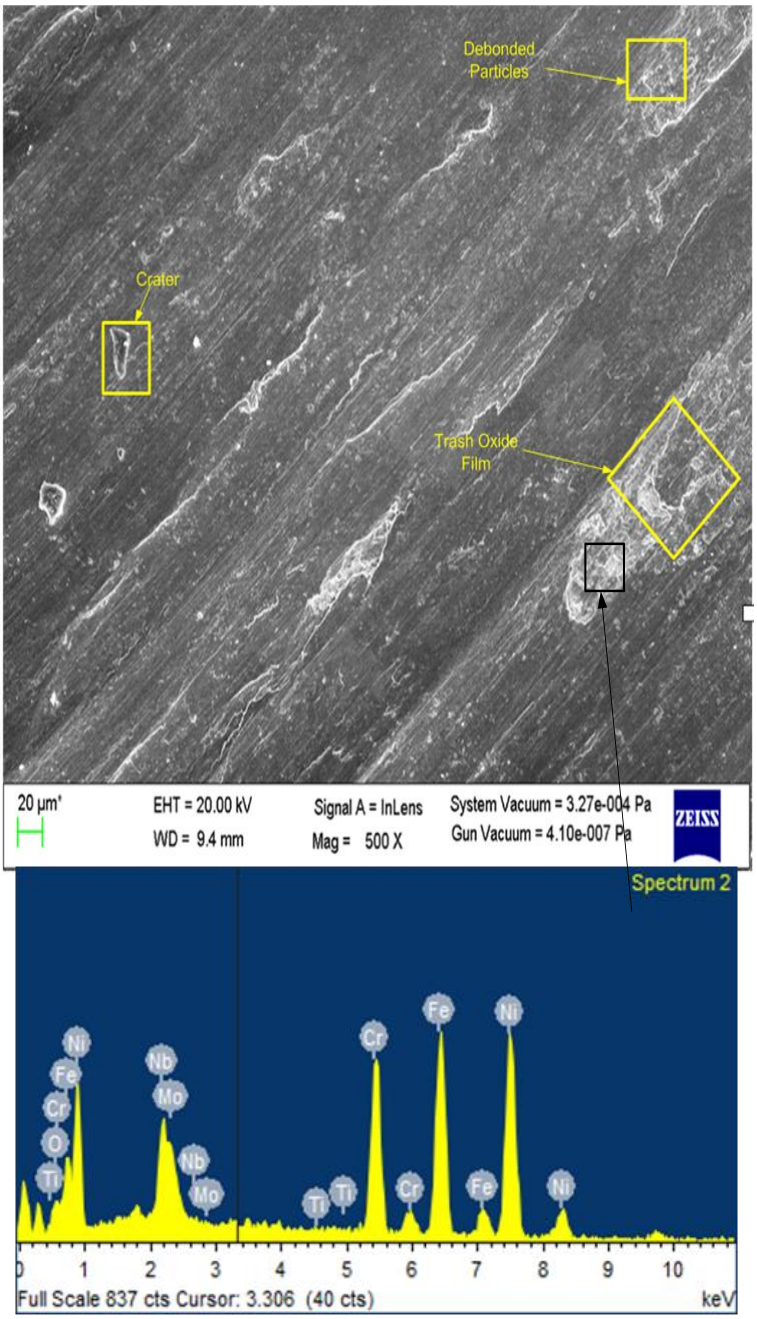

Fig6.9 Typical SEM/EDS image of the worn surface of BN3 specimen.

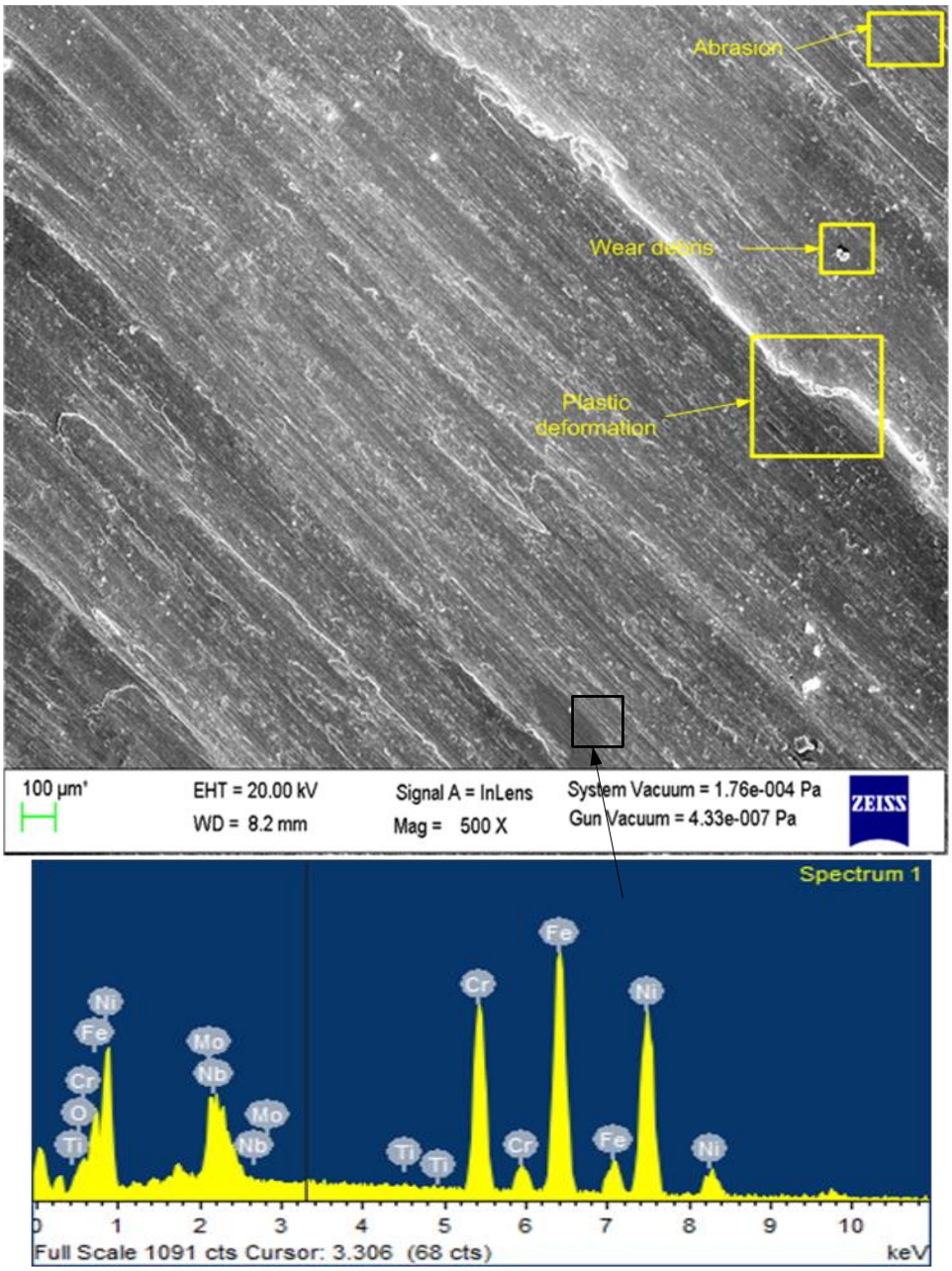

Fig 6.10 Typical SEM/EDS image of the worn surface of BN-2,

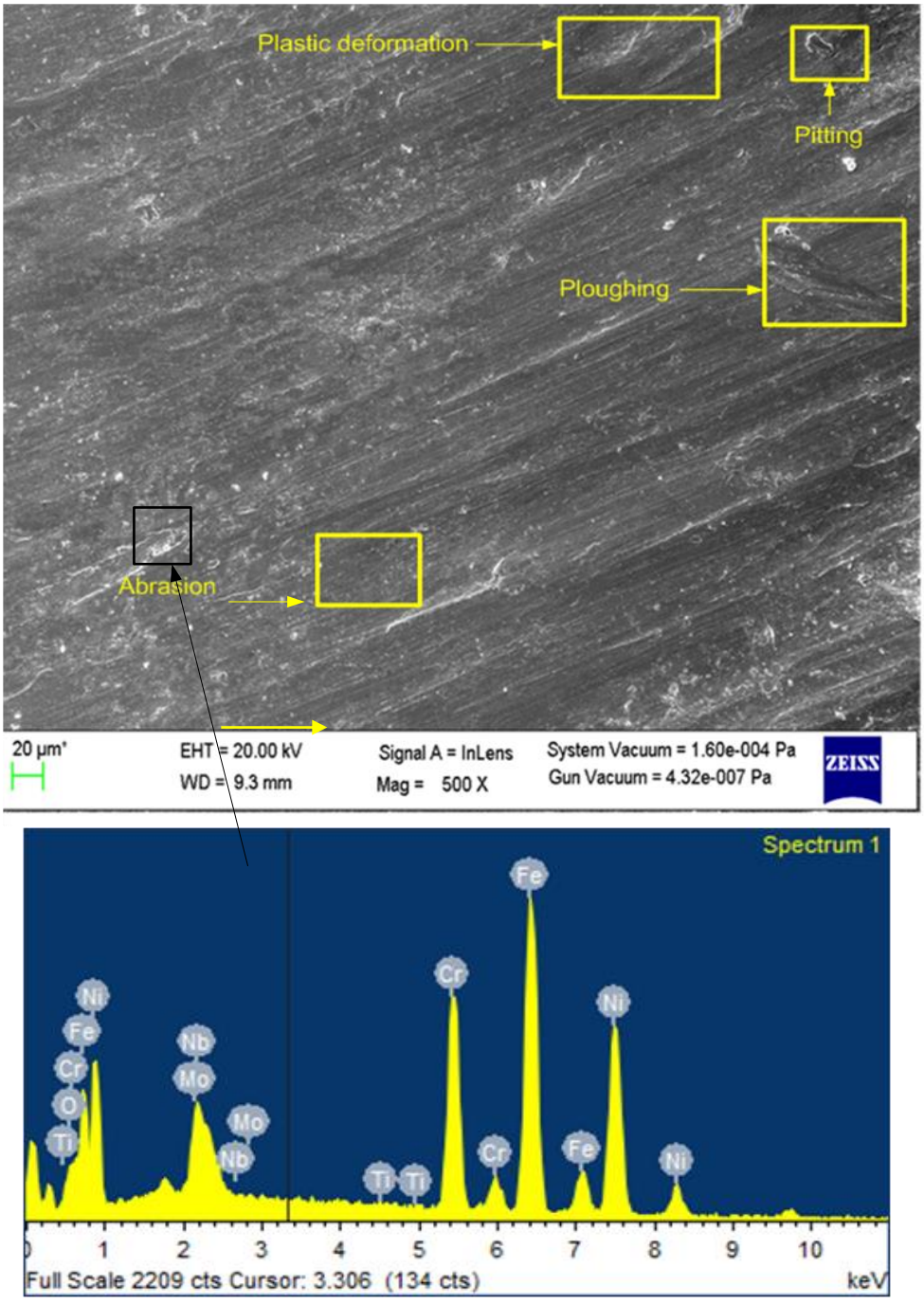

Fig 6.11 Typical SEM/EDS image of the worn surface of BN-1.

6.3 SUMMARY

The tribological aspects of the substrate, BN1, BN2 and BN3 specimens were discussed with suitable illustration in the present chapter. The erosive wear rate for BN2 was reduced by 3.2 times. This was attributed to the significant increase in the hardness and strength of the coatings due to presence of more cubic pahse of boron nitride. Whereas in the case of BN3 and BN1 specimen, it is reduced by 2.1, and 1.8 times compared. The dry sliding wear rate of BN2 specimens showed the 78% minimum abrasive wear coefficient from substrate (SS-316L) material, and 50% and 40% less abrasive wear compared with BN1 and BN3 specimens.

CHAPTER 7

7.1 CONCLUSIONS

The austenitic stainless steel (SS-316L) substrate material and BN thin films were used for the present study. The BN thin films were successfully developed on SS-316L substrates using the RF magnetron sputtering technique. A detailed description of the various steps in the RF magnetron sputtering technique has been described. A detailed description of different characterization techniques/tools (metallurgical, mechanical) used for finding the characteristics of developed BN thin film specimens has been presented in this study. The good quality of cBN film can be obtained by a combination of moderate substrate bias voltage, high substrate temperature and a certain N_2 partial pressure

- From the study it has been found that in comparison to BN-1 and BN-3 more cubic phase of boron nitride found in BN-2 sample as revealed by investigation of XRD differentiation peaks. It is because of the fact that there is a bombardment of high Ar ions in sample BN-2 which results in more Ar ions residing in the BN-2 film synthesised in Ar / N_2 plasma. Because of the contamination of these Ar ions within the BN coatings, the compressive stress increases during the formation of h-BN phase on the substrate interface to promote thermodynamically c-BN nucleation and growth.
- The bombardment ions energy is dissipated into phonons in what has been termed a thermal spike. The BN transforms from hexagonal phase to cubic phase at the action of thermal spike which results in very high temperature and pressure locally in a very brief period of time. At the low plasma energy and temperature, the bombardment ion energy is not high enough to make the hexagonal phase transform to cubic phase as shown in BN1 regime. Similarly in BN3 regime the high plasma energy and temperature high ion energy makes deposited atoms resputter from the substrate, which is not favorable to the cBN formation and lead to the decrease of cBN content and poor surface morphology. At moderate plasma energy and temperature there is sufficient bombardment ion energy and surface morphology is relatively smoother in BN2 regimes

- The XRD investigation shows the c-BN as a major phase in the deposited coating. However, soft phase h-BN is also found in the surface along with presences of phases such as amorphous-BN and t-BN phases. In contrast to the BN-1 and BN-3 samples, more peaks of c-BN have been identified in BN-2. Diffraction peaks of 43.254° and 50.306° in sample BN-2, are correspond to that of cubic phase of boron nitride while BN-1 coatings consisted of more softer boron nitride phases such as ortorombhic-BN, h-BN and rhombohedral-Boron Nitride with small amount of c-BN phase. In BN1 regime as more Ar ion are present in cpmarison to N_2 ions, the Ar+ bombardment leads to a nitrogen deficiency which could favor the formation of sp^2 bonds within the collision cascades. Ar ions induces a higher sputter rate at the film surface lead as well to an increased hBN content of the films. On the other hand in BN3 regime as N_2 supply increases the sputtering rate decreases which resulted in lower growth.
- In the SEM image relatively smoother coating morphology was found on the sample BN-2. The grain size of the coating on BN-3 sample is larger as compared to other regimes .From the corrosion test has been found that the BN-3 corrosion rate is the highest (CR (mpy)= 4.625) as compared to BN-1 and BN-2 samples. For BN-2 corrosion rate is the lowest (CR (mpy)= 1.114). The results from electrochemical corrosion test confirmed that BN-2 regimes have the lowest corrosion rate due to the presence of high c-BN contents in the coating. From the study of scratch tracks it has been found that BN-2 coatings have high adhesion strength and hardness in comparison to coatings deposited in other regimes.
- Tribological performance test for the measurement of friction coefficient was carried out on all samples. These tests were conducted with 80 g of load and velocity of 1.64 cm/s. Test result of BN-2 samples shows a constant friction coefficient of 0.052-0.148 and for BN-1 and BN-3 it is 0.074-0.103 and .091-0.125 both for 100 turns respectively. The literature review recorded coefficient of friction for c-BN within 30 cycles in the range of 0.158-0.20 and the elimination of some portions of the film (S. Miyake et al., 1992). For these

experiments the friction coefficient effects are constant and identical within a hundred cycles, during which the coefficients of friction increased.

- The BN-2 films had excellent wear resistance from these tests. The findings of Young's modulus obtained by system of approach curves confirmed cubic phase boron nitride structure deposited on BN films. The coatings deposited on BN-2 samples has possessed better adhesion than deposited on BN-1 and BN-3 , as indicated by higher value of critical load. Scratches were generated with the recording of acoustic emissions and friction force simultaneously. Based on microscopic observations, acoustic emission and friction force, critical load for the BN films was calculated. From these results, it is possible to see only a slight delamination present on the scratch track (Figure 8b), showing that the substrate has a high adhesion resistance of the BN-2 coating. This can be attributed to the behavior of elastic recovery that occurs next to the indenter path, triggered by the compressive stresses produced by the indenter and the failure of the coating to plastically deform. This mode of failure was observed among the three coating systems in L2 for BN-2 with the highest load (126 N), indicating thus the highest adhesive strength. Evidently, delamination for BN-1 and BN-3 coatings is also created in the scratch line. The load measured in L was 102 N and 96 N respectively for these coatings, which confirms that the coatings have lower adhesion strength. Therefore BN-2 is a coating with a higher adhesion strength, showing a combination of excellent durability and strength of adhesion.
- In porosity study due to volumetric and uniform ions bombardment associated with the sputtering technique, the porosity in the sputtered RF magnetron coating was found to be less than 0.5 per cent in all coating regimes. The porosity observed is normally very small compared to other commonly performed surface processes. The low porosity value in all the coating regimes is due to the low solidification rate and reduced thermal gradient of the process. The cumulative weight loss data showed the significant weight loss of substrate (SS-316l) followed by BN-1, followed by BN-3, and then followed by BN-2 as shown in figure 10(a). It is observed that the BN-2 coated sample was exhibited minimum weight loss among all the tested specimens. This was

attributed to the significant increase in the hardness and strength of the coatings. The BN-2 specimens showed the 78% minimum abrasive wear coefficient from the substrate (SS-316L), 60% minimum abrasive wear coefficient compared with as-deposited BN-1, and 50% and 40% less abrasive wear from the BN-3 and BN-2 specimens. The worn-out surfaces of the BN-3 specimen showed some deep grooves, craters and material deboned take places, abrasion marks on the surface with formation of pits as shown in SEM/EDS Fig.6.12. The scratches formed at some locations during the sliding. Furthermore, the ploughing can be seen on the surface and micro-cutting action takes place. The worn-out surface of the BN-2 specimen showed the abrasion and depressing impression of the counter surface which shows enhanced wear resistance of the BN-2 specimen shown in fig.6.11. It is observed that BN-1 treated samples suffered a severe material loss due to ploughing and pitting. Due to ploughing some scratches are shown in SEM/EDS image as shown in Fig.6.9. On the other hand, there is no material pull-out or deep grooves were shown in BN-2 treated specimens. The erosive wear rate for BN-2 was reduced by 3.2 times. Whereas in the case of BN-3 and BN1 specimen, it is reduced by 2.1, and 1.8 times compared. The dry sliding wear rate of BN-2 specimens showed the 78% minimum abrasive wear coefficient from substrate (SS-316L) material, and 50% and 40% less abrasive wear compared with BN-1 and BN-3 specimens. In terms of overall coating performance BN-2 sample has been found to be the excellent choice as it possessed superior mechanical, physical, tribological and chemical attributes.

7.2 FUTURE SCOPE:

This study can be further extended to provide quantitative expression to various coating phenomena under different coating parameters to formulate mathematical modelling for finite element analysis. Also various simulation technique can be used to predict the behaviours of coating under different coating regimes and operating conditions in order to optimize vast array of the parameters. The other parameters like pressure and temperature of inert gas environment could be taken for coatings.

References:

1. A Rivera-Tello C D, Broitman E, Flores-Ruir F J Jiménes 2016 Mechanical properties and tribological behavior at micro and macro-scale of WC/WCN/W hierarchical multilayer coatings Tribology.
2. A.Y. Liu and M.L. Cohen, Science 245, 841 (1989)
3. A.Y. Liu and M.L. Cohen, Science 245, 841 (1989).
4. Ananthakumar, R., et al. "Electrochemical corrosion and materials properties of reactively sputtered TiN/TiAlN multilayer coatings." (2019).
5. Audronis M., Valiulis A.-V., Silickas P., Recent Developments in the Deposition of c-BN Coatings, ISSN 1392–1320 Materials Science (MEDŽIAGOTYRA), Vol. 10, No. 2. (2015)
6. Auezhan . A, Tsukasa W. Ryo T, Shinya. Fretting wear and fracture behaviors of Cr-doped and non-doped DLC film deposited on Ti6Al$V alloy by unbalanced magnetron sputtering. Tribology International; 2020.
7. Bartl, S. Bohr, R. Haubner, and B. Lux, Int. J. of Refractory Metals and Hard Materials 14, 145 (2006)
8. Bartl, S. Bohr, R. Haubner, and B. Lux, Int. J. of Refractory Metals and Hard Materials 14, 145 (1996).
9. Bello, C.Y. Chan, W.J. Zhang, Y.M. Chong, K.M. Leung, S.T. Lee, Y. Lifshitz, Deposition of thick cubic boron nitride films: the route to practical applications. Diam. Relat. Mater. **14**, 1154–1162 (2005)
10. Bello, I.; Chan, C.Y.; Zhang, W.J.; Chong, Y.M.; Leung, K.M.; Lee, S.T.; Lifshitz, Y. Deposition of thick cubic boron nitride films: The route to practical applications. *Diam. Relat. Mater.* **2015**, *14*, 1154–1162.
11. Bewilogua K., Keunecke M., Weigel K., Wiemann E., Growth and characterization of thick cBN coatings on silicon and tool substrates, Thin Solid Films 469–470 (2004) 86–91.

12. Bin D, Ye Tao, Zhijie Hu. The microstructure, mechanical and tribological properties of TiN coatings after Nb and C ion implantation. Applied Surface Science; 2013.
13. Boyen ,Zhang, X.W.; Yin, H.;, H.G.; Ziemann, P.; Ozawa, M. Effects of crystalline quality on the phase stability of cubic boron nitride thin films under medium-energy ion irradiation. *Diam. Relat. Mater.* **2005**, *14*, 1482–1488.
14. Cheng ,Yang, H.S., A.L.; Qiu, F.M. Cubic boron nitride film residual compressive stress relaxation by post annealing. *Diam. Relat. Mater.* **2011**, *20*, 1179–1182
15. Chopra, KL 1969, 'Thin Film Phenomena', McGraw Hill, New York.
16. D. Ponnamma, A. Erturk, H. Parangusan, K. Deshmukh, M.B. Ahamed, M.A. Al-Maadeed, Stretchable quaternary phasic PVDF-HFP nanocomposite films containing graphene-titania- SrTiO3 for mechanical energy harvesting. Emergent Mater. 1,
17. D.M. Teter, MRS Bull. 23, 22 (1998).
18. D.R. Cote, S.V. Nguyen, W.J. Cote, S.L. Pennington, A.K. Stamper, and D.V. Podlesnik, IBM J. Res. Dev. 39, 437 (2005).
19. D.R. McKenzie, W.D. McFall, W.G. Sainty, C.A. Davis, and R.E. Collins, Diamond Relat. Mater. 2, 970 (2013)
20. Deng J., Wang B., Tan L., Yan H., Chen G., The growth of cubic boron nitride films by RF reactive sputter, Thin Solid Films 368 (2000) 312-31.
21. Deyneka, N.; Zhang, X.W.; Boyen, H.G.; Ziemann, P.; Fukarek, W.; Kruse, O.; Moller, W. Depth profiles of Argon incorporated into Boron Nitride films during preparation and their temperature dependent evolution. *Diam. Relat. Mater.* **2003**, *12*, 37–46.
22. Donald M Mattox 1998, 'Handbook of Physical Vapor Deposition (PVD) Processing', Second edition.
23. E. Weibmantel, T. Pfeifer, F. Richter, Electron microscopic analysis of cubic boron nitride films deposited on fused silica. Thin Solid Films **408**, 1–5 (2002)

24. E.M. Fayyad, A.M. Abdullah, M.K. Hassan, A.M. Mohamed, G. Jarjoura, Z. Farhat, Recent advances in electroless-plated Ni-P and its composites for erosion and corrosion applications: a review. Emergent Mater. 1, 3–24 (2018)
25. Essafti, E. Ech-chamikh, M. Azizan, Structural and chemical study of a-BC, a-CN, and a-BCN Thin films prepared by reactive RF sputtering*. Spectrosc. Lett. 41, 57–63 (2008)
26. F. Xu, M.F. Yuen, B. He, C.D. Wang, X.R. Zhao, X.L. Tang, D.W. Zuo, W.J. Zhang, Microstructure and tribological properties of cubic boron nitride films on Si 3 N 4 inserts via boron-doped diamond buffer layers. Diam. Relat. Mater. **49**, 9–13 (2014)
27. F.P. Bundy, H.T. Hall, H.M. Strong, and R.H. Wentorf, Nature 176, 51 (1955).
28. Freudenstein, R.; Klett, A.; Kulisch, W. Investigation of the nucleation of c-BN by AFM measurements. *Thin Solid Films* **2011**, *398*, 217–221
29. G. Bräuer, B. Szyszka, M. Vergöhl, R. Bandorf, Magnetron sputtering – Milestones of 30 years, Vacuum. 84 (2010).
30. G. Bräuer, B. Szyszka, M. Vergöhl, R. Bandorf, Magnetron sputtering – Milestones of 30 years, Vacuum. 84 (2010).
31. Grove, W.R., 1852: On the electro-chemical polarity of gases, Philosophical Donald M Mattox 1998, 'Handbook of Physical Vapor Deposition (PVD) Processing',Second edition.
32. H. Feldermann, C. Ronning, H. Hofs¨ass, Y.L. Huang, and M. Seibt, J. Appl. Phys. 90, 3248 (2001)
33. H. Feldermann, Dissertation, University of G¨ottingen (2002).
34. H. Hofs¨ass, C. Ronning, U. Griesmeier, M. Gross, S. Reinke, and M. Kuhr, Appl. Phys. Lett. 67, 46 (2015).
35. H. Yang, A. Chen, F. Qiu, Cubic boron nitride film residual compressive stress relaxation by post annealing. Diam. Relat. Mater. **20**, 1179–1182 (2011)

36. H.Oechsner, Growth conditions of the cubic phase cBN in boron nitride films, Thin Solid Films.515 (2006) 33-38.
37. H.S. Kim, J.K. Park, W.S. Lee, Y.J. Baik, Variation of residual stress in cubic boron nitride film caused by hydrogen addition during unbalanced magnetron sputtering. Thin Solid Films **519**, 7871–7874 (2011)
38. Helmer, John C., Kwok F. Lai, and Robert L. Anderson. "Physical vapor deposition employing ion extraction from a plasma." (1996).
39. Herman, H., & Sampath, S. Thermal spray coatings. In Metallurgical and ceramic protective coatings (pp. 261-289). Springer, Dordrecht (1996).
40. Hirama, K.; Taniyasu, Y.; Karimoto, S.I.; Krockenberger, Y.; Yamamoto, H. Single-crystal cubic boron nitride thin films grown by ion-beam-assisted molecular beam epitaxy. *Appl. Phys. Lett.* **2014**, *104*, 092113
41. Hofsass, H.; Ronning, C.; Griesmeier, U.; Gross, M.; Reinke, S.; Kuhr, M. Cubic boron-nitride films grown by low-energy B+ and N+ ion-beam deposition. *Appl. Phys. Lett.* **2015**, *67*, 46–48.
42. Janson, J. Minier-Matar, E. Al-Shamari, A. Hussain, R. Sharma, D. Rowley, S. Adham, Evaluation of new ion exchange resins for hardness removal from boiler feedwater. Emergent Mater. 1, 77–87 (2018)
43. Jiang L., Fitzgerald A.-G., Rose M.J., Lousa A., Gimeno S., Formation of cubic boron nitride by r.f. magnetron sputtering, Surface Interface Analysis 2012 , 34, 732-734.
44. K. Reichelt, X. Jiang, The preparation of thin films by physical vapour deposition methods, Thin Solid Films (1990).
45. K. Teii, S. Matsumoto, Impact of low-energy ions on plasma deposition of cubic boron nitride. Thin Solid Films **576**, 50–54 (2015)
46. Kelly, P. J., and R. D. Arnell. "Magnetron sputtering: a review of recent developments and applications." Vacuum, (2020).
47. Kelly, P. J., and R. D. Arnell. "Magnetron sputtering: a review of recent developments and applications." Vacuum, (2000).
48. Kelly, P. J., and R. D. Arnell. "Magnetron sputtering: a review of recent developments and applications." Vacuum, (2000).

49. Kelly, P.J.; Arnell, R.D. Magnetron sputtering: A review of recent developments and applications. Vacuum **2000**, 56, 159–172.
50. Keunecke M., Bewilogua K., Wiemann E., Weigel K., Wittorf R., Thomsen H., Boron containing combination tool coatings-characterization and application tests, Thin Solid Fils 494 (2016) 58-62.
51. Kim, H.S.; Park, J.K.; Baik, Y.J.; Choi, I.H. Origin of residual stress in the formation of boron nitride film by sputtering with Ar ions. *J. Appl. Phys.* **2013**, *94*, 3057–3060
52. Kiryukhantsev-Korneev, F.V.; Shirmanov, N.A.; Sheveiko, A.N.; Levashov, E.A.; Petrzhik, M.I.; Shtanskii, D.V. Nanostructural wear-resistant coatings produced on metal-cutting tools by electric-arc evaporation and magnetronic sputtering. Russ. Eng. Res. **2010**, 30, 910–920.
53. Konyashin, F. Aldinger, V. Babaev, V. Khvostov, M. Guseva, A. Bregadze, K.-M. Baumg¨artner, and E. R¨auchle, Thin Solid Films 355-356, 96 (2009).
54. L. Hultman, Thermal stability of nitride thin films, Vacuum. 57 (2020).
55. Le, Y.K.; Oechsner, H. On the influence of substrate temperature for cubic boron nitride growth. *Thin Solid Films* **2003**, *437*, 83–88
56. Lee, M. H., Shih, C. C., Chen, J. S., Huang, W. M., Gan, F. Y., Shih, Y. C., ... & Shih, I. S. (2009, June). 15.4: Excellent Performance of Indium- Oxide-Based Thin- Film Transistors by DC Sputtering.
57. Litvinov, D.; Clarke, R. Reduced bias growth of pure-phase cubic boron nitride. *Appl. Phys. Lett.* **2014**, *71*, 1969–1971
58. Lousa, J. Esteve, S. Muhl, E. Martínez, BN thin films near the B 4 C composition deposited by radio frequency magnetron sputtering. Diam. Relat. Mater. 9, 502–505 (2000)
59. M. A. Lieberman and A. J. Lichtenberg, Principles of plasma discharges and materials processing (John Wiley & Sons, Inc., New York, 1994).
60. M. Hebbache, Solid State Commun. 113, 427 (2000).

61. M. Mrlik, P. Sobolciak, I. Krupa, P. Kasak, Light-controllable viscoelastic properties of a photolabile carboxybetaine esterbased polymer with mucus and cellulose sulfate. Emergent Mater. 1, 35–45 (2018)
62. M. Ohring, The Materials Science of Thin Films, 2nd ed. (Academic Press Inc., San Diego, 2002).
63. M. Ohring, The Materials Science of Thin Films, 2nd ed. (Academic Press Inc., San Diego, 2002).
64. M. Ohring, The Materials Science of Thin Films, 2nd ed. (Academic Press Inc., San Diego, 2002).
65. M. Ohring, The Materials Science of Thin Films, 2nd ed. (Academic Press Inc., San Diego, 2002).
66. M.L. Cohen, Mater. Sci. Eng. A 209, 1 (1996)
67. M.L. Cohen, Phys. Rev. B 32, 7988 (1985)
68. M.L. Cohen, Solid State Commun. 45, 45 (1994).
69. Marco Annunziata, Adriana Oliva, Maria Assunta Basile, Michele Giordano, Nello Mazzola, Antonietta Rizzo, Alessandro Lanza & Luigi Guida 2011, 'The effects of titanium nitride-coating on the topographic and biological features of TPS implant surfaces.
70. Mateescu, A. O., et al. "Coating multilayer material with improved tribological properties obtained by magnetron sputtering." Materials Science and Engineering. (2017).
71. McKenzie, D.R.; McFall, W.D.; Sainty, W.G.; Davis, C.A.; Collins, R.E. Compressive stress-induced formation of cubic boron-nitride. *Diam. Relat. Mater.* **2019**, *2*, 970–976.
72. Mech, K., Kowalik, R., & Żabiński, P. (2011). Cu thin films deposited by DC magnetron sputtering for contact surfaces on electronic components. Archives of Metallurgy and materials.
73. Ming Lu, A. Bousetta, R. Sukach, A. Bensaoula, K. Walters, K. EipersSmith, and A. Schultz, Appl. Phys. Lett. 64, 1514 (2014)

74. N. Deyneka, X.W. Zhang, H.-G. Boyen, P. Ziemann, W. Fukarek, O. Kruse, and W. M¨oller, Diamond Relat. Mater. 12, 37 (2003)

75. Nagaraj, D. Govindaraj, M. Rajan, Magnesium oxide entrapped polypyrrole hybrid nanocomposite as an efficient selective scavenger for fluoride ion in drinking water. EmergentMater. 1, 25–33 (2018)

76. Navas, C., Colaco, R., De Damborenea, J., & Vilar, R., Abrasive wear behavior of laser clad and flame sprayed-melted NiCrBSi coatings. Surface and Coatings Technology (2006).

77. Neo K.-S., Rahman M., Li X.-P., Khoo H.-H., Sawa M., Maeda Y., Performance evaluation of pure c-BN tools for machining of steel, Journal of Materials Processing Technology 140 (2013) 326–331.

78. O. Mishima, in: Synthesis and Properties of Boron Nitride, J.J. Pouch, S.A. Alterovitz (eds.), Materials Science Forum, Vol. 54/55, Trans Tech Publications, Brookfield (1990), p. 313

79. O. Tsuda, Y. Yamada, T. Fujii, T. Yoshida, J. Vac. Sci. Technol A 13 (2011) 2843 Relat. Mater. 5 (2006) 1103

80. O.O. Fadiran, N. Girouard, J.C. Meredith, Pollen fillers for reinforcing and strengthening of epoxy composites. Emergent Mater. 1, 95–103 (2018).

81. P.B. Mirkarimi, K.F. McCarty, and D.L. Medlin, Mater. Sci. Eng. R 21, 47 (1997).

82. P.B. Mirkarimi, K.F. McCarty, D.L. Medlin, W.G. Wolfer, T.A. Friedmann, E.J. Klaus, G.F. Cardinale, and D.G. Howitt, J. Mater. Res. 9, 2925 (2004).

83. P.B. Mirkarimi, K.F. McCarty, G.F. Cardinale, D.L. Medlin D.K. Ottesen, H.A. Johnsen, J. Vac. Sci. Technol. A 14 (1)(2005) 251

84. Panich N, Wangyao P, Vattanaprateep N and Yong S 2006 Techniques to Improve Coating Adhesion of Superhard Coatings *Journal of Metals, Materials and Minerals,* **16 (**2) 19-23

85. Pelleg, Joshua, L. Z. Zevin, Sh Lungo, and N. Croitoru. "Reactive-sputter-deposited TiN films on glass substrates." Thin Solid Films 197, no. 1-2 (1991).

86. Popelka, P. Sobol, M. Mrlík, Z. Nogellova, I. Chodák, M.Ouederni, M.A. Al-Maadeed, I. Krupa, Foamy phase change materials based on linear low-density polyethylene and paraffin wax blends. Emergent Mater. 1, 47–54 (2018)
87. Prakash, K.B. Sundaram, Deposition and XPS studies of dual sputtered BCN thin films. Diam. Relat. Mater. 64, 80–88 (2016)
88. Pshyk, Oleksandr. "Cechy strukturalne i wlasciwosci trybo-mechaniczne powlok nanokompozytowych TiAlBSiN." (2017).
89. R.W. Hertzberg, ”Deformation and fracture mechanics of engineering materials”, Wiley, New York, 4th edn. (1995)
90. Reinke, P.; Oelhafen, P.; Feldermann, H.; Ronning, C.; Hofsass, H. Hydrogen-plasma etching of ion beam deposited c-BN films: An in situ investigation of the surface with electron spectroscopy. *J. Appl. Phys.* **2012**, *88*, 5597–5604.
91. Ronning, H. Feldermann, R. Merk, H. Hofs¨ass, P. Reinke, and J.-U. Thiele, Phys. Rev. B 58, 2207 (1998)
92. Rossnagel, S., Sputtering and sputter deposition, in “Thin- Film Deposition Processes And Techniques”. (2002).
93. S. Bohr, R. Haubner, and B. Lux, Diamond Relat. Mater. 4, 714 (2005).
94. S. Eyhusen, I. Gerhards, H. Hofsa¨ss, C. Ronning, M. Blomenhofer, J. Zweck, M. Seibt, Diamond Relat. Mater. 12 (2020) 1877.
95. S. Matsumoto and W. Zhang, Jpn. J. Appl. Phys. 39, 442 (2000)
96. S. Matsumoto and W.J. Zhang, Diamond Relat. Mater. 10, 1868 (2001)
97. S. Reinke, M. Kuhr, and W. Kulisch, Diamond Relat. Mater. 3, 341 (2014).
98. S. Veprek, J. Vac. Sci. Technol. A 17, 2401 (1999).
99. S. Veprek, J. Vac. Sci. Technol. A 17, 2401 (1999).
100. Schtze, K. Bewilogua, H. L¨uthje, and S. Kouptsidis, Diamond Relat. Mater. 5, 1130 (1996).

101. Setsuhara Y., Kumagai M., Suzuki M., Suzuki T., Miyake S., Properties of cubic boron nitride films with buffer layer control for stress relaxation using ion-beam-assisted deposition, Surface and Coatings Technology. 116–119 (2019) 100–107
102. T. Meng, C. Yi, L. Liu, A. Karim, X. Gong, Enhanced thermoelectric properties of two-dimensional conjugated polymers. Emergent Mater. 1, 67–76 (2018)
103. T. Taniguchi and S. Yamaoka, J. Cryst. Growth 222, 549 (2001).
104. T. Taniguchi, K. Watanabe, and S. Koizumi, Phys. Stat. Sol. (a) 201, 2573 (2004).
105. Taube, K. Bewilogua. Thin Films: Tribology. Encyclopedia of Materials: Science and Technology; 2018.
106. Tzeng, Y.; Zhu, H. Electron-assisted deposition of cubic boron nitride by r.f. magnetron sputtering. *Diam. Relat. Mater.* **2004**, *8*, 1402–1405
107. V.L. Solozhenko, D. Andrault, G. Fiquet, M. Mezouar, and D.C. Rubie, Appl. Phys. Lett. 78, 1385 (2000).
108. W. Kalss, R. Haubner, and B. Lux, Diamond Relat. Mater. 7, 369 (2008)
109. W. Kulisch and S. Ulrich, Thin Solid Films 423, 183 (2003)
110. W.J. Zhang, I. Bello, Y. Lifshitz, K.M. Chan, Y. Wu, C.Y. Chan, X.M. Meng, and S.T. Lee, Appl. Phys. Lett. 85, 1344 (2004)
111. Wang, Y. Qin, F. Jin, J.F. Yang, K. Ishizaki, Pulse electric current sintering of cubic boron nitride/tungsten carbide–cobalt (cBN/WC–Co) composites: effect of cBN particle size and volume fraction on their microstructure and properties. Mater. Sci. Eng. A **607**, 490–497 (2014)
112. Werbowy, J. Szmidt, A. Sokołowska, S. Mitura, RF plasma selective etching of boron nitride films. Diam. Relat. Mater. **9**, 609–613 (2000

113. Wiemann E., Keunecke M., Weigel K., Park S.T., Bewilogua K., Thick c-BN coatings –Preparation, properties and application tests, Thin Solid Films. 515 (2016) 967–972.

114. X. Yang, H. Li, Y. Li, X. Lü, S. Gao, P. Zhu, Q. Zhang, T. Zhang, G. Zou, Dependence of RF power on the phase transformation for boron nitride films deposited on graphite at room temperature. J. Cryst. Growth **311**, 3716–3720 (2009)

115. X.W,Zhang.. Doping and electrical properties of cubic boron nitride thin films: A critical review. *Thin Solid Films* **2013**, *544*, 2–12.

116. Yamamoto K., Keunecke M., Bewilogua K., Deposition of well adhering cBN films up to 2 mm thickness by B-C-N gradient layer system, Thin Solid Films 377-378 (2000)331-339

117. Yap, Y.K.; Aoyama, T.; Kida, S.; Mori, Y.; Sasaki, T. Synthesis of adhesive c-BN films in pure nitrogen radio-frequency plasma. Diam. Relat. Mater. 2018, 8, 382–385.

118. Ye J., Rothaar U., Oechsner H., Conditions for the formation of cubic boron nitride films by r.f. magnetron sputtering, Surface and Coatings Technology 105 (2009) 159–164.

119. Zhao Y.H, Hu L, Lin G.Q, Xiao J.Q, Dong C, Yu B.H. Deposition, microstructure and hardness of TiN/(Ti, Al)N multilayer films. Int. Journal of Refractory Metals and Hard Materials; 2019.

120. Vel L, Demazeau G, Etourneau J (1991) Mat Sci Eng B10: 149-164

121. A S Kamenetskikh *et al* 2017 *J. Phys.: Conf. Ser.* **857** 012017

122. McKenzie D R et al. 1996 *Surf. Coat. Technol.* **78** 255–62

123. Gomez-Aleixandre, A. Essafti, and J.M. Albella, J. Phys. Chem. B 104, 4397 (2000)

124. H.Hofsass, C.Ronning, U. Griesmeier, M.Gross, S.Reinke and M.Khuhr, *Appl Phy Lett* 67. 46(1995)